explorations

THE TEXAS A&M UNDERGRADUATE JOURNAL

VOLUME 13

FALL 2021

VOLUME 13 (FALL 2021)

Explorations: The Texas A&M Undergraduate Journal is a student-run, faculty/staff-guided publication dedicated to highlighting exceptional undergraduate research as well as scholarly and creative work in all fields. Submissions of broad interest should be submitted online at **explorations.tamu.edu**. Questions about publication, student membership, how to become a faculty/staff reviewer, or how to obtain a printed copy of the journal can be directed to **explorations@tamu.edu**. *Explorations'* home is in the LAUNCH: Undergraduate Research office located inside of Henderson Hall at Texas A&M University in College Station, TX 77840-4233.

ISSN 2668-7525 (print) | ISSN 2688-7533 (online)

explorations

THE TEXAS A&M UNDERGRADUATE JOURNAL

VOLUME 13
FALL 2021

THANKS & GIG 'EM!

Explorations would not be possible without the generous contributions of Mr. and Mrs. Ralph & Barbara Cox, as well as continued support from The Association of Former Students, Office of the Provost, and office of Undergraduate Studies at Texas A&M University. The *Explorations* Board and the LAUNCH office sincerely thank you.

SUPPORT US

For more information on how **you** can help us showcase the best and most vibrant undergraduate research by Aggies, contact the Texas A&M Foundation at **info@txamfoundation.com**. Donations are accepted online at **www.txamfoundation.com/give.aspx**. Checks may be made payable to:

Texas A&M Foundation
ATTN: UGR Explorations: The Texas A&M Undergraduate Journal
Acct. 510025-36000
$25 minimum for online donations

CONTACT US

★ **explorations.tamu.edu**

✉ **explorations@tamu.edu**

facebook.com/explorationstexasam

instgram.com/TAMU_UGR

twitter.com/TAMU_UGR

GET INVOLVED

Opportunities are open to all undergraduate students. Be part of a leadership and learning community through *Explorations* as a board member, an author, or an artist! The student board works year-round to meet the journal's annual publication schedule, and develop skills in areas such as leadership, public speaking, critical thinking, time management, editing, marketing, publishing, and graphic design. Board member applications are accepted in early-fall each year.

Publication in *Explorations* is a multi-stage, refereed process. The first step to publication in *Explorations* is the synopsis submission, which is an article pitch. Synopses are reviewed by faculty reviewers and student board members. If invited, prospective authors then submit a full manuscript. Full manuscripts are requested by mid-spring and undergo a second round of faculty and student review. Final articles are chosen from the full manuscript submissions. Provisionally accepted articles undergo further editing and a final review by a team of student editors, LAUNCH staff members, and a third-party professional editor. Final articles are due in late-spring each year.

Faculty at Texas A&M can mentor undergraduate researchers and encourage them to apply to the board and/or to submit synopses. Faculty and staff can also volunteer to review submissions for *Explorations*. The review process begins each spring semester.

FROM OUR FACULTY

DR. VALERIE BALESTER

Assistant Provost for Undergraduate Studies and the Executive Director of the University Writing Center and the Academic Success Center

I first started teaching writing in 1976. Then, the teaching of writing was considered at best an art, at worst, drudgery. Writing was viewed as the product of a solitary mind following a linear process and using the "correct" style: First, do the necessary research or thinking, then create an outline, translate that into a draft, and finally edit to conform to standard American English. Some students were considered "gifted" writers; others were expected to memorize and apply rules to produce adequate writing.

What changed that view, a change that was rapidly advancing in the late 1970s, was research. Teachers of writing realized with that empirical methods we could study the cognitive processes of writers at work and use that to improve teaching. In the 1980s and 1990s, we turned our attention to the social dimensions of writing, discovering that we write from a particular subject position and bring to our writing deeply ingrained, tacit ideas about language and genres. We acknowledged that writing could be oppressive in that it privileged certain styles and voices and censored or suppressed others.

We have not stopped studying the writing process, and the fact that we do now study it has not only resulted in better pedagogy but also has begun to give access to marginalized voices. We need research so we don't stagnate. We need research to improve our practice.

I suspect the authors whose work is represented in this journal went through an extensive and recursive writing process. When done well, the process of writing is messy. Not all of us start with an outline, for example. (I hate them.) Not all of us write only one or two drafts before they are ready to edit. While almost everything we write conforms to some degree to genre and audience expectations, those can vary widely and be altered. We may be working within the expectations of a defined genre (like an article reporting the results of a quantitative study using the Introduction, Method, Results and Discussion model) or we may be working in a less structured format (perhaps reporting the results of an ethnographic study in a narrative). In short, writing becomes a process of solving problems and making choices. It's been compared to master chess in its complexity.

No matter how you write, however, if you skimp on discovery, you will end up with a skimpy product. Discovery is not always done once the research is finished. As we draft, we ideally continue to invent or explore new avenues of thought, new things to say—we identify missing pieces, holes in logic, a problem in our data, and we have to go back to discovery and research before we can progress.

Writing is discovery. Writing is invention. Writing is exploration. The ancient Greek rhetoricians like Aristotle recognized the importance of heuristics (derived from the Greek, eureka, meaning "I found it") to the orator's process of composing.

Why name a journal Explorations? Obviously, the exploration isn't done once the research is done and written up. Readers, even the authors who are reading their own work, will be exploring as they peruse this issue, gaining knowledge, sparking ideas, perhaps discovering future research projects.

Even as infants, we explore the world, we discover, we make inferences, we test them, we create theories, we reject theories. In the academy, we formalize that process, and that gives us the potential to change the world. It is an awesome responsibility. Re-

search can open some avenues and close others. We can decide what and how to explore, and these decisions have real world consequences. That's why the peer review process is vital. Peers keep us honest, help us see the holes in our work, correct our missteps, and suggest ways to interpret or apply what we discover.

Research is collaborative, and as we move into the future, my hope is Texas A&M undergraduate researchers will collaborate extensively, opening access to alternative voices and visions and carrying on what they learned from the Texas A&M mentors. Research methodologies and subjects change. Commitment to the academic integrity, to the creation of knowledge, and to the freedom to explore, fostered by LAUNCH Undergraduate Research, endures.

CONTENTS

CONTENTS

The Impact of Genetic Background on Neurological Disease Outcomes

By Madilyn Feik '21

INTRODUCTION

Viral infection early in life is thought to contribute to greater susceptibility to neurological diseases later in life such as Parkinson's disease, multiple sclerosis (MS), epilepsy, and amyotrophic lateral sclerosis (ALS).[1] Humans show a wide range of responses to neurological diseases, ranging from mild symptoms to critical illness, but little is known about what makes an individual susceptible to grave consequences. People infected with the same antecedent virus show significantly different neurological outcomes later in life, suggesting that the genetic background of the individual influences the disease characteristics observed.

Although previous experimental studies with mice have investigated viral infection mechanisms, they utilized inbred strains, resulting in limited observable disease characteristics or phenotypic responses following viral infection.[2] The studies failed to reflect the wide range of genetic diversity in humans and consequently, our knowledge of human responses to previous viral infection is limited. Therefore, a specialized mouse model known as the Collaborative Cross (CC) is utilized in this study to model the complex genetic diversity of humans. The CC mouse model results from the deliberate crossbreeding of eight founder mice strains to achieve maximum genetic recombination, producing genetically and phenotypically distinct CC strains.[3] Variable gene expression in CC mice contributes to variation in their observed phenotypes.[4,5]

Theiler's murine encephalomyelitis virus (TMEV) causes neurological outcomes in mice analogous to human neurological disease outcomes. Individual CC strains show variable neurological disease responses to TMEV infection based on the strain's genetic background.[6] During the acute phase of TMEV infection, sudden onset neurological deficits can be measured; however, neurological deficits during the chronic phase of TMEV infection in mice are significant because neurological diseases in humans often develop long after their initial viral infection. Further classification of diverse neurological responses to a single virus based on host genetic background gives insight into why people with the same neurological condition suffer a wide range of responses from mild, transient symptoms to life-altering or fatal illness. The CC mouse model has previously been used to study diverse neurological responses with variable host genetic backgrounds for diseases such as SARS-CoV, influenza, Ebola, and West Nile virus.[7] Although this study investigated neurological disease pathologies in mice, parallels can be drawn to the wide range of disease response observed in humans to other neurological symptoms resulting from viral infections, such as the SARS-CoV-2 disease (COVID-19).

...PEOPLE WITH THE SAME NEUROLOGICAL CONDITION SUFFER A WIDE RANGE OF RESPONSES FROM MILD, TRANSIENT SYMPTOMS TO LIFE-ALTERING OR FATAL ILLNESS.

The purpose of the present work is to develop comprehensive phenotypic and histological profiles for genetically distinct mice based on neurological disease outcomes to TMEV infection. Analyzing diverse phenotypic outcomes, brain lesion locations, and cytokine expression levels can help characterize TMEV disease mechanisms and may ultimately improve neurological disease models for human conditions such as Parkinson's disease, MS, epilepsy, and ALS.

METHODS

To examine phenotypic and histological outcomes in mice with distinct genetic profiles, CC mice were examined at various time points throughout the infection period. **Figure 1** shows the comprehensive experimental timeline for CC mice with TMEV infection. Non-infected CC mice were also studied throughout the infection period to serve as experimental controls.

GENETIC DIVERSITY IN CC STRAINS RESULTED IN VARIABLE PHENOTYPIC OUTCOMES AND CNS LESIONS FOLLOWING TMEV INFECTION.

Mice were infected with TMEV at four weeks old, marking the 0-days post-infection (dpi) time point. Critical time points in the experimental timeline were 14- and 90-dpi, representing the ends of the acute and chronic phases of infection, respectively. Qualitative phenotyping was performed twice daily during the acute infection phase and once weekly during the chronic infection phase to evaluate observable disease characteristics. Weights were also recorded during qualitative phenotyping. The second row of **Figure 2** shows the neurological disease characteristics documented in qualitative phenotyping. Although **Figure 2** only displays up to 3-dpi, qualitative phenotyping was recorded twice daily until 14-dpi and then once weekly until 90-dpi.

After weighing, CC mice were placed on a flat surface to look for neurological deficits such as hunched posture, seizures, backing up, circling, encephalitis, ruffled fur, and stiff/spastic tail. Reflex deficiencies were tested in each mouse by measuring reaction times turning from a supine position back onto their paws. CC mice were then placed onto a metal grate as depicted in **Figure 3**. The metal grate was rotated 180° to test the mouse's ability to grip and move around a grate while hanging underneath it, as shown in **Figure 4**. Most notably, the grate helped identify limb weakness, indicated by the mouse's difficulty with or inability to grip the metal grate. Each of the neurological disease symptoms displayed in **Figure 2** were evaluated based on their presence or absence, but several symptoms were evaluated based on their severity, including limb weakness, limb paralysis, reflex deficiency, and seizure.

In addition to qualitative phenotyping, three established quantitative behavioral assays were used to evaluate motor function in mice: 1) Rotarod Assessment, 2) DigiGait Imaging, and 3) open-field test. These behavior assays were performed at three points throughout the experimental period: pre-infection, 21-, and 90-dpi, as indicated by asterisks in **Figure 1**. Motor evaluations helped understand disease progression in TMEV-infected mice.

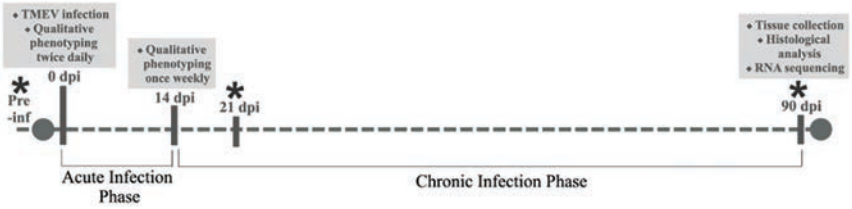

Figure 1. *TMEV infection experimental timeline. Quantitative phenotyping behavioral assay time points are indicated by *.*

The Rotarod Assessment detects motor defects by measuring a mouse's motor coordination, balance, strength, and endurance.[8] **Figure 5** shows the Rotarod experimental setup. The rotating rod divided into isolat-

Animal ID:

Date	Days Post-Infection	AM/PM	Seizure	Reflex Deficiency	Hunched Posture	Backing Up on Ground	Circling on Ground	Circling on Grate	Clonus (Limb Clasping)	Encephalitis	Twirling When Held by Tail	Ruffled Fur	Stiff/Spastic Tail	Limb Weakness on Grate				Limb Paralysis			
														Right Hind Limb	Left Hind Limb	Right Fore Limb	Left Fore Limb	Right Hind Limb	Left Hind Limb	Right Fore Limb	Left Fore Limb
	Pre-infection																				
	1dpi	AM																			
	1dpi	PM																			
	2dpi	AM																			
	2dpi	PM																			
	3dpi	AM																			
	3dpi	PM																			

Figure 2. *Qualitative phenotyping data collection form used twice daily to record neurological disease characteristics.*

Figure 3 and 4. *Qualitative phenotyping method to identify limb weakness.*

ed segments allowed for up to five mice to be tested at a time. Small ridges allowed the mice to grip the rod effectively as it rotated. The rod rotated at 4 rotations/minute initially and increased by 4 rotations/minute every thirty seconds. CC mice were kept on the rod for a maximum of five minutes. Inability to stay on the Rotarod for five minutes indicated neurological deficits such as hindlimb weakness and paralysis, hunch, or loss of motor coordination. Paper towels were placed beneath each segment to cushion CC mice if they were unable to stay on the Rotarod for the full five minutes. The trial was repeated three times for each mouse with a fifteen-minute rest period between each trial.

DigiGait Imaging was used to determine peripheral nerve and spinal cord injury in TMEV mice by measuring the length and width of limb stride.[10] The DigiGait Imaging system (**Figure 6**) used a ventral

Figure 6. *DigiGait Imaging experimental setup.*

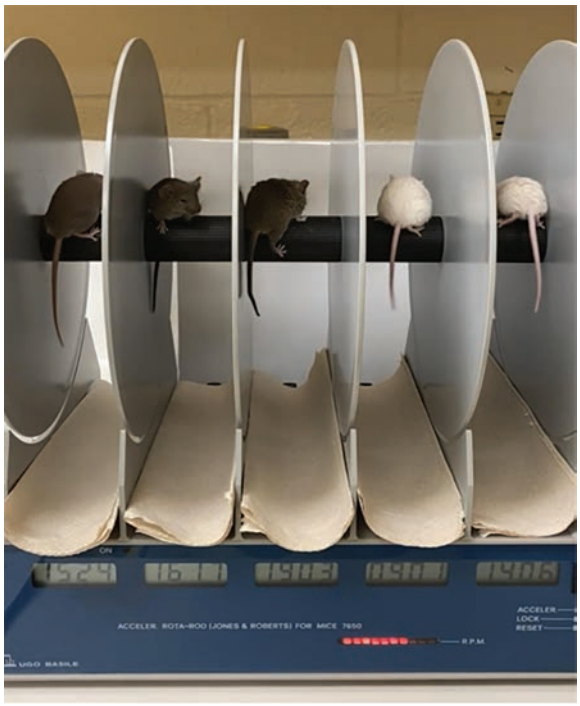

Figure 5. *Rotarod Assessment experimental setup.*

plane camera to record gait patterns. The plantar surface of each paw was painted with a red washable marker to make paw placement easy to detect. At a treadmill belt speed of 15 cm/s, each mouse's gait was recorded until five consistent, consecutive steps of each paw could be isolated from the DigiGait Imaging video.

The open-field test assesses rodents' natural avoidance of unprotected, open areas; exposure often induces anxiety and measurable behavioral patterns.[11] The open-field arena (**Figure 7**) had four overhead lamps, illuminating eight empty 10 cm by 10 cm enclosed experimental boxes with 25-cm-high walls. As shown in **Figure 8**, a dorsal plane camera recorded the movement of each mouse in a silent room lit only by the overhead lamps over a thirty-minute experimental period.

At the end of the chronic infection phase, tissue samples were obtained from the hippocampus, cerebellum, spinal cord, heart, and spleen of each CC mouse for histological analysis and RNA sequencing. To determine if similar lesion burdens existed within distinct CC strains, central nervous system (CNS) lesion location and frequency were analyzed in addition to

Figure 7. *Open-field experimental setup.*

Figure 8. *Open-field experimental trial.*

qualitative and quantitative phenotyping results. RNA extraction techniques isolated RNA from each tissue sample to investigate which genes were active in each specialized cell type. RNA sequencing measured gene expression in each tissue sample.

RESULTS

The most immediate difference between CC strains was daily weight change. During the acute phase of infection, non-infected mice naturally weighed more in the morning and steadily gained weight as they grew over time. TMEV-infected CC mice exhibited various weight differences from 0- to 14-dpi including minor weight loss, significant weight loss, or steady weight gain mirroring non-infected CC mice weight patterns. Interestingly, some strains showed an observable difference in weight change between males and females.

...SPECIFIC HUMAN GENETIC VARIANTS CAN MAKE SOME PEOPLE MORE SUSCEPTIBLE THAN OTHERS TO NEUROLOGICAL DISEASES LATER IN LIFE.

Qualitative phenotypic profiles of distinct CC strains are displayed in **Figure 9** with neurological disease outcomes represented as a percentage of the total deficit. **Figure 9** includes TMEV-infected CC strains that developed significant neurological conditions; however, several TMEV-infected CC mice showed qualitative phenotyping profiles analogous to profiles for non-infected CC mice of the respective strain.

Specific phenotypic outcomes were observed more frequently in certain TMEV-infected CC strains. Ruffled fur, circling while hanging underneath the metal grate, and clonus (limb clasping) were common in certain strains but did not always result from TMEV infection. Seizures, paralysis, and encephalitis were never observed in non-infected CC mice. Limb paralysis was always a result of TMEV infection, often affecting a mouse's hindlimbs earlier and more severely than the mouse's forelimbs. Significant limb paralysis was observed in CC023 and CC078 mice. The overall

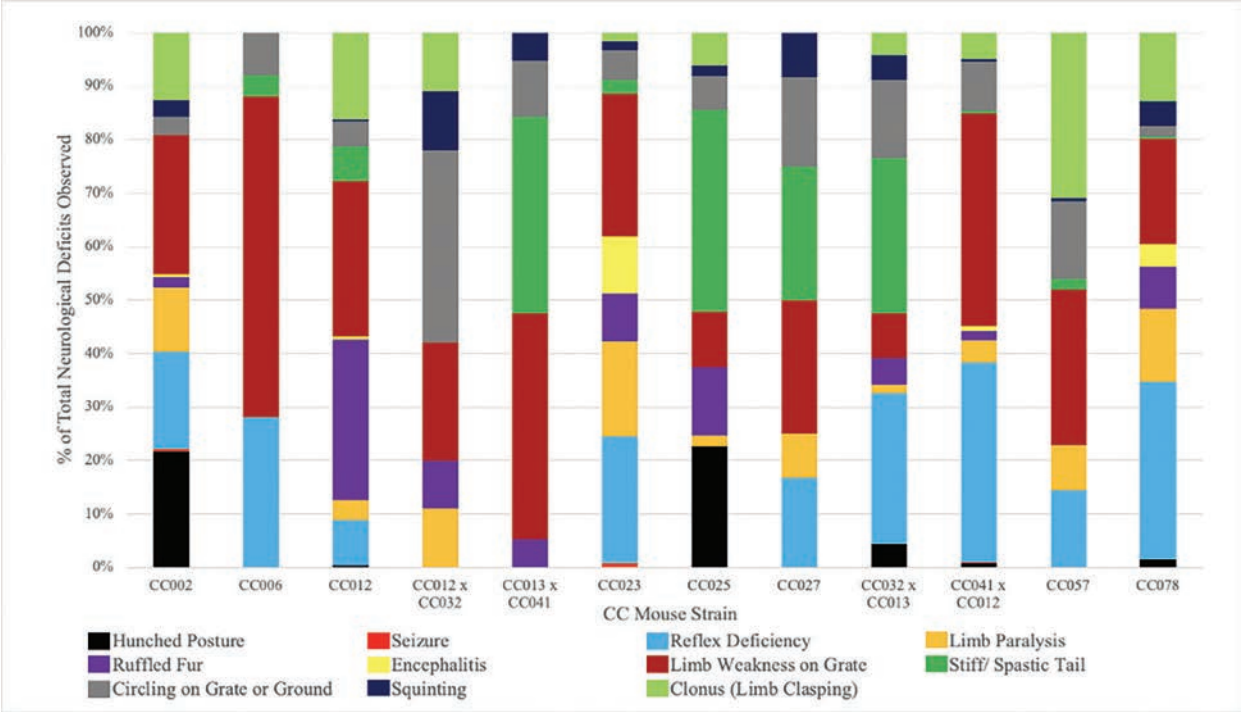

Figure 9. *Qualitative phenotypic frequencies as a percentage of total neurological deficits observed in distinct CC strains.*

progression of phenotypic outcomes was measured during the chronic infection phase; CC078 and CC023 phenotypic frequencies worsened between 14- and 90-dpi, but CC002 and CC025 phenotypic frequencies improved between 14- and 90-dpi.

Typically, TMEV-infected CC mice with severe hunch and hindlimb paralysis were unable to stay on the Rotarod for more than a few seconds. Less severely affected mice could stay on the Rotarod for longer, but often fell off before the five-minute period due to decreased strength and endurance. However, results with the Rotarod Assessment behavioral assay were not always related to neurological disease outcomes; some mice jumped off the Rotarod before the five-minute period. The pre-infection motor evaluation time point often helped train the mice to stay on the Rotarod to achieve accurate experimental results during the 21- and 90-dpi time points.

While DigiGait analysis showed differences between strains and sexes at the pre-infection time point, DigiGait imaging profiles varied over the infection period for both strain and sex. Several CC strains had wider steps and a longer gait, while others unevenly distributed their weight between each paw. Foot and leg paralysis could also be evident in DigiGait analysis. In severely affected CC mice, gait deficit severity increased between the motor evaluation time-points. The footprints of non-infected CC mice showed the mouse's toes fanned out from the center of the foot, but severely TMEV-infected CC mice with foot paralysis had clenched or limp toes during DigiGait trials. Severe leg and foot paralysis were evident when CC mice were unable to walk at the treadmill belt speed of 15 cm/s, which prevented recording of gait pattern.

Brain and spinal cord lesion locations were analyzed to determine if there was an association between brain lesion sites and outward phenotypic characteristics observed in distinct strains. CNS lesion burden profiles of CC mice are displayed in **Figure 10**. Lesion locations varied significantly between strains. Notable differences were found between males and females of certain TMEV-infected CC strains. The most common lesion burden across all CC mice was in the hippocampus and thalamus; however, CC012xCC032 females, CC013xCC041 females, all CC032xCC013 mice, and CC041xCC012 males did not have lesion burdens in the hippocampus or thalamus.

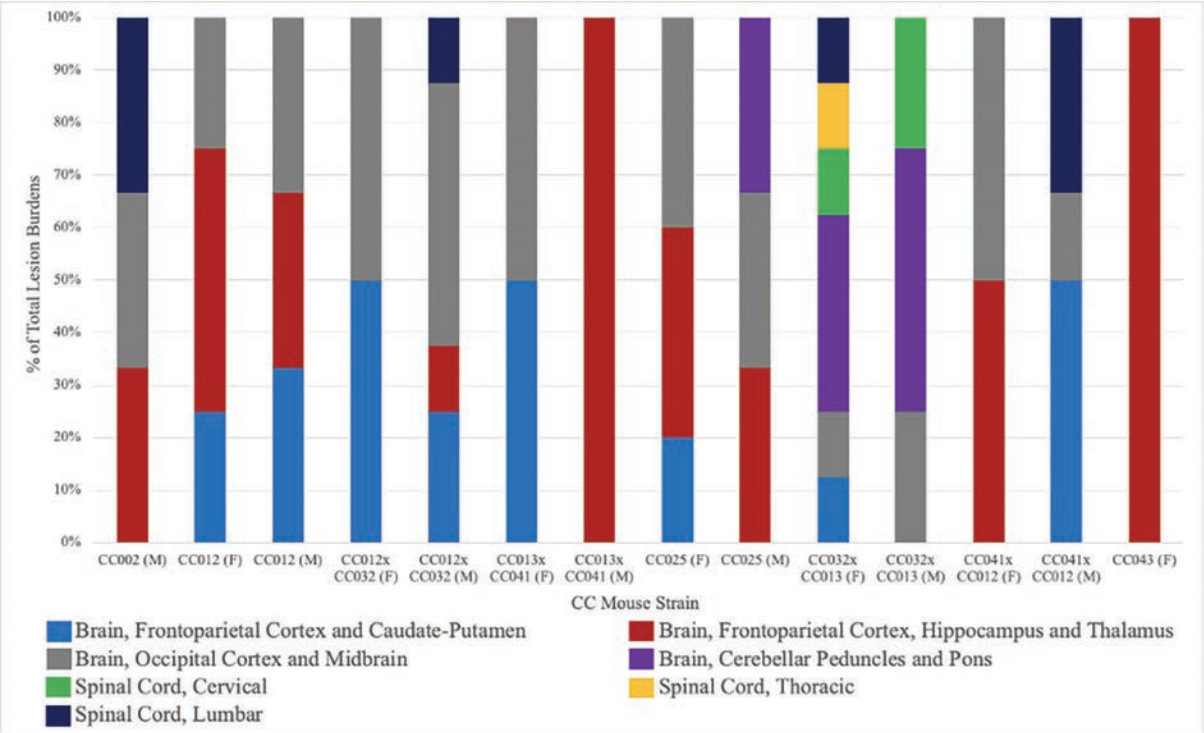

Figure 10. *Brain and spinal cord lesions as a percentage of total lesion burdens for distinct CC strains and sexes. Females are indicated by (F), and males are indicated by (M).*

Genetic diversity in CC strains resulted in variable phenotypic outcomes and CNS lesions following TMEV infection. Similar neurological disease profiles could suggest shared genetic loci or mechanisms between strains. A consistent cytokine protein expression level was not found for mice with most neurological disease outcomes. Open-field test results, cytokine level profiling, and further histological analysis during the chronic infection period continue to be investigated.

DISCUSSION

It was found that TMEV infection in genetically diverse CC mice results in a variety of phenotypic differences and CNS lesions. Common phenotypic and histological profiles could be indicative of shared viral mechanisms between strains, suggesting that the presence of specific human genetic variants can make some people more susceptible than others to neurological diseases later in life.

Cytokine level profiling is currently being investigated in relation to specific disease phenotypes. Measuring relative cytokine expression will determine if there is a relationship between cell protein signaling levels and similar phenotypic outcomes. Continuing to map out CNS lesion locations and frequencies will investigate the correlation between specific phenotypic outcomes and CNS lesions. Inducing further genetic variation by crossing more CC parent strains will explore if mice of a specific parental sex contribute to phenotypic outcomes in the offspring. Cohorts of 4- and 14-dpi CC mice are in progress to evaluate initial viral effects on distinct strains. The differences in phenotypic outcomes and CNS lesions between male and female mice continues to be investigated. Analysis of the viral load at 90-dpi will see if there is a difference between the CNS- and systemic-viral load. Identification of quantitative trait loci will hopefully indicate regions of the genome harboring genes associated with the phenotypic traits.

This study further developed phenotypic and histological profiles for genetically distinct mice based on neurological disease outcomes to TMEV infection. Investigation of TMEV disease mechanisms aims to explain the wide range of virally induced disease outcomes in humans with neurological conditions such as Parkinson's disease, MS, epilepsy, and ALS.

ACKNOWLEDGMENTS

I would like to thank Dr. Candice Brinkmeyer-Langford for encouraging me to accomplish my goals and including me in her research team through the Veterinary Integrative Biosciences Department at Texas A&M University for the past two years. I would also like to thank Koedi Lawley, Aracely Perez, and Katia Amstalden for always being willing to teach me and allowing me to follow my passion for working with mice within our research. This project is funded by DHHS-NIH-National Institute of Neurological Disorders and Stroke (NIH NINDS R01 NS103934-01 [PI: Brinkmeyer-Langford]).

REFERENCES

1. C. L. Brinkmeyer-Langford et al., "Host genetic background influences diverse neurological responses to viral infection in mice," Scientific Reports 7, no. 1 (2017): 1–17, **https://doi.org/10.1038/s41598-017-12477-2**.
2. Brinkmeyer-Langford et al., "Host genetic background," 1–17.
3. D. W. Threadgill, D. R. Miller, G. A. Churchill, F. P.M. de Villena, "The Collaborative Cross: A Recombinant Inbred Mouse Population for the Systems Genetic Era," ILAR Journal 52, no. 1 (2011): 24–31, **https://doi.org/10.1093/ilar.52.1.24**.
4. Brinkmeyer-Langford et al., "Host genetic background," 1–17.
5. R. Eldridge et al., "Antecedent presentation of neurological phenotypes in the Collaborative Cross reveals four classes with complex sex-dependencies," Scientific Reports 10, no. 1 (2020): 1–13, **https://doi.org/10.1038/s41598-020-64862-z**.
6. Eldridge et al., "Antecedent presentation of neurological phenotypes," 1–13.
7. Brinkmeyer-Langford et al., "Host genetic background," 1–17.
8. D. B. McGavern, L. Zoecklein, K. M. Drescher, M. Rodriguez, "Quantitative Assessment of Neurologic Deficits in a Chronic Progressive Murine Model of CNS Demyelination," Experimental Neurology 158, no. 1 (1999): 171–81, **https://doi.org/10.1006/exnr.1999.7082**.
9. R. M.J. Deacon, "Measuring Motor Coordination in Mice," Journal of Visualized Experiments, no. 75 (2013): e2609, **https://doi.org/10.3791/2609**.
10. D. B. McGavern, L. Zoecklein, S. Sathornsumetee, M. Rodriguez, "Assessment of hindlimb gait as a powerful indicator of axonal loss in a murine model of progressive CNS demyelination," Brain Research 877, no. 2 (2000): 396–400, **https://doi.org/10.1016/S0006-8993(00)02710-4**.
11. V. Carola, F. D'Olimpio, E. Brunamonti, F. Mangia, P. Renzi, "Evaluation of the elevated plus-maze and open-field tests for the assessment of anxiety-related behaviour in inbred mice," Behavioral Brain Research 134, no. 1–2, (2002): 49–57, **https://doi.org/10.1016/S0166-4328(01)00452-1**.

AUTHOR BIO

MADILYN FEIK '21

Madilyn Feik '21 is a biomedical sciences major with a neuroscience minor, public health minor, and biomedical research certificate from Houston, Texas. Her left brain and right brain get along well; she has enjoyed combining her passions for writing, neuroscience, and animal model optimization in her two undergraduate research projects. After graduating, Madilyn plans to earn her Doctor of Medicine degree and prioritize research while working in the medical field.

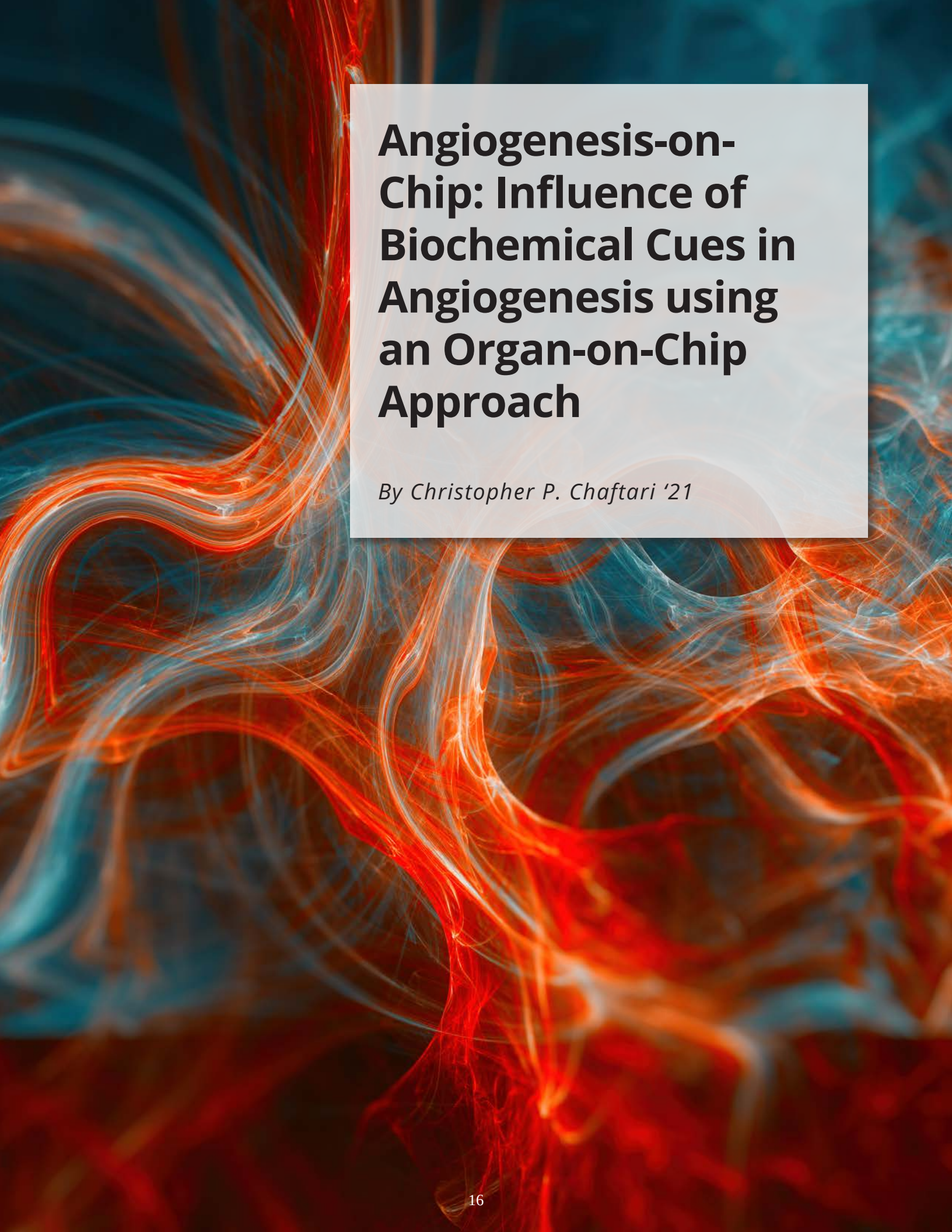

Angiogenesis-on-Chip: Influence of Biochemical Cues in Angiogenesis using an Organ-on-Chip Approach

By Christopher P. Chaftari '21

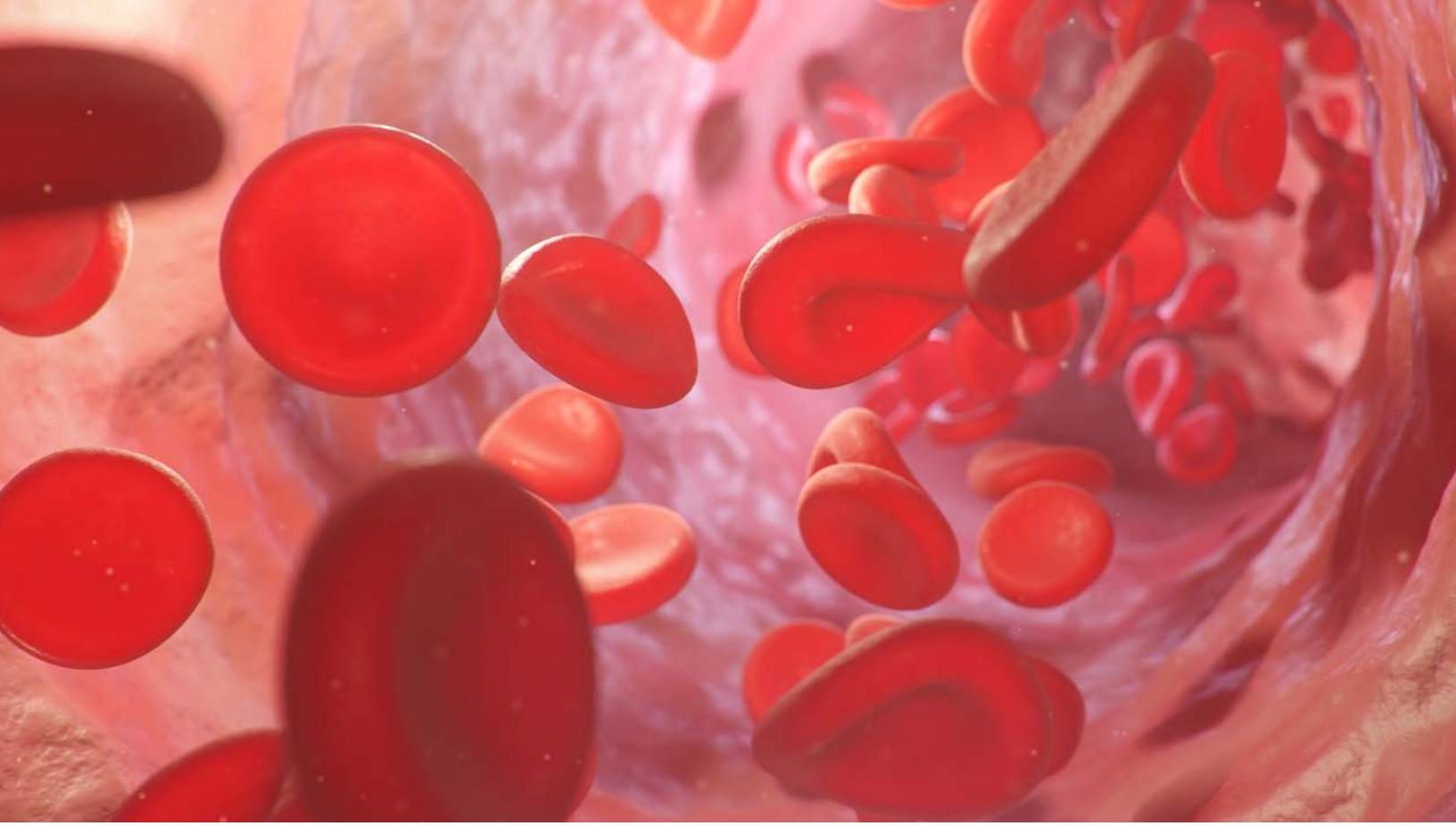

INTRODUCTION

Microfluidic organs-on-a-chip, or microphysiological systems, are contemporary devices used to recreate healthy or pathological human-specific tissue microenvironments. One such process is angiogenesis, where a parent blood vessel made of individual endothelial cells (ECs) sprouts into new daughter blood vessels. Angiogenesis occurs in many biological processes, including during inflammation, wound repair, and growth of tumors.[1] Studying angiogenesis allows scientists to better understand how these processes occur and how to better treat them. At the cellular level, angiogenesis requires individual endothelial cells of a blood vessel to receive a pro-angiogenic stimulus, migrate toward that stimulus, proliferate, and form a cylindrical tube.[2] These three events are commonly referred to as tip cell selection and migration, stalk cell proliferation, and tube maturation, respectively.[3]

Angiogenesis can be induced on chip devices by adding biochemical cues that stimulate angiogenesis in endothelial cells. Additionally, these biochemical cues have varied roles and differing effects on the various stages of angiogenesis (**Table 1**). In the literature, angiogenesis chips are regularly reported, but culturing conditions widely vary because no standard protocol or quantification method exists.[4,5] Additionally, many reports misclassify endothelial cell sprouting as angiogenesis, whereas in physiology, angiogenesis also requires the final two stages of angiogenesis (endothelial cell proliferation and final maturation to cylindrical tubes). Due to the many outcomes that are possible with the plethora of biochemical cues and cell lines currently available, the standard culturing protocols for angiogenesis-chips are missing. By developing a standard for angiogenesis-on-a-chip, the findings of

STUDYING ANGIOGENESIS ALLOWS SCIENTISTS TO BETTER UNDERSTAND HOW THESE PROCESSES OCCUR AND HOW TO BETTER TREAT THEM.

future studies will be more accurate and reflective of angiogenesis due to the implementation of these standards.

To address these gaps, this study was aimed at identifying several cocktails of biochemical cues to set a standard for angiogenesis, which can readily be replicated and used for other scientific applications. The study first investigated the basic building blocks of angiogenesis: endothelial cells and biochemical cues. Using tri-channel microfluidic devices (**Figure 1**), parent vessels were seeded in a fluidic channel adjacent to a hydrogel that acts as a scaffold for angiogenic sprouts. In a third channel situated on the other side of the hydrogel, previously identified critical growth factors were supplied to one or all the events of angiogenesis: endothelial cell migration, proliferation, and tube maturation. The makeup and potency of the growth factor cocktails was analyzed to determine basal angiogenesis conditions, as well as cocktails that improve quantifiable sprout metrics such as maximum sprout length and average sprout diameter. With these results, standard culturing conditions were established and a quantification pipeline was introduced that can be adopted by other research groups.

Table 1. *Roles of Biochemical Cues in Angiogenesis.*

Category	*Growth Factor*	*Role in Angiogenesis*
Tip Cell Migration	VEGF	Motility, tip cell selection
	S1P	Motility, upregulate matrix metalloproteinase (MMP) secretion
	HGF	Motility
	MCP-1	Signaling, activation, MMP secretion
Stalk Cell Proliferation	VEGF	Mitogen, tube morphogenesis
	PMA	Mitogen, enhances other growth factor effects
	HGF	Mitogen, tube morphogenesis, branching
	bFGF	Mitogen, tube morphogenesis
Tube Maturation	VEGF	EC maintenance
	S1P	Tight junction formation, vascular maintenance

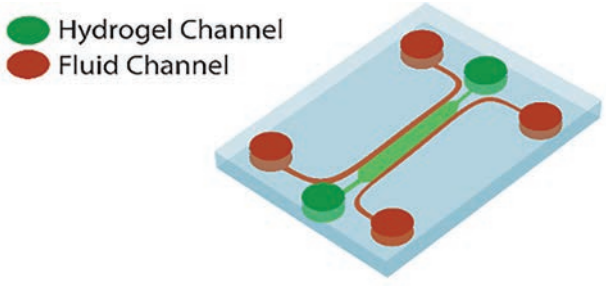

Figure 1. *Diagram of a tri-channel microfluidic device used in these experiments.*

METHODS

Microfluidic Device Fabrication

Three-channeled microfluidic chips were used to analyze the effects of various growth factor cocktails (GFCs). These microfluidic chips were made of polydimethylsiloxane (PDMS). To fabricate the chips, a 10:1 PDMS base to curing agent mixture was made. This concentration allows for the optimization of mechanical properties for fluid flow and cell adhesion to form parent vessels in the device. The mixture was poured onto a silicon wafer master mold with channel features of the device. Next, the PDMS was degassed for 15 minutes and then baked at 70°C for 2 hours to cure. Cured PDMS slabs were peeled off the wafer and inlet and outlet ports were punched using 1 mm and 5 mm biopsy punches. Cut slabs and glass microscope slides were then plasma treated and bonded. Microchannels were then coated with 100 µg/mL poly-D-lysine (PDL) for 6 hours in a humidified chamber at 37°C.[6] PDL facilitates a stronger PDMS-hydrogel bond that prevents cell slippage during culturing. The devices were subsequently washed with 1X phosphate buffer solution (PBS) and put into an oven to dry overnight. The following day, a 2.5 mg/mL fibrin hydrogel was

Table 2. *Composition of growth factor cocktails (GFCs). All growth factors are supplied at a final concentration of 75 ng/mL, excluding S1P, which has a final concentration of 500 nM.*

Cocktail	Growth Factors
Control	N/A
GFC 1	VEGF, S1P, PMA
GFC 2	VEGF, S1P, PMA, bFGF
GFC 3	VEGF, S1P, PMA, HGF
GFC 4	VEGF, S1P, PMA, MCP-1
GFC 5	VEGF, S1P, PMA, HGF, MCP-1
GFC 6	VEGF, S1P, HGF, bFGF, MCP-1
GFC 7	VEGF, S1P, PMA, HGF, bFGF, MCP-1

injected into the middle channel.

Cell Culture

While the devices were being fabricated, human umbilical vein endothelial cells (HUVECs) were cultured from cryopreservation. Endothelial Basal Medium was supplemented with Growth Medium-2 (EGM-2) packs. The EGM-2 allows for cell proliferation and growth. Once cells reached 80% confluence, HUVECs were trypsinized and spun down into a pellet. Trypsin is an enzyme which breaks down the peptide anchors attaching the cells to the surface of the container in which they were being cultured. The pelleted cells were resuspended in fresh EGM-2 at a concentration of 10 million cells/mL and injected into the left-most-channel of the previously fabricated chips. Cells were left at a 90° angle for 30 minutes to allow cells to attach to the side of the hydrogel. After seeding, devices were flushed with fresh medium and left in a humidified chamber at 37°C overnight. The following day, growth factor cocktails (**Table 2**) were injected into the rightmost channel to induce angiogenesis. Daily media changes were performed for the following two days.

Immunofluorescence and Network Quantification

The staining process occurred in three main steps, each of which was followed by a wash with 1X PBS. Devices were first fixed with 4% paraformaldehyde for 30 min at room temperature and washed. Fixing halts cellular decomposition and keeps cellular components in place. Then, the devices were permeabilized with 0.1 % Triton X-100 in 1X PBS for 30 min at room temperature and washed again. Permeabilization is required to allow for the staining compounds to enter the cells. Next, the devices were stained with rhodamine phalloidin (1:100) and Hoechst (1:2000) in 3 % BSA in 1X PBS for one hour at room temperature. Rhodamine phalloidin stains F-actin in the cell, which is a common protein found in the cell membrane. Hoechst stains DNA found in the nucleus. Stained devices were then imaged under a microscope by collecting tiled Z-stacks, which were then orthogonally projected to render a 2D image from the 3D data. Images were analyzed using REAVER, a previously standardized MATLAB GUI, which quantifies the total vascularized area, total vascularized length, mean sprout length, mean sprout diameter, and maximum sprout length.[7] To compare the various groups to each other, Principal Component Analysis (PCA) was used to reduce the dimensionality of the data, resulting in two principal component scores (PC 1 and PC 2); these explain at least 80% of the variance of the data. PC 1 scores, which explain the most variance, were normalized and represented as the vas-

ADDITIONALLY, THIS PROJECT FOUND THAT INCREASING THE CONCENTRATION OF BIOCHEMICAL CUES DOES NOT HAVE A SIGNIFICANT EFFECT ON ANGIOGENESIS...

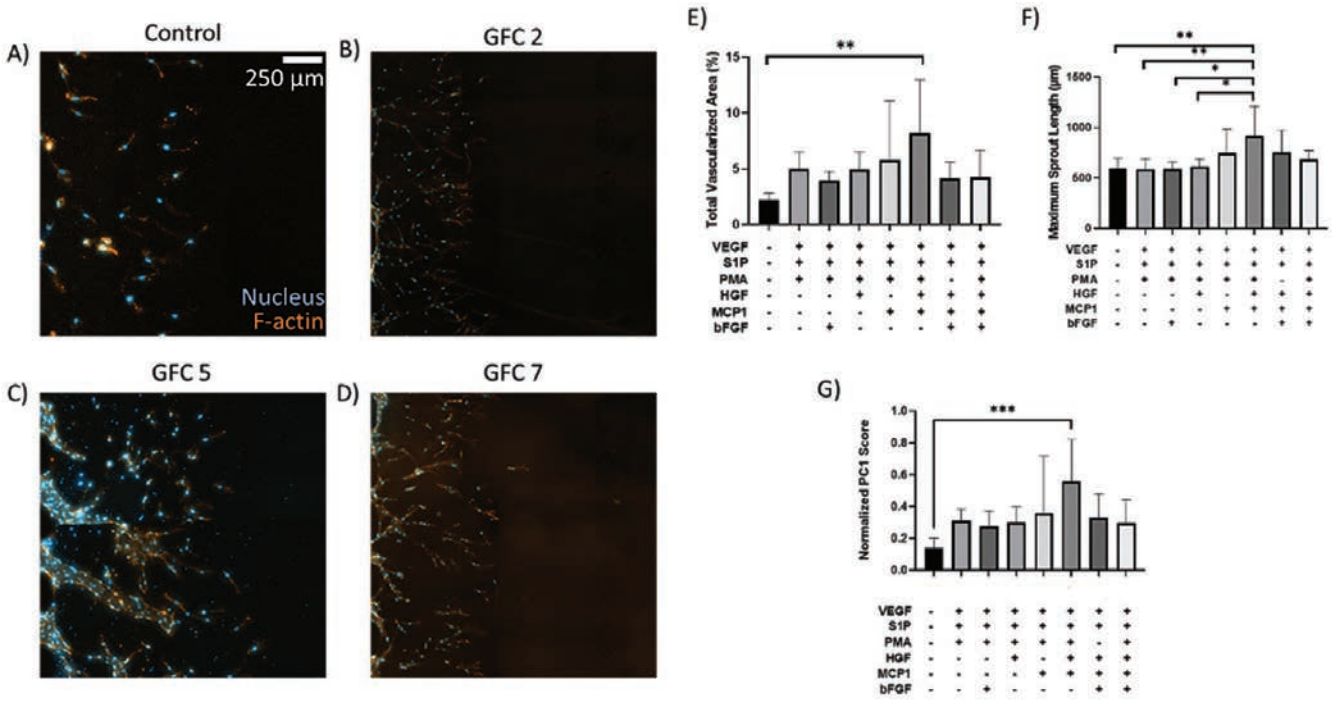

Figure 2. *Representative and quantitative results of angiogenesis-chips. A-D) Immunofluorescence images of angiogenesis-chips showing qualitative differences in sprout length, average sprout diameter, and total vascularized area. A) Control; B) GFC 2; C) GFC 5; D) GFC 7. E-G) Quantification of angiogenesis-chips. E) Total vascularized area; F) maximum sprout length, and; G) PC 1 score.*

cularization index that describes an optimized vascular network.[8] For all results, data is represented as mean ± the standard deviation, and one-way ANOVA was used to compare all the groups to each other.

RESULTS

In this project, the composition and concentration of biochemical cues were analyzed. Quantification of immunofluorescence images showed that the composition of biochemical cues can be a significant contributor in angiogenesis (**Figure 2**). First, controls, which had culturing medium without supplemental growth factors (containing 5 ng/mL VEGF and bFGF for EC maintenance and proliferation), show that some tip cells migrate into the hydrogel (**Figure 2A**). Because there are no additional cells following the tip cells, it appears that stalk cell proliferation does not occur, thus showing that angiogenesis is not faithfully recreated on-chip without growth factor supplementation. When we increased the concentration of VEGF and bFGF to 75 ng/mL and added 75 ng/mL PMA and 500 nM S1P, tip cells migrated followed by a thin trail of stalk cells, yet tube morphogenesis is not seen. When adding HGF instead of bFGF, which are two factors responsible for tube morphogenesis (**Table 1**), there is no significant differences in angiogenic sprouting. However, when adding monocyte chemotactic protein-1 (MCP-1) to this cocktail, wide sprouts yield a high vascularized area (**Figure 2C**). However, when adding all factors together (**Figure 2D**), the vascularization is decreased, possibly due to overstimulation.

When quantifying the images of each angiogenesis-chip after a 3-day culture with the GFCs, we saw that only GFC 5 had a significant difference compared to the culture in total vascularized area (**Figure 2E**) and PC 1 score (**Figure 2G**). We used these metrics as a vascularization index that linearly combines all quantified metrics into a dimensionless unit. GFC 5 has a significant difference between the control and three of the other six GFCs when quantifying maximum sprout length (**Figure 2F**). Because the key difference between GFC 5 and the other cocktails is the use of MCP-

1 instead of bFGF for tube morphogenesis without overloading the system, we theorize that MCP-1 plays a significant role in angiogenesis on-chip. This is also noted in literature, which suggests that MCP-1 induced angiogenesis is mediated by MCP-1 induced protein (MCPIP) and plays a key role in tube formation.[9]

Based on the results in **Figure 2,** the three-best performing GFCs (4, 5, and 6) were selected as possible standard cocktails for on-chip angiogenesis and doubled the concentrations of the biochemical cues in them to investigate if increasing the concentration affects angiogenesis. As shown in **Figure 3**, increasing the concentrations of biochemical cues does not seem to affect the scoring of angiogenesis within the same GFC. Figures 3G-J do not indicate any significant differences in angiogenesis between different concentrations of the same GFCs. This suggests that GFC composition is more important for angiogenesis than concentration of biochemical cues within the GFC. In addition, as seen in the 2x images (**Figure 2**), increasing the concentration may overstimulate the migrating tip cell, causing the migration rate to exceed tube formation and maturation rates. This inequality in rate might result in suboptimal angiogenesis as the networks are not fully perfusable because the ECs are not connected to each other.[10]

CONCLUSION

The purpose of this project was to determine basal angiogenesis conditions, establish standard culturing procedures, and introduce a scoring method to quantify angiogenesis in chip devices. This is important because there is no current standard for modelling and quantifying angiogenesis, thus limiting the use of angiogenesis-chips in drug toxicity and efficacy evaluation as well as healthy and pathological tissue modeling. In this project, we identified several key biochemical cues which are essential to inducing angiogenesis in chip devices. Furthermore, we identified three potential

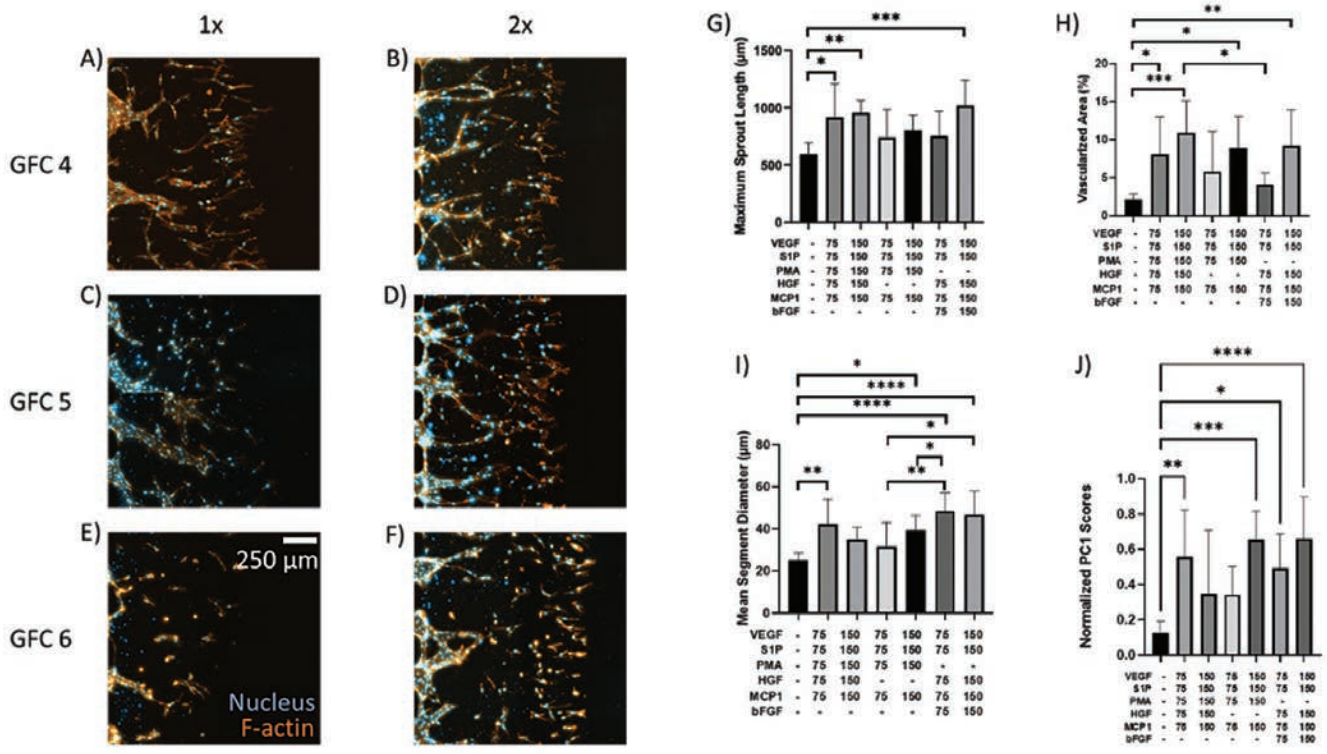

Figure 3. *Immunofluorescence images and quantification of angiogenesis-chips with 1X and 2X concentration of GFCs. A-F) immunofluorescence images A) GFC 4 at 1X concentration; B) GFC 4 at 2X concentration; C) GFC 5 at 1X concentration; D) GFC 5 at 2X concentration; E) GFC 6 at 1X concentration, and; F) GFC 6 at 2X concentration. G-J) Quantified results comparing each of the six immunofluorescence results. G) maximum sprout length; H) total vascularized area; I) mean segment diameter. Results from G-J were used to develop a normalized PC 1 score to compare overall vascular network quality between all groups and a control.*

WE IDENTIFIED THREE POTENTIAL COMBINATIONS OF BIOCHEMICAL CUES WHICH COULD BE USED AS STANDARDS FOR ANGIOGENESIS.

combinations of biochemical cues which could be used as standards for angiogenesis. Also, we presented how PCA can be used as a possible quantitative method to score angiogenesis and standardize angiogenesis across research studies. By using PCA, we can combine multiple variables to reduce dimensionality as opposed to presenting single network metrics and better analyze the overall quality of the angiogenic sprouts.

Additionally, this project found that increasing the concentration of biochemical cues does not have a significant effect on angiogenesis when compared to a 1X concentration. This can be an important consideration for projects limited by material availability. In fact, higher concentrations may overload the biological system and lead to suboptimal angiogenesis due to unequal rates of tube formation, cell migration and tube cell maturation. Increasing the concentrations of biochemical cues caused the tip cell migration to occur much faster than the stalk cells proliferated, resulting in the separation of tip and stalk cells and the elimination of stalk cells' guide to angiogenic factors. Therefore, it is important to use a concentration which precisely induces angiogenesis without overwhelming the biological system.

In conclusion, the findings of this project can be implemented into future studies mimicking biological environments, which include microphysiological systems and microfluidic technology. Since organs and tissues are usually highly vascularized in vivo, incorporating a perfusable endothelium into a model will yield better biomimetic results in future experiments and will lead to significant advances in types of studies which can implement organ-on-a-chip technology.[11] Additionally, pathological tissue models such as cancer-on-a-chip require angiogenesis to mimic how a tumor supports itself and subsequent metastasis. Besides the GFC makeup and potency, the scoring standard for microvascular self-assembly developed can be implemented in further studies, which require microvascular networks to have a complete model.

ACKNOWLEDGMENTS

I would like to acknowledge my faculty advisor, Dr. Abhishek Jain, and my Ph.D. student mentor, Jim Tronolone, for their guidance and mentorship in the research project. I would also like to thank the other members in the Bioinspired Translational Microsystems Laboratory research lab and my family for their continuous support along the way.

REFERENCES

1. L. J. Chen and H. Kaji, "Modeling angiogenesis with micro- and nanotechnology," Lab Chip 17, no. 24 (2017): 4186–219. **https://doi.org/10.1039/c7lc00774d**.

2. W. Y. Wang et al., "Functional angiogenesis requires microenvironmental cues balancing endothelial cell migration and proliferation," Lab Chip 20, no. 6 (2020): 1153–66. **https://doi.org/10.1039/c9lc01170f**.

3. Wang et al., "Functional angiogenesis," 1153–66.

4. D. H. Nguyen et al., "Biomimetic model to reconstitute angiogenic sprouting morphogenesis in vitro," Proceedings of the National Academy of Sciences 110, no. 17 (2013): 6712–7. **https://doi.org/10.1073/pnas.1221526110**.

5. G. S. Jeong et al., "Sprouting angiogenesis under a chemical gradient regulated by interactions with an endothelial monolayer in a microfluidic platform," Analytical Chemistry 83, no. 22 (2011): 8454–9. **https://doi.org/10.1021/ac202170e**.

6. S. Chung et al., "Surface-treatment-induced

three-dimensional capillary morphogenesis in a microfluidic platform," Advanced Materials 21, no. 47 (2009): 4863–7. https://doi.org/10.1002/adma.200901727. **https://www.ncbi.nlm.nih.gov/pubmed/21049511**.

7. B. A. Corliss et al., "REAVER: A program for improved analysis of high-resolution vascular network images," Microcirculation 27, no. 5 (2020): e12618. **https://doi.org/10.1111/micc.12618**.

8. J. Lam et al., "Functional Profiling of Chondrogenically Induced Multipotent Stromal Cell Aggregates Reveals Transcriptomic and Emergent Morphological Phenotypes Predictive of Differentiation Capacity," Stem Cells Translational Medicine 7, no. 9 (2018): 664–75. **https://doi.org/10.1002/sctm.18-0065**.

9. J. Niu et al., "Monocyte chemotactic protein (MCP)-1 promotes angiogenesis via a novel transcription factor, MCP-1-induced protein (MCPIP)," Journal of Biological Chemistry 283, no. 21 (2008): 14542–51. **https://doi.org/10.1074/jbc.M802139200**.

10. Wang et al., "Functional angiogenesis," 1153–66.

11. James J. Tronolone and Abhishek Jain, "Engineering New Microvascular Networks On-Chip: Ingredients, Assembly, and Best Practices," Advanced Functional Materials (2021): 2007199. **https://doi.org/10.1002/adfm.202007199**.

AUTHOR BIO

CHRISTOPHER P. CHAFTARI '21

Christopher Chaftari '21 is biomedical engineering major from Bellaire, Texas who went to Strake Jesuit College Preparatory. Christopher has participated in undergraduate research since his sophomore year, studying several topics ranging from deep vein thrombosis to the modeling of angiogenesis in microfluidic devices. Following graduation, Christopher hopes to attend medical school to become a physician.

Investigating the Effects of Arginine and Interferon Tau on Obesity and Non-Alcoholic Fatty Liver Disease in Zucker Diabetic Fatty (ZDF) Rats

By Cristina Caldera Garza ‘23 and Ashton Corporon ‘23

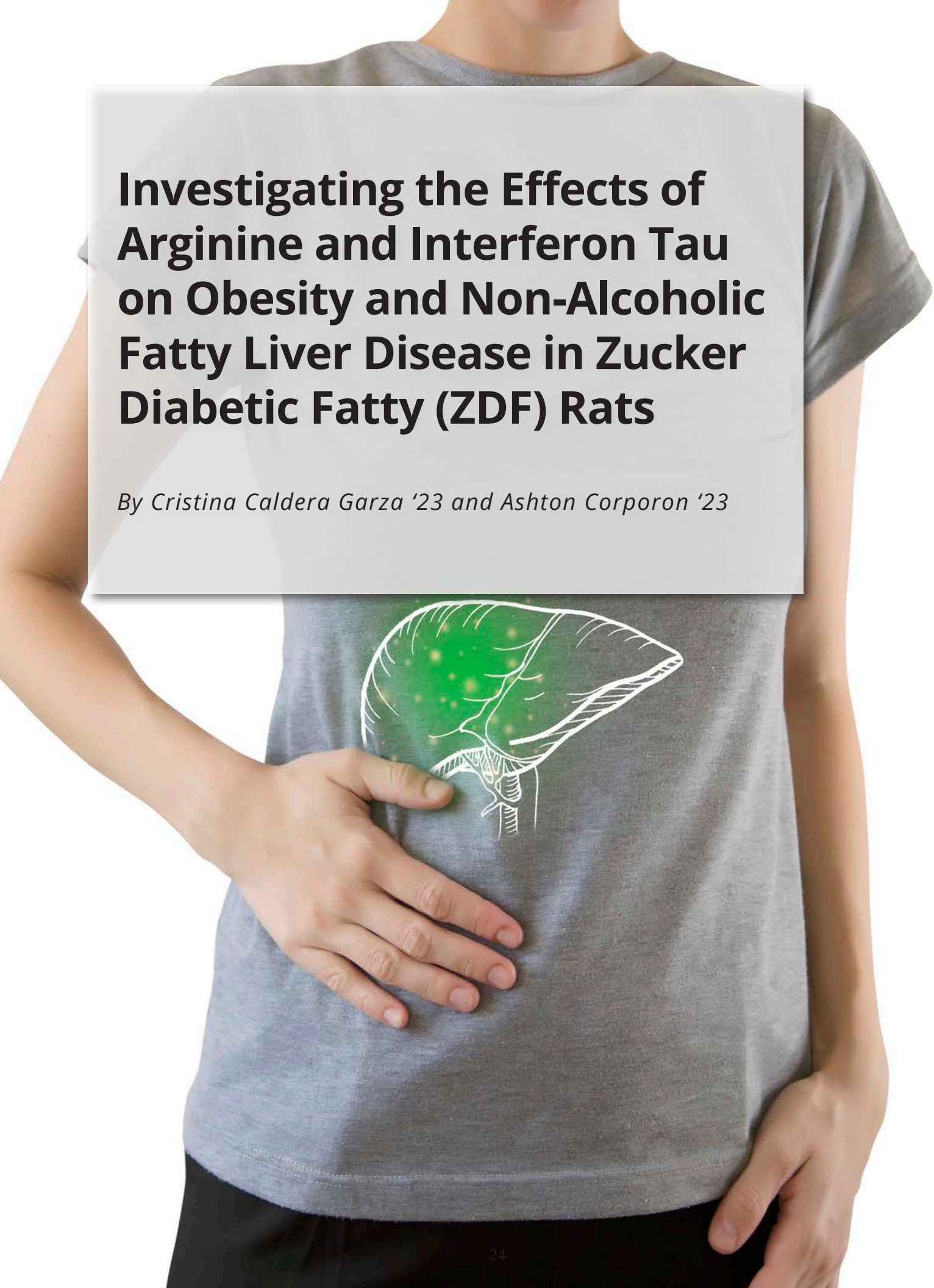

INTRODUCTION

Obesity is a worldwide epidemic. In the US alone an estimated 42.4% of the population is considered obese.[1] Obesity is caused by excess body fat accumulated through disproportionate energy intake as opposed to output. Obesity is associated with an increased risk of developing type II diabetes (T2DM), hypertension, cardiovascular disease, and non-alcoholic fatty liver disease (NAFLD).[2]

NAFLD is a common chronic liver disease affecting 30-40% of men, 15-20% of women, and 70% of men and women with T2DM. NAFLD is a result of excess lipid deposition in the liver that can lead to liver damage and cirrhosis. Factors that can induce NAFLD are T2DM, age, and obesity. There are no current therapies approved for treatment of NAFLD; thus, there is a clear need for investigations into possible treatments.[3]

Arginine (Arg) and interferon tau (IFNT) supplementation are potential therapies for NAFLD and obesity. Arg is a conditionally essential amino acid with great biological importance. It is vital for ammonia detoxification and increased insulin sensitivity, both of which improve liver function.[4] IFNT is a type I interferon that signals pregnancy recognition in ruminants, such as cows and sheep. It has been shown that IFNT can reduce inflammation because of its ability to promote immunological tolerance, meaning that it increases the numbers of anti-inflammatory immune cells.[5] IFNT targets expression of cytokines and adipokines in fatty tissues that are pro-inflammatory, causing IFNT to be anti-inflammatory and giving IFNT the ability to affect expression of specific genes shown to decrease white adipose tissue (WAT), and increase brown adipose tissue (BAT).[6] BAT expends more energy to produce heat whereas WAT stores excess energy

...THERE WERE INTERESTING NUMERICAL DIFFERENCES BETWEEN THE TREATMENT GROUPS AND THE CONTROL GROUP...

as triglycerides. Because BAT consumes more energy than WAT, increasing the amount of BAT and decreasing WAT, decreases body weight to reduce or prevent obesity.[7]

In a previous study by our same lab, IFNT was orally administered to Zucker Diabetic Fatty (ZDF) rats, and measured the effects of onset diabetes, accumulation of WAT and BAT, and reducing obesity.[8] Eighteen ZDF rats were assigned to receive either 0, 4, or 8 µg IFNT/kg body weight per day for eight weeks. Water consumption was recorded every two days and food and body weight were recorded weekly. It was found that oral administration of 8 µg INFT/kg body weight/day reduced body weight and adiposity, delayed the onset of diabetes, and increased BAT, while decreasing WAT.[9]

This current study, using the previous study as a foundation, aimed to determine: 1) whether Arg alone, IFNT alone, or Arg+IFNT in combination delivered orally would have similar results; and 2) how genes associated with NAFLD were expressed. We hypothesized that Arg and IFNT, either alone or in tandem, would decrease the expression of genes encoding for proteins involved in the transport and binding of fatty acids, decrease body weight, and, therefore, decrease the severity of obesity and NAFLD to enhance the well-being of the ZDF rats.

METHODS

Male Zucker diabetic fatty (ZDF) rats (n=24) were obtained from Envigo at approximately five weeks of age. After a three-day acclimation period to assess basal water consumption, treatments began. Rats were assigned randomly to one of four treatment groups: Control–2.55% Alanine; Arg only–1.51% Arg; IFNT only–8µg IFNT/kg body weight; or Arg and IFNT in combination–1.51% Arg and 8µg INFT/kg body weight. Treatments were given via the rats' drinking water, and water consumption as well as the weight of the rats were recorded daily. Rats were treated for nine weeks, after which time they were euthanized. Body weights of rats were determined and then several organs were collected for analyses.

We performed quantitative polymerase chain reaction (qPCR) analyses to determine the expression of candidate genes and to assess how effectively treatment with IFNT and/or Arg decreased the expression of genes associated with fatty acid transport and binding. In this study, we determined the expression of messenger RNAs (mRNAs) for fatty acid binding proteins (FABP), fatty acid transport proteins (FATP), peroxisome proliferator-activated receptor alpha (PPARA), CD36, a fatty acid translocase protein, and C-reactive protein (CRP). These genes have central roles in the transport, binding, and oxidation of fatty acids in the liver.

Table 1. *Body weights of ZDF rats are summarized by treatment for each week of treatment (means (g) + standard error of the mean)*

Treatment	Week 1	Week 2	Week 3	Week 4	Week 5	Week 6	Week 7	Week 8	Week 9
Control	148.7 ± 4.2	203.4 ± 5.5	269.3 ± 4.6	320.3 ± 7.6	391.3 ± 9.9	447.7 ± 11.3	508.7 ± 12.8	550.0 ± 14.1	583.3 ± 17.8
Arg	150.4 ± 3.6	197.81 ± 4.9	275.5 ± 4.3	324.8 ± 10.7	384.1 ± 4.3	438.2 ± 4.8	483.9 ± 5.9	516.4 ± 6.6	547.3 ± 8.2
IFNT	157.4 ± 3.3	208.5 ± 5.8	273.7 ± 5.3	340.2 ± 6.2	396.4 ± 6.5	446.4 ± 7.2	489.2 ± 8.2	530.7 ± 9.0	567.1 ± 8.8
Arg+IFNT	155.66 ± 4.2	205.2 ± 4.7	269.9 ± 5.6	321.9 ± 6.7	365.5 ± 8.3	406.4 ± 9.4	456.1 ± 8.4	492.8 ± 7.9	519.5 ± 8.9

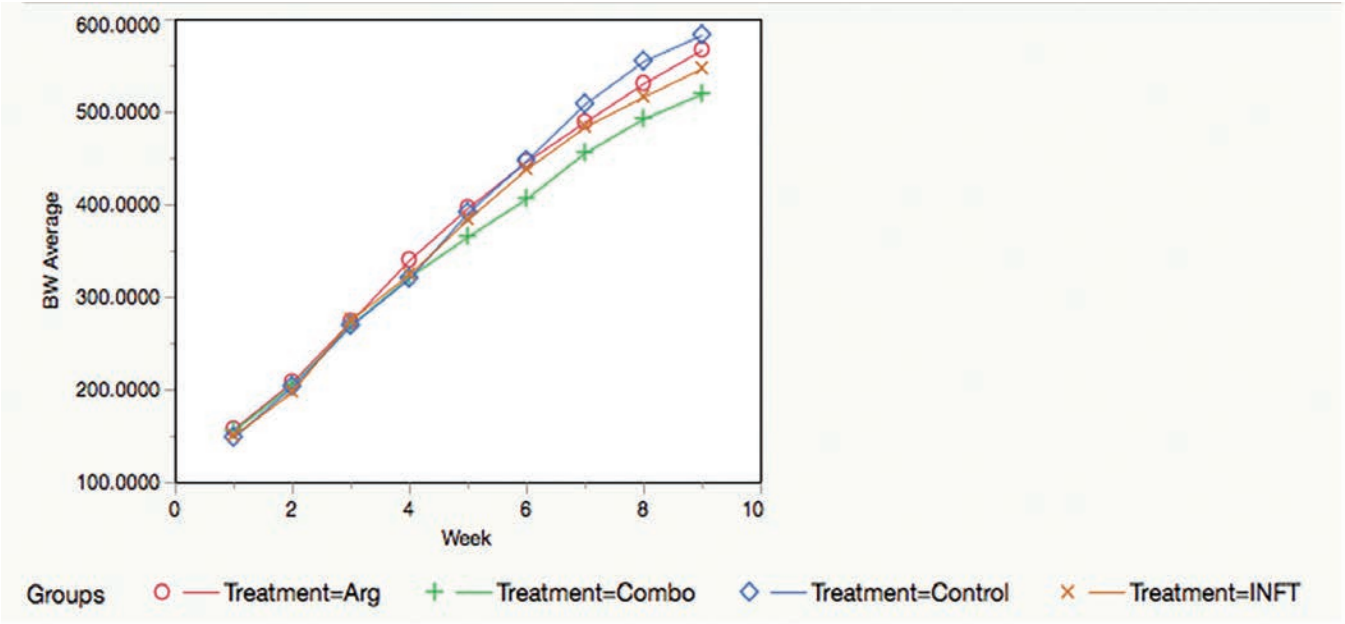

Figure 1. *Body weight (kg) changes by treatment, Reproduced by permission of Erin Posey.*

RNA was extracted from 30–50 µg of snap-frozen liver samples as described previously.[10] Complementary DNA (cDNA) was synthesized from 1.0 µg of RNA with SuperScript III reverse transcriptase and oligo (deoxythymidine) primers (Invitrogen, Carlsbad, CA), as per the manufacturer's instructions. Quantitative polymerase chain reactions (qPCR) were performed using the ABI prism 7900HT system (Applied Biosystems, Foster City, CA, United States) with Power SYBR Green PCR Master Mix (Applied Biosystems), as specified by the manufacturer to determine the levels of expression of mRNAs encoded for by genes of interest. Serial dilutions of pooled cDNA in nuclease-free water ranging from 1:2 to 1:256 were used as standards. All primer sets used amplified a single product. Each well contained 10% cDNA, 30% nuclease-free water, 10% primer, and 50% SYBR Green reaction mix in a 10 µl reaction volume. All reactions were performed at an annealing temperature of 60ºC.

ACTB (beta actin) and YWHAZ (tyrosine 3-monooxygenase/tryptophan 5-monooxygenase activation protein zeta) were utilized as reference genes. These genes were found to have stable expression by geNORM V3.5 (Ghent University Hospital, Centre for Medical Genetics). GenStat (Version 13.1; VSN International Ltd.) was used to statistically confirm that the treatments did not affect the expression of ACTB and YWHAZ, both individually and the mean of the two reference genes. The level of expression of each of the candidate mRNAs in the liver samples were quantified using the ΔΔCq statistical method. The normality

Table 2. *Effects of treatment with arginine (Arg), interferon tau (IFNT) and their combination on amounts of white and brown adipose tissue (mg, mean+standard error of the means). Reproduced by and with permission of Erin Posey.*

Tissue Type	Control	Arg	IFNT	Arg+IFNT
White Adipose Tissue	40.5 ± 1.15	30.3 ± 1.27	39.2 ± 1.20	5.0 ± 0.75
Brown Adipose Tissue	1.65 ± 0.60	1.90 ± 0.38	1.96 ± 0.34	2.49 ± 0.30

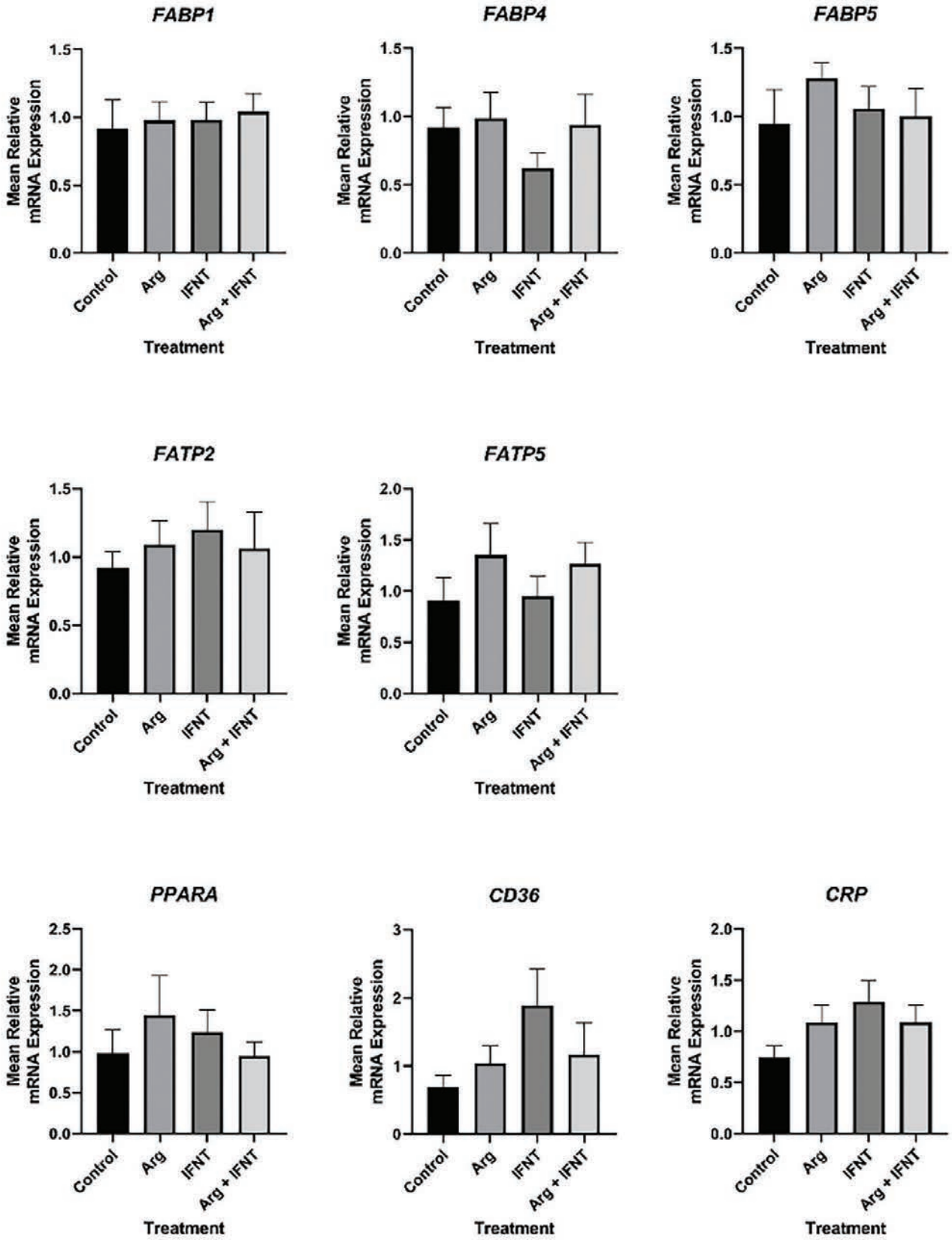

Figure 2. *Effects of Arginine (Arg) and Interferon Tau (IFNT) and their combination on the expression of mRNAs encoding for proteins involved in fatty acid transport and binding.*

of the distribution of the data was assessed using the Anderson-Darling test. If a P value of < 0.05 was obtained, then the data were not considered to have a normal distribution. Log10 transformations were carried out if necessary to achieve a Gaussian distribution. Outliers identified by a ROUT outlier test were excluded.

RESULTS

Treatment of ZDF rats with Arg alone, IFNT alone, and Arg and IFNT in combination significantly decreased total body weight when compared with control rats as shown in **Table 1**. Body weight loss using the Arg+IFNT treatment group compared to the control group was significant ($p<0.05$). Body weight loss with the Arg+IFNT group compared to the Arg only group was also significant ($p<0.05$). **Table 2** shows that an increase in BAT and a decrease in WAT was observed for all treatment groups, with the Arg+IFNT group being the most effective, although not statistically significant. This result suggests that treatment with Arg and/or IFNT may be a potential therapeutic target for the treatment of obesity.

Although differences in the expression of genes between control and treatment groups were not statistically significant, there were interesting numerical differences between the treatment groups and the control group as shown in **Figure 2**. For the fatty acid binding proteins (FABP), expression of FABP1 mRNA was not different due to treatment, while expression of FABP4 mRNA decreased in response to the IFNT only treatment, and expression of FABP5 mRNA was greater for the Arg only treatment group compared to the other treatments. For the fatty acid transport proteins (FATP), FATP2 mRNA expression was numerically greater for all treatment groups compared to the control group, particularly for the IFNT only treatment group. FATP5 mRNA expression was greater for the Arg only and Arg+IFNT groups compared to the alanine supplemented control group and IFNT only group. The expression of peroxisome proliferator-activated receptor alpha (PPARA) mRNA increased slightly for the Arg alone group, but the effect was not statistically significant. The expression of CD36 mRNA, a fatty acid translocase protein, increased in the IFNT only group, but there was only a slight increase in the Arg and Arg+IFNT groups, with all instances being insignificant statistically. C-reactive protein (CRP) mRNA expression increased slightly in all treatment groups, particularly for the IFNT only group, but those changes were not statistically significant.

THIS TREATMENT COMBINATION HAD MINIMAL EFFECTS ON THE EXPRESSION OF GENES INVOLVED IN FATTY ACID TRANSPORT AND BINDING OF FATTY ACIDS IN THE LIVER.

The Arg only group had increased expression in all genes evaluated as compared to the control group, suggesting that Arg has an important role in lipid deposition and changes in body mass due to its important roles in liver function. Treatment with Arg alone tended to increase FATP5 mRNA expression in the liver which would increase surface binding of fatty acids on the cellular membrane. The Arg only treatment also tended to increase expression of FABP5 mRNA which could result in less arginase participating in other metabolic pathways, thus allowing more arginine to be circulated in the liver,[11] perhaps to increase the expression of PPARA which is the oxidative pathway for metabolism of fatty acids.[12]

The IFNT only treatment had the greatest expression of FATP2, CD36, and CRP mRNAs. The increase in FATP2 mRNA expression could increase the transport of fatty acids into the cell. In the liver, fatty acids that reach the cell membrane are bound by FABP1 after which time they are oxidized.

Rats treated with the combination of Arg and IFNT had modest increases in expression of FABP4, FATP5, CD36, and CRP mRNAs compared to the con-

TREATMENT OF ZDF RATS WITH ARG ALONE, IFNT ALONE, OR ARG + IFNT IN COMBINATION...LED TO A SIGNIFICANT DECREASE IN BODY WEIGHT IN ALL TREATMENT GROUPS.

trol group. Results of this current study have provided interesting insights into the potential of Arg and IFNT as therapies for the mitigation of NAFLD and obesity. In this study, the rats treated with Arg+IFNT had the most effective weight loss among the treatments. However, this treatment combination had minimal effects on the expression of genes involved in fatty acid transport and binding of fatty acids in the liver. Given these findings, further analyses are necessary to assess the long-term effects of these treatments on lipid accumulation and liver function in ZDF rats. Furthermore, one may speculate that Arg+IFNT is the most effective treatment for weight loss; however, Arg or IFNT alone may be a more appropriate therapy for patients showing signs of NAFLD because these treatments showed more promise in regard to decreasing fatty acid accumulations in the liver.

CONCLUSION

Treatment of ZDF rats with Arg alone, IFNT alone, or Arg + IFNT in combination increased BAT, decreased WAT, and led to a significant decrease in body weight in all treatment groups. Treatment with Arg only resulted in the greatest overall increase in expression of mRNAs for proteins involved in transport and binding of fatty acids. The IFNT only treatment yielded similar results in mRNA expression but was less effective than Arg. The IFNT only treatment also resulted in greater expression of mRNAs for inflammatory proteins as compared to the Arg only treatment. Arg+IFNT resulted in the most significant body weight loss but had the least overall effect on changes in mRNA expression compared to the other treatment groups. More research is needed to fully understand how the Arg+IFNT treatment resulted in the most significant body weight loss without having a significant effect on expression of mRNAs for fatty acid binding and fatty acid transport proteins in the liver.

Although this experiment has not led to a definite treatment for obesity and NAFLD, the results are promising and give insight on how best to move forward. Future studies are needed to assess the role of FABP5 in interactions with arginase in the urea cycle to determine if that could play a role in increasing the abundance of Arg in the circulation and therefore providing more clarity as to how treatment works in the body.

ACKNOWLEDGMENTS

We would like to acknowledge Texas A&M University for providing the T3 grant from the Office of the VP for Research. We would like to thank Dr. Fuller, W. Bazer, and Dr. Claire Stenhouse for inviting us into their laboratory and supporting us through this process. We would like to thank Erin Posey for her prior work that set the foundation for this project. We would also like to thank Katherine Halloran, Robyn Moses, and Nirvay Sah for their support.

REFERENCES

1. Center for Disease Control and Prevention, "Adult Obesity Facts," Center for Disease Control and Prevention, last modified June 7, 2021,. **https://www.cdc.gov/obesity/data/adult.html**.

2. Carmen D. Tekwe et al., "Oral administration of interferon tau enhances oxidation of energy substrates and reduces adiposity in Zucker diabetic fatty rats," International Union of Biochemistry and Molecular Biology 39, no. 5 (September-October 2013): 552–63, **https://doi.org/10.1002/biof.1113**.

3. Christopher D. Byrne and Giovanni Targher, "NAFLD: A multisystem disease." Journal of Hepatol-

ogy 62, no. 1 (April 2015): S47-S64. https://doi.org/10.1016/j.jhep.2014.12.012.

4. Guoyao Wu et al., "Arginine metabolism and nutrition in growth, health, and disease." Amino Acids 37, (November 2008): 153–68. https://doi.org/10.1007/s00726-008-0210-y.

5. Fuller W. Bazer et al., "Select nutrients, progesterone, and interferon tau affect conceptus metabolism and development," Annals of the New York Academy of Sciences 1271, no. 1 (October 2012): 88–96. https://doi.org/10.1111/j.1749-6632.2012.06741.x.

6. Christoph H. Saely, Kathrin Geiger, and Heinz Drexel, "Brown versus white adipose tissue: a mini-review," Gerontology 58, no. 1 (December 2010): 15–23. https://doi.org/10.1159/000321319.

7. Tekwe et al., "Oral administration of interferon tau," 552–63.

8. Tekwe et al., 552–63.

9. Tekwe et al., 552–63.

10. Claire Stenhouse et al., "Novel Mineral Regulatory Pathways in Ovine Pregnancy: I. Phosphate, Klotho Signaling, and Sodium Dependent Phosphate Transporters," Biology of Reproduction, (February 2021). https://doi.org/10.1093/biolre/ioab028.

11. Sherri M. Moore et al., "Fatty acid-binding protein 5 limits the anti-inflammatory response in murine macrophages," Molecular Immunology 67, no. 2 (June 2015): 265–75.

12. David H. Ipsen, Jens Lykkesfeldt, and Pernille Tveden-Nyborg, "Molecular mechanisms of hepatic liver accumulation in non-alcoholic fatty liver disease," Cellular and Molecular Life Sciences 75 (June 2018): 3313–27. https://doi.org/10.1007/s00018-018-2860-6.

AUTHOR BIOS

CRISTINA CALDERA GARZA '23

Cristina Caldera Garza '23 is a Genetics major with minors in Spanish and Health from Laredo, TX. Cristina was motivated to pursue research as a way to expand her knowledge in the fields of reproduction and physiology. She plans to attend medical school and one day practice as an OBGYN.

ASHTON CORPORON '23

Ashton Corporon '23 is a Biomedical Sciences Major with a minor in Psychology from Hutto, Texas and went to Hutto High School. Ashton is involved in an Animal Reproduction lab at Texas A&M, which sparked her interest in research and allowed for the opportunity to study different processes and lab techniques inspiring her to write for Explorations. Ashton plans to continue her academic career with medical school, and eventually pursue a career in Obstetrics and Gynecology.

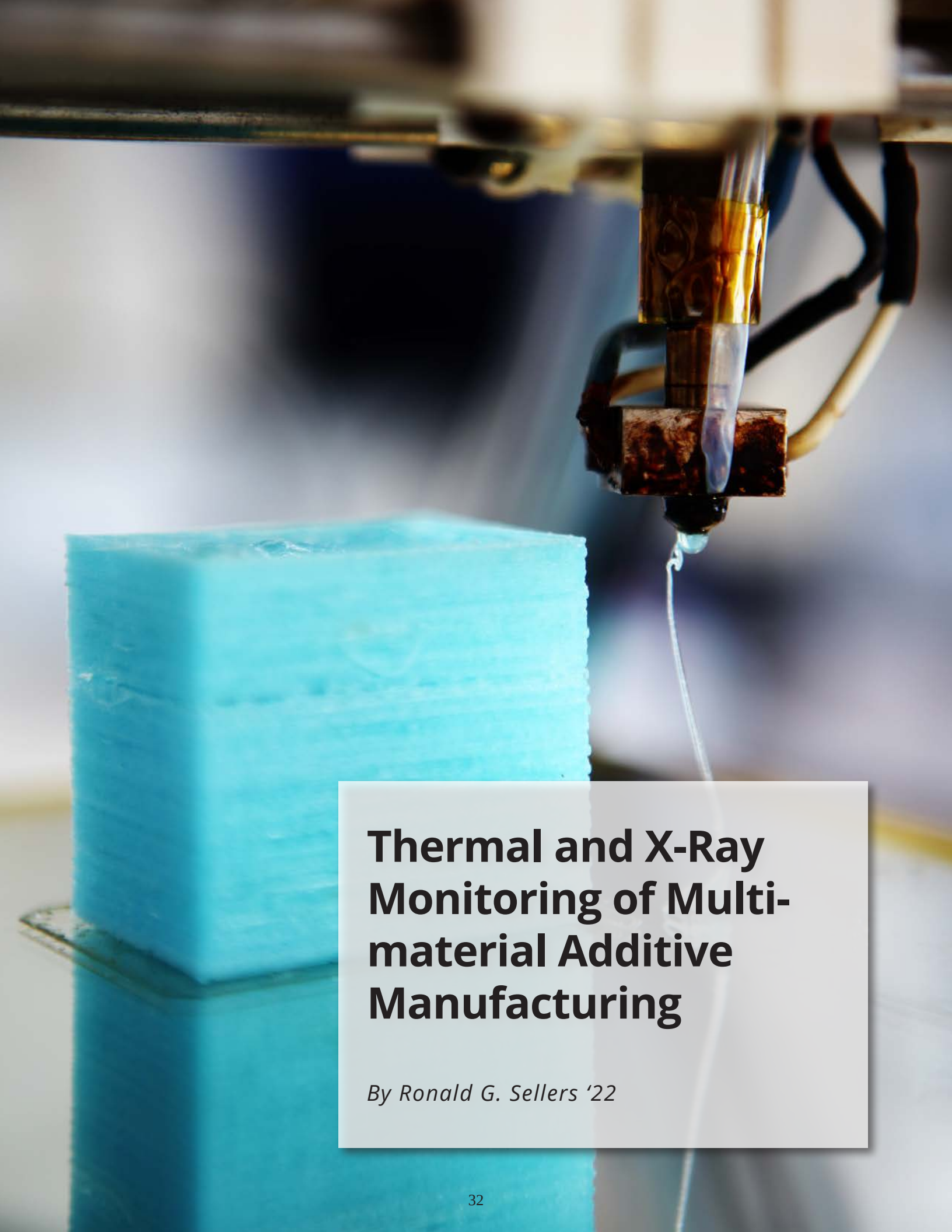

Thermal and X-Ray Monitoring of Multi-material Additive Manufacturing

By Ronald G. Sellers ‘22

INTRODUCTION

Additive manufacturing (AM) is a process that creates an object layer-by-layer in the 3D space from a computer-aided design software. Over the past few years, the AM industry has seen rapid expansion and is now used in automotive, nuclear, aerospace, biomedical, and other industries due to its versatile applications. This era is called Industry 4.0, or the Fourth Industrial Revolution.[1] AM includes processes such as laser bed powder fusion, 3D printing, directed energy deposition (DED), and more. DED fuses two materials together through the method of powder deposition and laser melting. This research deals with DED experiments of Molybdenum (Mo) particles fusing onto a titanium alloy, Ti-6Al-4V (Ti64), substrate. Specifically, I observed the thermal and x-ray imaging of the fusing between these two metals as shown from the lab setup in **Figure 1**. Monitoring this process allows for the collection of melt-pool characteristics, particle velocity, temperature gradients, flow paths, and other useful phenomena for analysis. The main parameters changed throughout the experiments are shown in **Table 1**. These changes are important to understand because they can affect the behavior of the Mo particles that collide, flow, and fuse with the substrate.[2] Understanding parameter changes is critical to producing consistent, high-quality parts using the AM process.

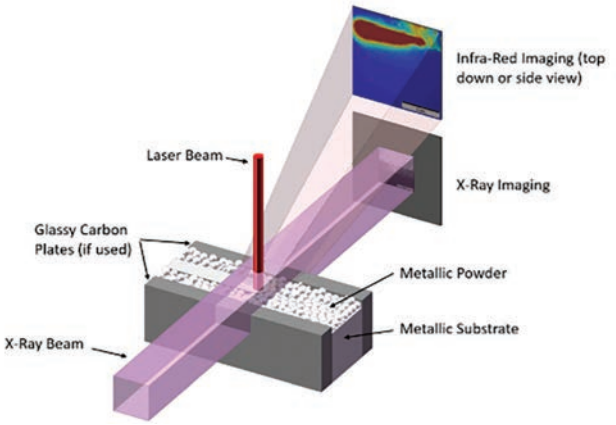

Figure 2. *Infra-red and X-Ray camera setup at the lab.*[4]

METHODS

MATLAB Conversions

Image processing and analysis necessitates that the thermal images captured in the lab be converted from .htc files to .tiff files or tiff images. The thermal imaging camera was placed above the experiment to capture a scan of the top layer of the substrate (**Figure 2**). Infrared (IR) cameras compressed images into .htc files and converted them into tiff images with a 128x128 matrix of numbers. Each cell in the matrix represents one pixel from the camera and the number for each cell is the temperature detected from the experiment. For every frame of the experiment video, one tiff image was created, meaning that an 8-millisecond video is 80 tiff images.

Temperature Plots

After converting files, the temperature gradient of the substrate surface was analyzed. Experiments were selected with different parameters such as laser power, scan speed, gas pulse, and wheel pulse (**Table 1**). These parameters determined the temperature, velocity, angle of deposition, and intensity of the Mo particles, which in turn affected the Ti64 adhesion and microstructure. MATLAB was used to cycle through each tiff image and plot cells as graphs

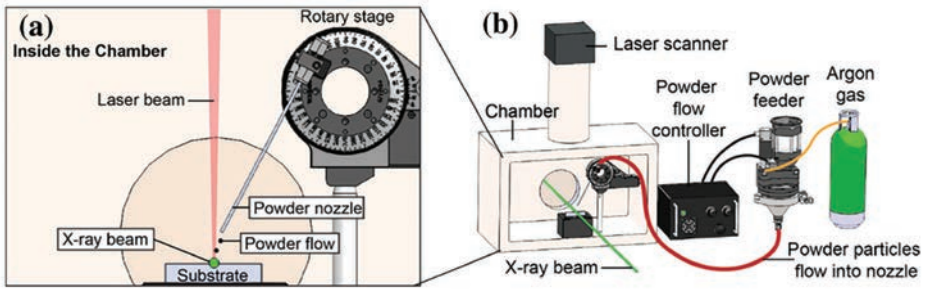

Figure 1. *Directed energy deposition experiment setup with a 520-Watt laser positioned 90° above the Ti64 substrate. The powder nozzle expels the argon shielding gas and the Mo particles at an angle that allows all three elements to collide.*[3]

Table 1. *Experiment Parameters of Directed Energy Deposition Setup.*

Experiment	Laser Power (W)	Scan Speed (m/s)	Gas Pulse (ms)	Wheel Pulse (ms)
1	208	0.1	1,000	0.1
2	312	0.1	400	0.1
3	312	0.1	0	0
4	312	0.1	1,000	0.1
5	312	0.1	0	0
6	520	0.2	0	0

of temperature versus time (**Figure 3**). An important note about IR images and the experiment is that each pixel represents 30 microns. When picking cells based on the image itself, this factor had to be understood to translate from picture to matrix to graph. The peaks of the graph are marked to show how the substrate will increase in temperature in different fluctuations over time. Each peak represents a pass from the laser. In this case, the laser made four side-to-side passes across the Ti64. The number of passes for each experiment was considered when deciding how to analyze. To get the most accurate results, the graph-making process was done for multiple experiments with different spots from each sequence of tiff images.

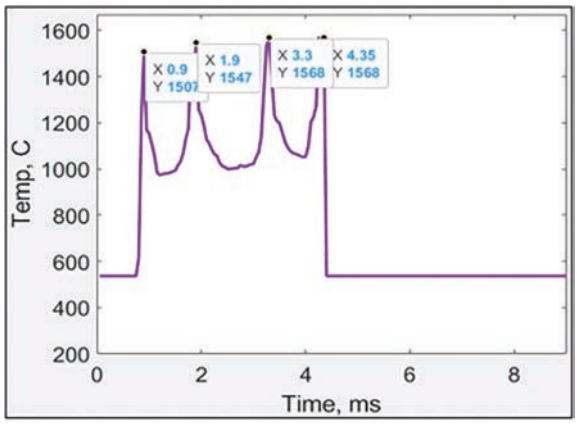

Figure 3. *Temperature vs time of single pixel from experiment 6 generated with MATLAB.*

3D Contour Plotting and Pixel Intensity

2D graphs can be useful for analysis, but they only reflect a limited portion of the experiment at a given time. For this reason, MATLAB plotted a single tiff image, or layer, on a 3D contour surface plot as shown in **Figure 4**. This plot represents a 128x128 matrix of temperatures captured from a single video frame of the experiment to show a gradient of temperature along the substrate. This was done to observe rate of change, temperature gradient, and how the melt pool around the laser was affected when passing over.

X-Ray Image Processing

After saving and analyzing graphs of particle temperature, x-ray images were analyzed. The x-ray camera shot at 30,000 frames per second (fps) at a side cross section of the experiment using a third-party program ImageJ for image processing. ImageJ allows for measurements, brightness and contrast alterations, and other post-image analysis techniques on an image or sequence of images. The first step for the x-ray image data processing was to change the set-scale. Each pixel is about 1.97 μm which had to be calibrated in the settings for future measurements. After this step, the contrast of the image needed to be changed to view the particle and melt-pool definitions using the line function of ImageJ, which can measure distance-to-scale on the image. The melt-pool distance was measured

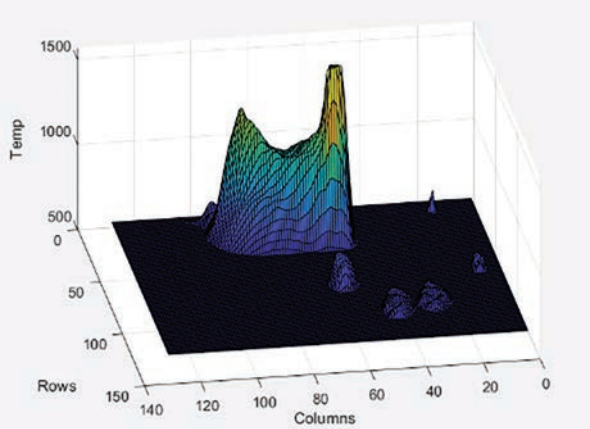

Figure 4. *Surface plot of layer 21, which corresponds to the time at 2.1 milliseconds from experiment 5 generated with MATLAB.*

at multiple time periods throughout the experiment to analyze the shape, length, and duration (**Figure 5**). Average size, shape, and height were recorded in an Excel file for future calculations.

Along with the line function in ImageJ, the ellipse tool was used to measure circular objects. Ellipses have a major and minor axis which describe the length and height of said object. This can be useful in understanding the dimensions of the ellipse and how it can be changed. Particles were separated into two categories: in-air and in-substrate. Particles were measured with the ellipse tool and recorded in an Excel sheet for calculations afterwards. Recording multiple data points was extremely important as each particle is not the same, which is crucial in understanding how and why they react to different situations.

As the laser makes a pass, it forms a keyhole which looks like a liquid key inserted into the substrate but instead of rotating, it travels along the path (**Figure 6**). Depending on parameters, such as laser power or speed, the keyhole can form bubbles of air trapped in the molten liquid which is known as porosity. To understand porosity, the ellipse tool measured the size of the bubbles formed in the experiments (**Figure 6**). Since each experiment had different porosity percentages, the number of frames was divided into four increments to acquire a better average of measurements. The average number of bubbles over a certain time frame was also recorded to understand how porosity changed with parameters of the experiment.

RESULTS

Pixel and Temperature Analysis

Analysis of temperature versus time graphs found that post-peak slopes from experiments with lower laser power exhibit a faster decrease in temperature. That is, the slopes on lower laser power are more expanded and shorter than those of higher laser power slopes. The second observation from these graphs is that with each pass of the laser, the material reaches a higher temperature. This is observed numerically with the text box placed at the peak of each pass as well as visually with the positive slope in between. The peaks shown in **Figure 3** reached temperatures of 1507°C, 1547°C, 1568°C, and 1568°C for each pass, respectively. One reason for this occurrence is that the material reached a high temperature with the first pass, cooled slightly, then was reheated from a new position. When comparing multiple graphs of single cells to each other, it was shown that as the powder flow decreases, the cooling rate decreases. This is represented by the slopes of the graphs either being compressed or expanded depending on the powder flow.

Contour Plot Analysis

For better analysis of the tiff matrix, multiple surface contour plots were compared to each other. The comparison included plots at the same time as each

AMIDST THE INCREASED USE OF ADDITIVE MANUFACTURING, IT IS CRUCIAL TO UNDERSTAND HOW MATERIALS COMBINE EFFICIENTLY THROUGH DIFFERENT PROCESSES.

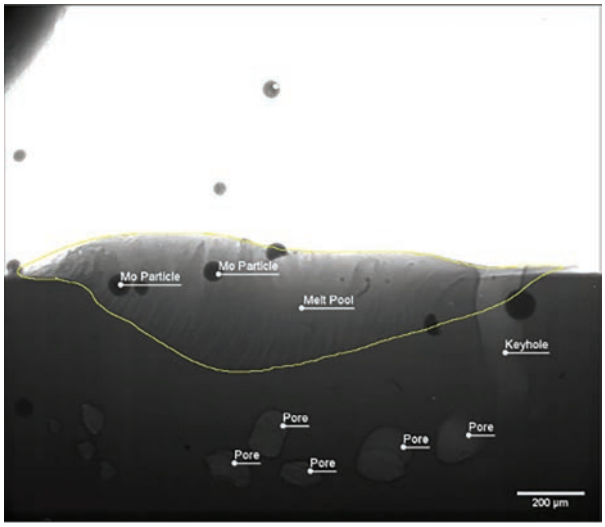

Figure 5. *Melt-pool measurements from experiment 3 using ImageJ.*

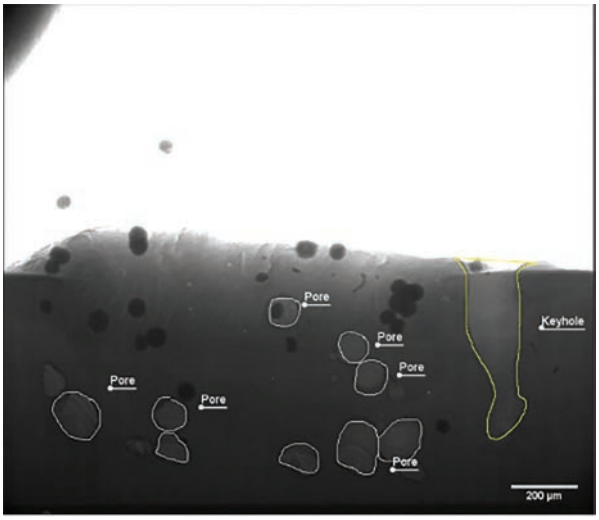

Figure 6. *Keyhole and porosity markings from experiment 2 using ImageJ.*

other, different times, and based on their respective experimental parameters. The color gradient in Figure 4 indicates the temperature of the layer ranging from purple being around 512°C to red which was around 1,600°C. A surface plot is integral to observing how the area of pixels that represent the melt pool is affected by the surrounding molten liquid. **Figure 3** had a slope of 2,577.5°C/ms heating up and -2,168°C/ms cooling down, which was found by dividing temperature by time with differentiation to analyzing how fast each part of the slope is changing. Along with the color shift, contour plots also allow for visual aid in vector lines. These vector lines appear stretched when increasing significantly, as observed on the slope from the laser (**Figure 4**).

THE PEAK TEMPERATURES FROM THE GENERATED CONTOUR PLOT ALLOW OBSERVATION OF HOW THE SUBSTRATE AROUND THE CONCENTRATED LASER AND MOLTEN METAL REACTS.

Melt Pool Characteristics

When analyzing melt-pools, there are a few phenomenon that must be accounted for. The first is that as laser power increases, the melt-pool increases. Experiment one had a melt-pool size of 577 µm while experiment five had a max melt pool of 837 µm. The laser power for these experiments was 208 W and 312 W, respectively. This shows that not only does the temperature cause the melt-pool to have a larger width, but also a greater depth.

Number of particles present in the melt-pool is also a determining factor for melt-pool characteristics. Particles melting or not melting influences the melt-pool size as it will take more heat per time to break down. This is evident in experiments one and two with gas pulses of 1,000 ms and 400 ms, respectively. Since experiment one had a higher gas pulse along with lesser laser power, more particles were mixing in the substrate, but not melting. Experiment two had a higher laser power and lesser gas pulse, resulting in a decrease in un-melted particles in the melt-pool. This proves that as gas pulse increases, the likelihood of un-melted particles will increase, causing a buildup of solid material.

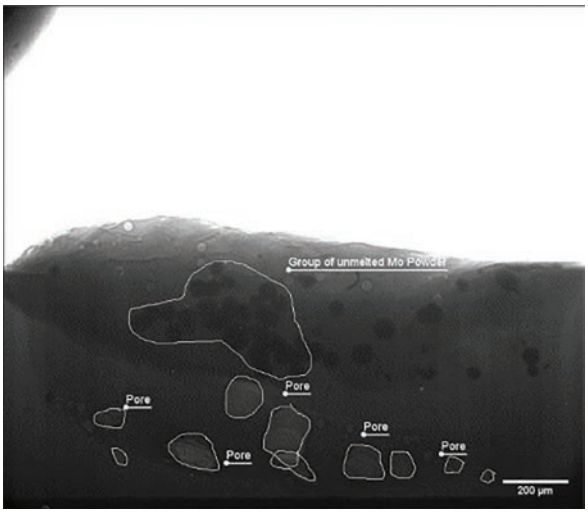

Figure 7. *Porosity and un-melted Mo particles representation from experiment 3 using ImageJ.*

Porosity Analysis

Increasing the laser power not only results in larger melt-pools but also affects porosity. A higher laser power means hotter temperatures, more powerful focus, and a larger keyhole.[5] These three attributes contribute to the creation of bubbles in the metal. Since molten flow is uneven, certain areas get mixed poorly, causing pockets of air to become trapped. Looking at experiments one, two, and three, the average number of bubbles was 0.25, 14.5, and 17.75, respectively. The average area of those bubbles was 0.000258, 0.005172, and 0.004859 mm², respectively. Not only does an increase in laser power raise the average size of the pores, but decreasing the gas pulse leads to an increase in porosity percentage in the substrate. Another factor of porosity is laser absorption.[6] A certain percentage of particles will travel directly into the melt-pool, while others will collide mid-air with the laser. If the latter occurs, the number of particles melting due to the offset of distributed heat from the laser decreases. This is represented by the dark circles being un-melted particles and the grey spots as the bubbles (**Figure 7**).

Another useful technique in analyzing melt-pools for DED is pixel intensity. Pixel intensity is the brightness of a pixel in an image and is generally plotted on histograms which show how many pixels are at a given intensity level in an image. The x-axis ranges from 0 to 255, where 255 is white. Plotting pixel intensity will show the relative size of a melt-pool.

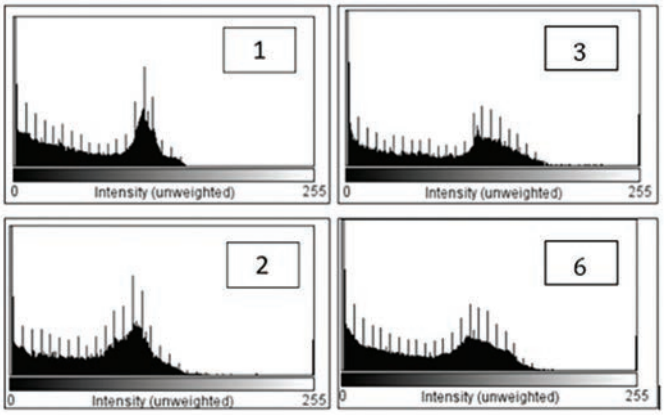

Figure 8. *Pixel intensities of experiments one (top left), three (top right), two (bottom left), and six (bottom right) generated using MATLAB.*

This is determined from the substrate and particles having around the same, dark-value brightness. Liquid metal will appear brighter in these images, which will be present in the graph. Pixel intensity was performed on experiments one, two, three, and five. Each experiment had differing parameters, which is why they were specifically chosen to analyze. Melt pool size increased with temperature, as shown from the graphs of pixel intensities (**Figure 8**).

CONCLUSIONS

Amidst the increased use of additive manufacturing, it is crucial to understand how materials combine efficiently through different processes. Laser-based directed energy deposition requires understanding the characteristics of materials and their microstructure before, during, and after the experiment. This research presents evidence that the characteristics of a melt-pool are influenced by the parameters of the laser and particles. A higher laser power means faster and more efficient melting. However, it also leads to a larger melt-pool as well as higher chance to generate porosity in the metal. This understanding is important as it allows for manipulation of the melt-pool by changing the parameters of the experiment. With pixel intensity, it was observed that a larger melt-pool is present with a higher laser power due to the number of pixels within a certain brightness range. Increase in powder flow also generates plots of higher temperature due to the increase in solid and molten particles in the substrate.

INDUSTRY 4.0 IS HERE, AND A BETTER UNDERSTANDING OF THE DED PROCESS WILL ENABLE NEW, STRONGER MATERIALS TO BE FABRICATED WITH ADDITIVE MANUFACTURING.

The peak temperatures from the generated contour plot allow observation of how the substrate around the concentrated laser and molten metal reacts.

Future work could analyze particle flow or trajectory in and out of the melt pool, as well as a more in-depth analysis of melt-pool characteristics including major and minor axes, eccentricity, radius of curvature, and other properties that help describe the shape. A larger melt-pool is able to produce parts faster due to the increases melting area, reach certain sections of the part for a more complete melting, and can be altered to made in a specific shape needed by certain industries. Particle flow is important when analyzing the substrate as the trajectories can impact melting, temperature gradients, and porosity. Some industries, such as medical devices, need more porosity to make a device lighter, while others, such as aerospace companies, need less porosity to strengthen the part. Industry 4.0 is here, and a better understanding of the DED process will enable new, stronger materials to be fabricated with additive manufacturing.[7]

ACKNOWLEDGMENTS

The author would like to thank Tao Sun, Niranjan Parab, Kamel Fezzaa, and Alex Deriy at the beamline. This research used resources of the Advanced Photon Source, a U.S. Department of Energy (DOE) Office of Science User Facility operated for the DOE Office of Science by Argonne National Laboratory (ANL) under Contract No. DE-AC02-06CH11357 and support through Laboratory Directed Research and Development (LDRD) funding from ANL under the same contract. I would like to acknowledge my research advisor, Dr. Sarah J. Wolff, who has guided me through my experience and has been an inspiration to what I can do in the field. You have helped me through the submission process as well as supported my ideas for personal research projects.

I would also like to acknowledge my roommate, Eduardo Gonzalez, who helped me stare at X-Ray images and figure out how to calculate certain values.

Lastly, I would like to thank my parents, who have helped support me and the decisions I have made. Without them, I would not be here today to do this research and understand the world more.

REFERENCES

1. Ugur M. Dilberoglu et al., "The Role of Additive Manufacturing in the Era of Industry 4.0," Procedia Manufacturing 11, (2017): 545–54. **https://doi.org/10.1016/j.promfg.2017.07.148**.

2. Qilin et Guo al., "In-Situ Full-Field Mapping of Melt Flow Dynamics in Laser Metal Additive Manufacturing," Additive Manufacturing 31, (October 2020). **https://doi.org/10.1016/j.addma.2019.100939**.

3. Sarah J. Wolff et al., "In-Situ Observations of Directed Energy Deposition Additive Manufacturing Using High-Speed X-Ray Imaging," JOM 73, no. 1 (2020): 189–200. **https://doi.org/10.1007/s11837-020-04469-x**.

4. Benjamin Gould et al., "In Situ Analysis of Laser Powder Bed Fusion Using Simultaneous High-Speed Infrared and X-Ray Imaging," JOM 73, no. 1 (2020): 201–11. **https://doi.org/10.1007/s11837-020-04291-5**.

5. Ranxi Duan et al., "In Situ Alloying Based Laser Powder Bed Fusion Processing of β Ti–Mo Alloy to Fabricate Functionally Graded Composites," Composites Part B: Engineering 222 (October

1, 2021). **https://doi.org/10.1016/j.compositesb.2021.109059**.

6. Wolff et al., “In-Situ Observations,” 189-200.

7. Reem Ashima, et al., “Automation and Manufacturing of Smart Materials in Additive Manufacturing Technologies Using Internet of Things towards the Adoption of Industry 4.0,” Materials Today: Proceedings 45, no. 6 (February 22, 2021): 5081–8. **https://doi.org/10.1016/j.matpr.2021.01.583**.

AUTHOR BIO

RONALD SELLERS '22

Ronald Sellers ’22 is an industrial and systems engineering major with a minor in mathematics from Dallas, Texas. Ronald has been part of the research team with Dr. Sarah Wolff at Texas A&M since the fall of 2020 and will continue on this journey to pursue more publications as well present at additive manufacturing conferences around the United States. Ronald hopes to pursue a master’s degree in Biomedical engineering and a Ph.D. in Mechanical engineering.

Building a Recovery Oriented System of Care in Rural Texas Amidst a Global Pandemic

By Elizabeth M. Kappil '22

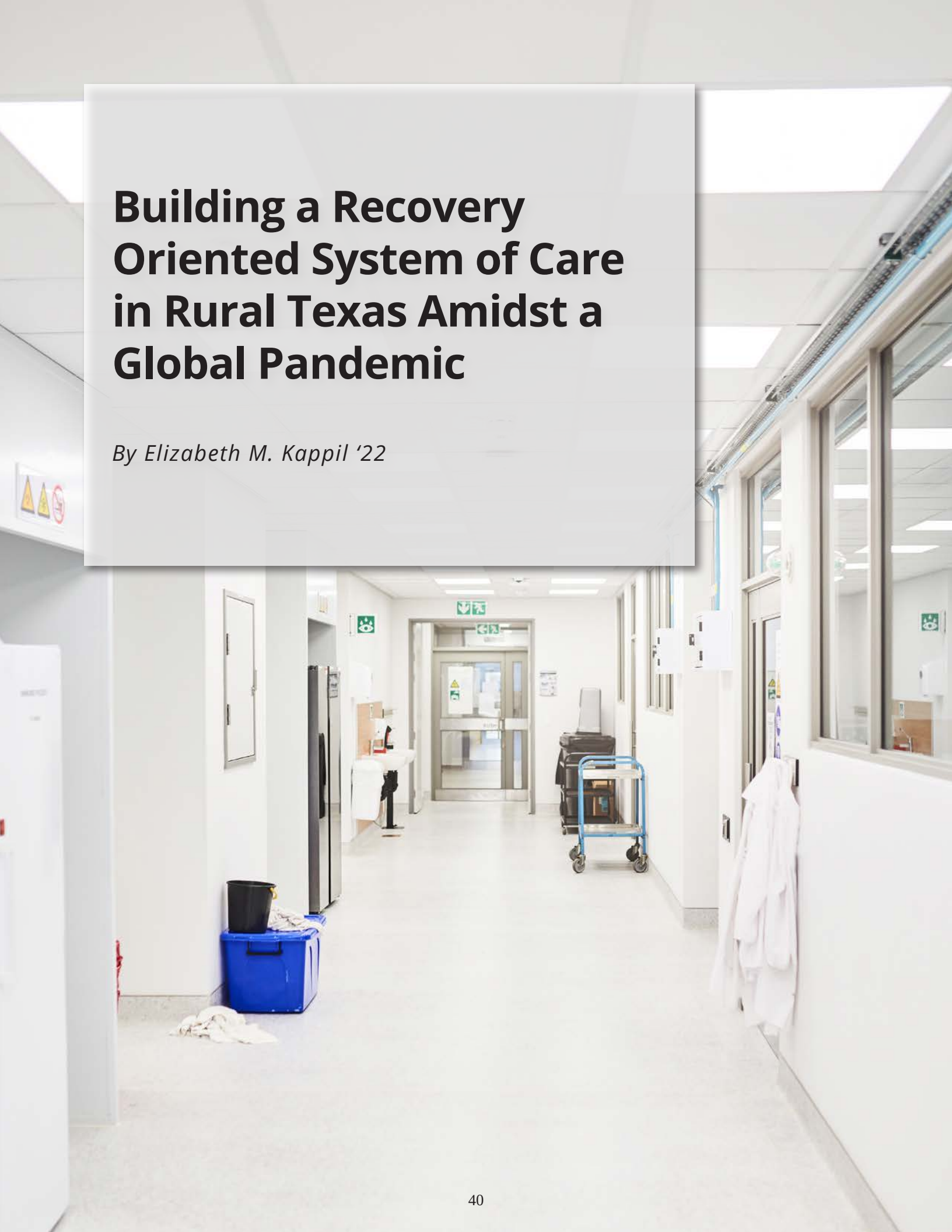

INTRODUCTION

RURAL US RESIDENTS AND COMMUNITIES SUFFER A DISPROPORTIONATE BURDEN FROM OPIOID MISUSE COMPARED TO THEIR URBAN COUNTERPARTS.

Substance use disorder (SUD), which includes opioid use disorder (OUD), is a public health crisis that has been magnified by the global pandemic due to social distancing policies increasing the likelihood of deaths from overdoses.[1] The most common reason people seek medical care is related to pain, and opioids are one of the most widely prescribed classes of drugs in America.[2] Due to the high frequency of prescribed opioids, there was an inevitable upsurge in the use and abuse of prescription and illicit opioids termed "The Opioid Epidemic," which resulted in a staggering number of opioid-related fatalities in the United States. Prescription for opioid analgesics quadrupled in the United States between 1999 and 2010, with a sharp increase in deaths due to opioid misuse and a similar trend for prescription opioid deaths over the same period.[3] In 2016, over 63,000 Americans died of a drug overdose, primarily involving an opioid, while 2.1 million people suffered from an OUD.[4] In 2017, the opioid crisis was declared a nationwide public health emergency.[5] Provisional data indicates that more than 81,000 Americans died from a drug overdose between June 2019 and May 2020, which is the largest number of drug overdose deaths recorded in the United States.[6]

Rural US residents and communities suffer a disproportionate burden from opioid misuse compared to their urban counterparts.[7] This is primarily due to the lack of resources within rural communities that are essential to combat this crisis. SUD is a complex and multifaceted public health issue, which requires community buy-in for prevention, treatment, and recovery strategies to be effective.[8] The proposed solution to SUD is a community-driven solution referred to as the Recovery Oriented System of Care (ROSC) to address SUD/OUD despite the challenges brought by the global pandemic, such as shifting to virtual lunches, video conferencing, and an online presence.

From the fall of 2019 through the fall of 2020, the Texas A&M University College of Nursing led a team to complete a strategic plan directed toward the assessment and prevention of SUD/OUD by establishing a community consortium in the rural coastal bend of Texas known as the Golden Crescent (**Figure 1**). This 200,000-resident region of seven counties is predominantly rural.[9] Funded by a one-year federal planning grant, the multidisciplinary team spent a year formalizing partnerships with local stakeholders, and formally investigating the inequities in SUD treatment in the Golden Crescent. The community consortium affirmed that rural communities in the Golden Crescent face numerous challenges in providing and accessing SUD services. The consortium created a plan to improve access to services and care for prevention, treatment, and recovery with the aim of reducing opioid mortality and morbidity rates in the community. Subsequent grant funding was pursued to address the

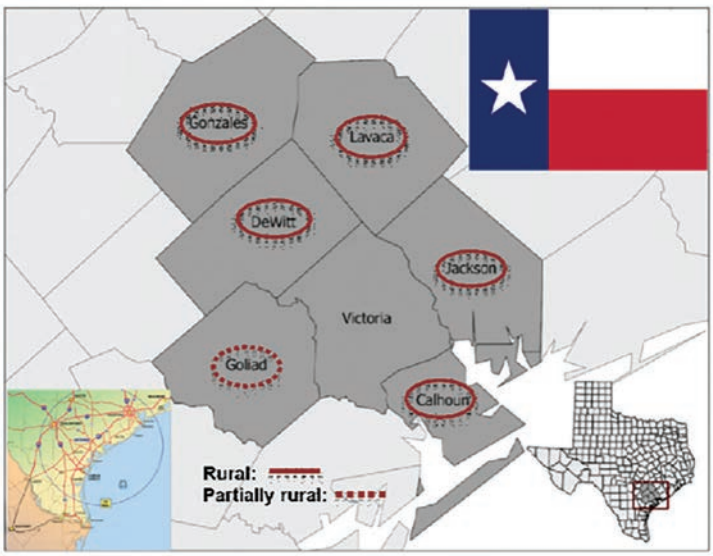

Figure 1. *Map of Golden Crescent Counties in Texas.*

inequities in access and delivery of SUD services in the Golden Crescent.

As with the rest of the nation responding to COVID-19 threats, our consortium members spent much of the spring of 2020 "sheltering in place." Some of our consortium members noted the following benefits with the use of telehealth: resources and information for telehealth regarding SUD/OUD were quickly distributed and shared among consortium members as it became available, and quick access of multiple forms of educational materials, webinars, and contact points were provided directly from our national funding agency. This early success in communication and collaboration set the stage for future accomplishments. During this time, two federal grant applications were submitted to request funds to implement activities to address SUD/OUD in the Golden Crescent. The proposals detailed adaptations to the original consortium plan due to the pandemic and activities were limited to those without direct physical contact.

Both funding mechanisms were awarded, and in September of 2020, work began that allowed the established consortium and other collaborating partners in the Golden Crescent to move forward with the long-term goal of reducing SUD/OUD morbidity and mortality by improving prevention, treatment, and/or recovery services. One project is focused on increasing awareness of SUD/OUD and the associated stigma of seeking help: providing SUD/OUD resources for prevention, treatment, and recovery while developing a peer recovery support specialist program. The other project aims to increase recovery capital to support pregnant women, mothers, women of childbearing age, children, families, and caregivers who are affected by SUD/OUD.

With sustainability in mind for the community after the funding period ends, both projects depend on the expansion of the existing consortium to a self-sustaining Recovery Oriented System of Care (ROSC) as a community network to coordinate and support SUD/OUD activities. The ROSC is a community-driven framework chosen as the central methodology of the grant projects. The ROSC recognizes recovery in the context of health and wellness for a community while focusing on services that are person-centered, strength-based, trauma-informed, inclusive of family, individualized and comprehensive, connected to the community, outcome-driven, and evidence-based. While there are ROSCs in neighboring regions of Texas, none serve the Golden Crescent area. Creating an ROSC in the Golden Crescent fills this significant gap. In the planned process of improving SUD/OUD prevention, treatment, and recovery services, a key activity in the initial six months of funding was the development of an ROSC. This foundational activity has been met with increased challenges amid the global pandemic.

RECOVERY ORIENTED SYSTEM OF CARE DEVELOPMENT

An ROSC is a coordinated community network of services and support for SUD/OUD activities that work to achieve abstinence from opioids and to improve health in the Golden Crescent. The ROSC model is designed to build upon the strengths of the individuals, families, and communities to take charge for sustained health, wellness, and recovery from SUDs which inevitably improves the quality of life.[10] The development of recovery-oriented care is a vital approach to combat opioid abuse, misuse, and overdose.[11] An

Figure 2. *Proposed Golden Crescent Recovery Oriented System of Care (ROSC) Membership.*

ROSC tries to capture the key components of personal, social, and community recovery capital and to translate this into a summary of recovery strengths and barriers to improved health that can be used to support the ongoing recovery pathway and journey. The Golden Crescent ROSC is currently working to extend and augment the existing consortium with formal and informal networks and collaborations between organizations and agencies to implement the planned activities. These activities include care coordination, community education, peer recovery, and provider training.

THE RECENT SUCCESS OF THE GOLDEN CRESCENT ROSC HAS BEEN THE BUILDING OF RELATIONSHIPS.

Building the ROSC has taken time and commitment. During the pandemic, the ROSC has been challenged with learning to utilize videoconferencing tools and hosting virtual meetings, in an already technologically taxed region in rural Texas. The outcome has been increased collaboration and focus on the goals of increasing resources for prevention, treatment, and recovery for those with SUD. In October of 2020, the consortium was gathered via videoconferencing for an open discussion with immediate plans to move forward with ROSC development. The next month, a two-hour ROSC training for the consortium was hosted by the Statewide Opioid Coordinator of Texas with presentations by ROSC coordinators in adjacent areas. By December, a handful of stakeholders met over a virtual lunch to define plans for regularly scheduled meetings with educational activities and community workgroups. Since the beginning of 2021, the Golden Crescent ROSC has met on the second Wednesday of each month through video conferencing. The 45-minute virtual meetings include community updates on activities of the funded projects and a 15–20 minute presentation on a SUD/OUD topic followed by discussion. The virtual meetings allow attendance and convenience from across the Golden Crescent without a need for travel.

The recent success of the Golden Crescent ROSC has been the building of relationships. Existing partnerships have been leveraged to establish a consortium dedicated to expanding the capacity of the rural communities to address substance abuse, specifically OUD, and its tragic side effects. Local advertising has grown the consortium and ROSC meetings to almost 40 engaged stakeholders. We are currently attracting a variety of consortium members such as healthcare providers, social workers, community advocates and volunteers, substance use treatment providers, emergency services personnel (i.e. fire and prehospital emergency responders), investigators for child protective services, hospital and health clinic administrators, community health workers, law enforcement, and members of the recovery community as outlined in our proposed ROSC membership (**Figure 2**).

The immediate impact of the first few monthly ROSC meetings involved education on reducing stigma associated with SUD. Unintentional use of stigmatizing language was noted by first responders, health care providers, community members, and various stakeholders during the planning phase of the grant. The ROSC identified the need to address stigma and built this priority into the education component of each meeting. A virtual community town hall organized by the ROSC included a speaker from the recovery community to address stigma, language, and to witness the successes and challenges faced by those with SUD. Partnership with our own Texas A&M Opioid Taskforce for trainings and Naloxone kit distributions provided Opioid Overdose Education and Naloxone Administration (OENA), a 90-minute standardized intensive training to educate the community on opioid abuse and naloxone administration, which includes an introduction to non-stigmatizing language and naloxone rescue kit distribution. Adaptations have been made to accommodate virtual education sessions of the OENA.

A committed community coalition of stakeholders to address prevention, treatment, recovery, workforce needs, and existing gaps in SUD/OUD resources noted during the planning grant has been

solidified. The consortium has grown in momentum as well as in affiliations to a functioning ROSC. With time and continued collaboration, the ROSC will be a substantial network of resources for the Golden Crescent. The work together has shown that SUD/OUD is an important health issue and additional training is needed to promote community preparedness. Priority workforce and sustainability plans for education, training, and awareness are in progress for meeting immediate and future needs. In some ways, the COVID-19 pandemic has facilitated growth of the consortium through forced use of technology to collaborate. Video conferencing has facilitated growth and engagement. As momentum grows, the planning of what could happen is more solidified. The impact to the consortium in assessment, planning, and collaboration is powerful as we are moving forward from planning to implementation.

DISCUSSION

We aimed to develop an ROSC in the primarily rural Golden Crescent of Texas. We have succeeded in developing a Golden Crescent ROSC as a value-driven approach to structuring behavioral health systems and a network of clinical and non-clinical services and support. The ROSC aims to recognize recovery in the context of community health and wellness, focusing on services that are person-centered, individualized, strength-based, trauma-informed, inclusive of family, comprehensive, outcome-driven, and evidence-based.

Significant findings from the in-depth community assessment pointed to numerous challenges in providing and accessing any services for SUD. These challenges have been heightened with the COVID-19 pandemic. However, rapid adaptations in consideration of the pandemic resulted in the progress of a resilient community consortium in building an ROSC in the Golden Crescent of Texas.

The key to our success has been a focus on relationships. Over the year-long planning period we engaged in monthly conference calls, produced newsletters, co-hosted town hall meetings, conducted online surveys, and met with multiple stakeholder groups for interviews and discussions. We listen, share, and engage in dialogue pertinent to the community's needs. This engagement is our greatest accomplishment and will lead to implementation success.

The next steps include a robust media campaign to introduce and engage the community and recruit a diverse group of stakeholders (**Figure 2**) to the ROSC. Support and guidance will be sought through consultation with regional ROSC facilitators in adjacent communities identified through Texas Health and Human Services. The ROSC will seek natural partnerships with county and state agencies as it begins to meet regularly and build momentum. Momentum has been established to strengthen and expand SUD/OUD prevention, treatment, and recovery services to enhance the rural communities' ability to access treatment and move towards recovery.

ACKNOWLEDGMENTS

This publication/program is supported by the Health Resources and Services Administration (HRSA) of the U.S. Department of Health and Human Services (HHS) as part of financial assistance awards totaling $1,700,000 with 100% percentage funded by HRSA/HHS and $0 amount and 0% percentage funded by non-government source(s). The contents of the article are those of the author(s) and do not necessarily represent the official views of, nor an endorsement, by HRSA/HHS, or the U.S. Government.

The projects would not be possible without the consortium members and community stakeholders who provided valued input into the strategies that are now in implementation. The community of focus has taught us to listen and provide a wealth of information to understand issues in order to construct and implement a feasible plan. We acknowledge the work of the consortium as true navigators within the community. Significant partnerships and relationships have blossomed during our project that have led to further collaborations and sustainable strategies to address substance related morbidity and mortality in the rural communities. This work is uniquely tailored by the community, for the community.

REFERENCES

1. B. F. Henry et al., “COVID-19, mental health, and opioid use disorder: Old and new public health crises intertwine,” Psychological Trauma: Theory, Research, Practice, and Policy 12, no. S1 (2020): S111–2. **http://dx.doi.org/10.1037/tra0000660.**

2. Paul J. Jannetto, "The North American Opioid Epidemic," Therapeutic Drug Monitoring 43, no. 1 (2021): 1–5. **https://doi.org/10.1097/FTD.0000000000000817.**

3. John Strang et al., "Opioid use disorder," Nature reviews Disease primers 6, no. 1 (2020): 1–28. **https://doi.org/10.1038/s41572-019-0137-5**.

4. "National survey on drug use and health," Substance Abuse and Mental Health Services Administration, 2016, **https://www.samhsa.gov/data/sites/default/files/NSDUH-DetTabs-2016/NSDUH-DetTabs-2016.htm.**

5. “HHS Acting Secretary Declares Public Health Emergency to Address National Opioid Crisis,” US Department of Health and Human Services Press Release: October 26, 2017, **https://www.hhs.gov/about/news/2017/10/26/hhs-acting-secretary-declares-public-health-emergency-address-national-opioid-crisis.html**.

6. Centers for Disease Control and Prevention, "Increase in fatal drug overdoses across the United States driven by synthetic opioids before and during the COVID-19 pandemic," CDC Health Alert Network, December 17, 2020, **https://emergency.cdc.gov/han/2020/han00438.asp**.

7. L. C. Palombi et al., “A scoping review of opioid misuse in the rural United States,” Annals of Epidemiology 28 no. 9 (2018): 641–52. **https://doi.org/10.1016/j.annepidem.2018.05.008**.

8. David Best et al., "Recovery networks and community connections: Identifying connection needs and community linkage opportunities in early recovery populations," Alcoholism Treatment Quarterly 35, no. 1 (2017): 2–15.

9. "HPSA Find," US Department of Health and Human Services, **https://data.hrsa.gov/site-map**.

10. Robert D. Ashford et al., "Building recovery ready communities: The recovery ready ecosystem model and community framework," Addiction Research & Theory 28, no. 1 (2020): 1–11. doi/full/10.1080/16066359.2019.1571191.

11. A. Azar and A. B. Giroir, "Strategy to combat opioid abuse, misuse, and overdose: A framework based on the five-point strategy," Department off Health And Human Services, 2018.

AUTHOR BIO

ELIZABETH M. KAPPIL ‘22

Elizabeth M. Kappil '22 is a pre-med public health major from Deer Park, TX. Elizabeth went to the Texas Academy of Mathematics & Science at UNT where she participated in undergraduate research pertaining to biomedical engineering. After coming to Texas A&M, Elizabeth conducted research on substance use disorder and opioid use disorder. After graduating, Elizabeth plans to pursue an M.D. and Ph.D. degree.

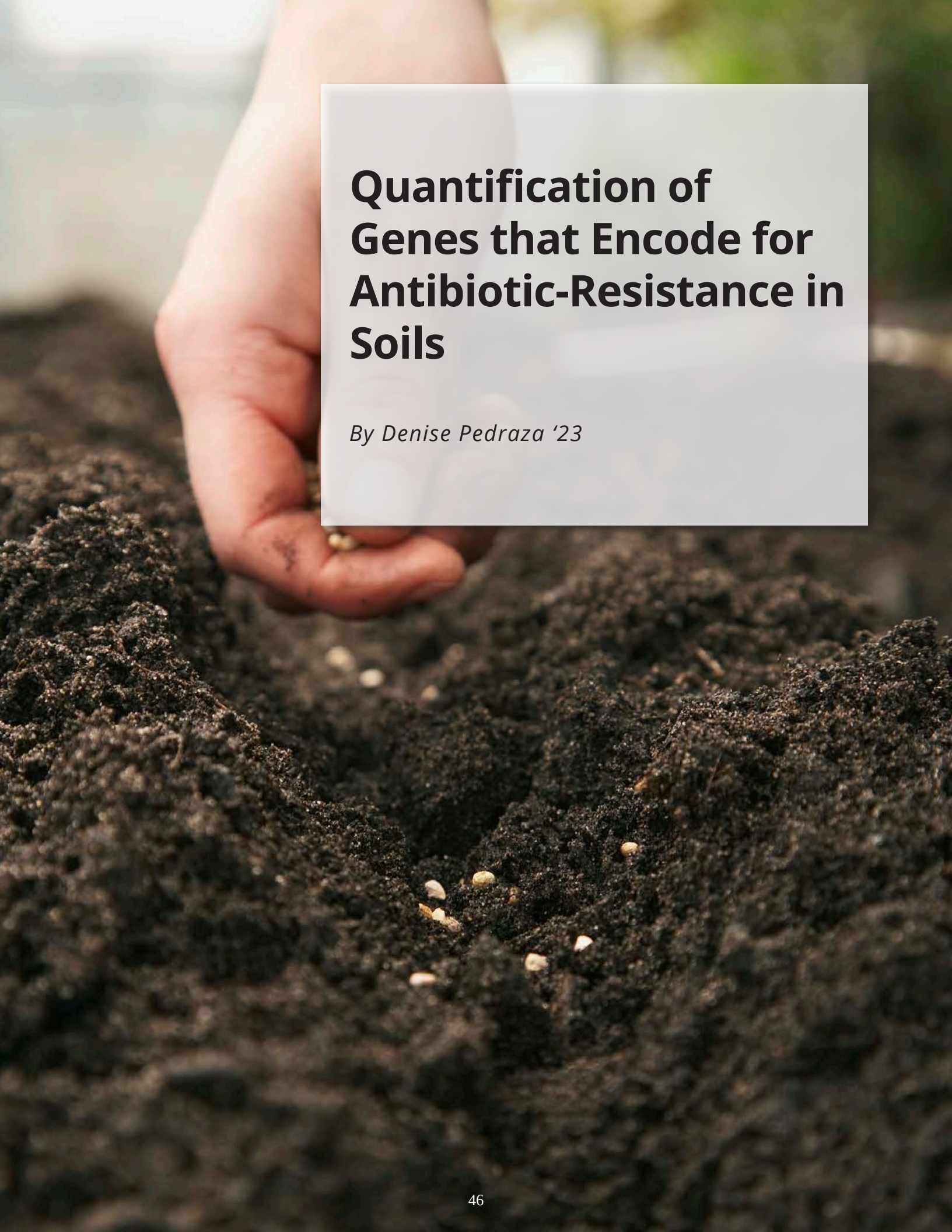

Quantification of Genes that Encode for Antibiotic-Resistance in Soils

By Denise Pedraza ‘23

INTRODUCTION

Antibiotic resistance has negative impacts since it decreases the effectiveness of antibiotics, and they no longer stop an infection caused by bacteria. Antibiotics are introduced into an environment through animal waste and other sources, which give rise to antibiotic resistant bacteria strains.[1] Since many animals are treated with antibiotics, their environment will usually have contact with these antibiotics too. With a given exposure of antibiotics comes a resistance to them, which is how the soil these animals interact with will contain antibiotic resistant genes. It has been observed that when the levels of antibiotics increase, the antibiotic-resistant bacteria and genes increase as well which leads to a greater risk of exposure to this bacteria when people work consistently with soils that are being treated with antibiotics.[2] Human contact with antibiotic-resistant bacteria in the environment can lead to infection.[3] Soils contaminated with antibiotics have been recognized as a threat for those working in the agricultural sector. Although there has been some research in antibiotic resistant genes there are few studies on soils, especially those using quantitative polymerase chain reaction (qPCR) or even digital droplet polymerase chain reaction (ddPCR). We hypothesized that with a defined concentration of antibiotics introduced to the soil there will be an increase in the resistance genes observed throughout a period, which can be determined through the quantification of specific antibiotic-resistant genes (ARG) in soils. Our work will aid in the work being done in this field, since we will be able to report problems we encountered and how we decided to troubleshoot.

METHODS

Sampling and experimental settings

Soils were collected from the Howdy Farm, placed in sterile containers and stored at 4 °C. Soils were exposed to the antibiotics Tetracycline (TC) and Sulfamethazine (SMZ) in experimental soil microcosms. Each microcosm, a small version of the original environment, consisted of glass vials containing soil plus the antibiotic. SMZ and TC were selected for the exposure experiments because they are commonly used in livestock facilities. The antibiotics given to livestock are found in the soil of these facilities through the animals' feces. Soil samples were obtained from the microcosms at day 0, 4, 6, 16, 35 and 56. DNA was extracted from the samples and tested for the presence and concentration of sul2, an antibiotic-resistant gene resistant to the antibiotic sulfonamide. It has been established that long-term use of an antibiotic will cause bacteria to develop resistance to not only that antibiotic, but to other antibiotics not associated with it, which is why we tested for sul2 in samples that were treated with TC (not related) and SMZ (related).[4]

SOILS CONTAMINATED WITH ANTIBIOTICS HAVE BEEN RECOGNIZED AS A THREAT FOR THOSE WORKING IN THE AGRICULTURAL SECTOR.

Real-time q-PCR of ARG in Soils

PCR is used to amplify DNA segments. Conventional PCR includes three temperature stages. The first is denaturing, where the DNA separates into two single strands due to the heat, which is 98°C for 2 minutes. The second is annealing where the primers attach to the DNA due to the decrease in temperature, 60°C, for 0.50 minutes. The third is extension, where the Taq polymerase enzyme makes new DNA strands due to the increase in temperature to 72°C for 2 minutes. The three stages are repeated for several cycles to achieve observable amplification of the DNA segment. The presence of the DNA segment is measured at the end.[5]

The main difference between PCR and qPCR is in the quantification of the resistance gene. In qPCR the fluorescence is measured at each amplification cycle. The fluorescence depends on how many copies of the gene are obtained. Since the dye binds to the DNA, the fluorescence will be detected proportionally to the

amount of amplified DNA.[6] qPCR helps determine the concentration of the DNA segment specific to the antibiotic resistance gene sul2 by setting up controls (or standards) with a range of known sul2, determining the cycle at which those concentrations produce fluorescence and comparing the cycle at which unknown samples produces fluorescence to the standards as seen in Figure 1. Since the standards are E. coli with the sul2 amplicon (191bp) cloned we already know their concentration (copy gene/ uL).

Quantification of the target resistant genes was done by qPCR in a LightCycler®96 System, the qPCR machine where reactions take place. Each qPCR reaction was conducted using PowerUp SYBR Master Mix [2X], template DNA from the samples and sul2 forward and reverse primers in a final volume of 10 µL as seen in **Table 1**. The primers used were previously reported.[7]

A total of 30 DNA soil samples were tested using a combination of six samples from the experiment with added TC, 12 samples with added SMZ, and 12 samples with no antibiotic added over the 56 days.

Table 1. *Volume for the components in a qPCR for one 10µL reaction . The PCR mix volume is 9µL for a subsequent sample input of 1µL/reaction. These components are needed in order for the DNA amplification to take place during the 3-step-amplification.*

Component	Volume (10 µL/ well)
Nuclease-Free Water	3.6
PowerUp SYBR Master Mix [2X]	5
Forward primer	0.2
Reverse primer	0.2
DNA template	1

Only six samples with added TC were used, because not all of the samples needed to be tested in order to find a correlation with this antibiotic and sul2. For the soil treated with SMZ and no antibiotic, samples of each time interval were tested to quantify the concentration of sul2 over time. For the soil treated with TC, samples of only three interval times (T0, T2, T5) were tested to see if there was a selection for bacteria that are resistant to several other antibiotics.

For each reaction, triplicates of the standards were included. Triplicates are important to see if the reaction can be replicated in the same environment and obtain similar results. Standards included serial 10-fold dilutions of the original strain from 1:1000 through 1:1000000, a negative sample without DNA, and the DNA extracted from soil samples. One µL of DNA and 9 µL of master mix was pipetted into each well. The temperature profile of the reaction in the LightCycler®96 System had conditions shown in **Table 2**.

During troubleshooting, cross contamination was an issue with the negative controls (the negative sample without DNA). Reactions were done under a clean bench to have a clean and sterilized environment; however, contamination in the non-template controls persisted. Although there was amplification, the threshold cycle (Ct) was higher than the most diluted standard. A limit of detection (LOD) was established to identify the lowest concentration of resistance genes that will be detected. If a sample had triplicates where two out of the three were negative or the Ct values lower than those of the negative controls, then they were defined as below the limit of detection (LOD) or negative. This means that although we would get positives in the negative controls if samples were below the set limit of detection, they will be considered negative for this experiment. This procedure was similar in a previous publication by Devarajan.[8] The absolute quantification settings in the LightCycler®96 System's program were set to a minimal end point fluorescence (EPF) to 0.2, which is appropriate for the dye used (PowerUp SYBR Master Mix).

Q-PCR standard curves and quantification

The log copy number of genes per µL DNA template solution for the calibration curve and the copy of genes/ gram of sediment were calculated using the previously published equation.[7] In this equation, when b is Avogadro's constant (6.022×10^23 mol), c is the

Table 2. *Profile for LightCycler® 96 Application software . The experiment run parameters have the following temperature profile for the heating and cooling cycles in order to achieve the 3-step-amplification of denaturing, annealing, and extension in order to amplify DNA segments. During the denaturing cycle the temperature needs to increase in order to separate the DNA into two single strands. Then, the temperature decreases during the annealing cycle in order for the primers to attach and finally for the extension cycle the Taq polymerase enzyme makes new DNA strands due to the increase in temperature.*

Programs	**Steps**			
Name	**Number of cycles**	**Duration (s)**	**Target (°C)**	**Acquisition Mode**
Preincubation	1	120	50	None
Preincubation	1	120	95	None
3-step amplification	40	15	95	None
		15	60	Single
		60	72	None
Melting	1	15	95	None
		60	60	None
		15	95	Continuous 7 readings/ °C

concentration of the target DNA (0.000322 (µg)/(µL)), L is the length of template containing the target gene (0.191kb), a is the weight of kb DNA per pmol (0.66 (µg)/pmol). The result of this equation with the data filled in from the experiment results in the copy gene/ µL DNA which is used for the calibration curve of the samples.

Equation 1

$$\frac{(copy\ gene)}{\mu L\ DNA} = \frac{(6.022\times10^{23}\,mol)(0.000322\frac{\mu g}{\mu L})}{(0.191kb)(0.66\frac{\mu g}{pmol})(10^{12})} = 9.18701 \rightarrow 10^{9.1870} = 1.53\times10^{9}$$

RESULTS

The DNA concentration found for the samples are shown in **Figure 2**. The detection limit for each gene was determined by the standard that was most diluted and a Ct value was still defined. We defined the concentration in the samples under the orange line seen on **Figure 2** to be negative, since they were below the limit of detection (LOD). Although fluorescence occurred, meaning that the sample has a concentration of ARG, it is too low to quantify. In **Figure 2**, TC corresponds to the samples with the antibiotic TC added to the soil, SMZ to the samples with SMZ added, and C-0 are the samples with no antibiotics added. Resistance to sulfonamides (sul2) for TC was not observed for times 0a, 2a, and 5b; however, it was detected for all samples in SMZ and C-0. Additionally, we found that the results of the samples with no antibiotic added were like those with SMZ.

The error bars in the bar graphs (**Figure 2**) were calculated by the difference between the average of the triplicates minus the lowest concentration for the negative error and the difference between the maximum concentration and the average of the triplicates for the positive error.

CONCLUSION

Although the findings are preliminary, results show that the introduction of antibiotics in soils may

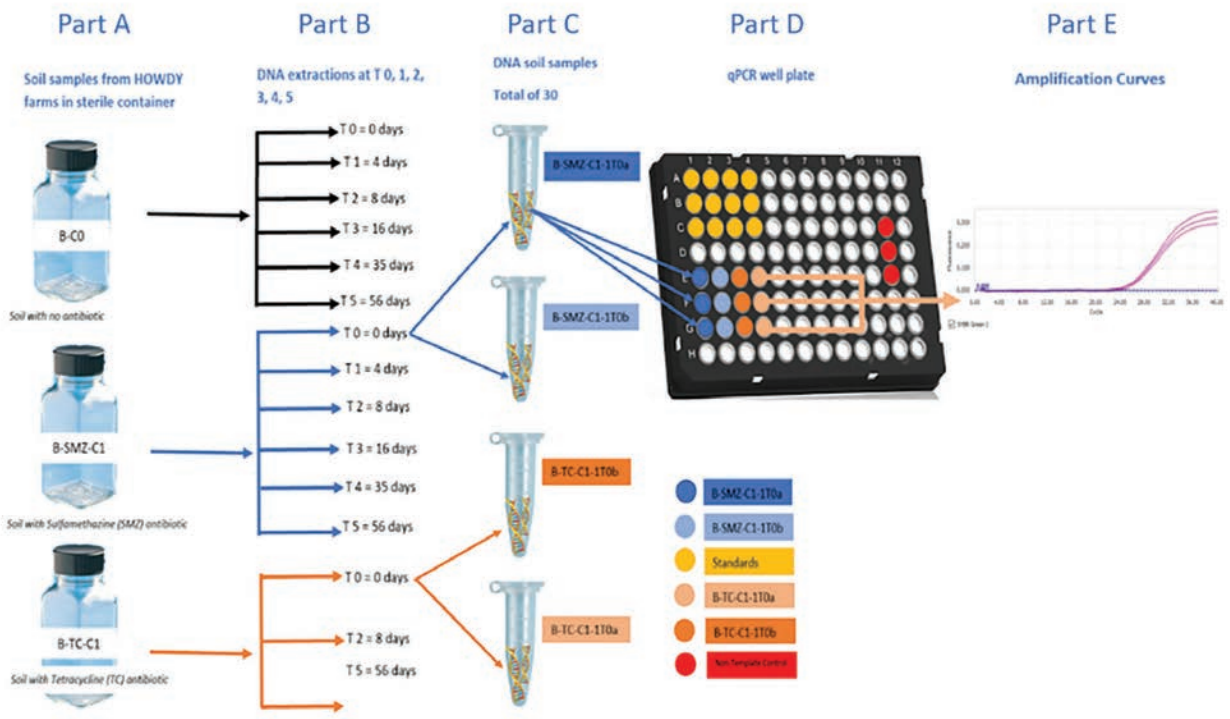

Figure 1. *Overview of experiment. In part A of the figure are the sterile containers with the soils that were collected. In part B the DNA was extracted at different times from each container. In part C two samples were taken from the extractions of one time. For each DNA soil sample in the qPCR reaction triplicates were pipetted in the well plate as well as standards and non-template controls as seen in part D. After the qPCR reaction, we obtain amplification curves as seen in part E where we are then able to determine the concentration of the genes. Image of well plate by Brooks Life Science.9 Image of microcentrifuge tube by ThermoFisher Scientific.10 Image of sterile container by Kimble Kontes.*[11]

Figure 2. *Results of microcosms using Howdy Farm soil.*

influence antibiotic-resistance development. However, we must conduct more tests under differing conditions. If a positive correlation is observed in further studies, results would be especially concerning for agricultural workers who work with soils. Future directions for the progress of this experiment are to test the samples in a digital droplet PCR to compare quantification of the antibiotic-resistance gene sul2 in the soil samples using two different technologies. For improvements of this experiment getting the cross contamination to a minimum would help in determining a more accurate limit of detection. Another limitation of this experiment is the number of antibiotic resistant genes being used. In the continuation of this experiment more ARG's will be tested against the soil samples. A point of interest could be to examine the soil type (sandy, muddy, etc.) and see if there is some correlation with the DNA concentration.

ACKNOWLEDGMENTS

I would like to thank Dr. Mendoza for inspiring my interest in this experiment and for her guidance throughout my research journey. For this, I am extremely grateful. Financial support was provided from Texas A&M Triads for Transformation and the Feasibility Studies Program at Southwest Center for Agricultural Health, Injury Prevention, and Education through Cooperative Agreement # U54-OH007541 from CDC/NIOSH and Texas A&M T3 Award. Antibiotic resistance in soils after flooding events.

REFERENCES

1. J. C. Chee-Sanford et al., "Fate and transport of antibiotic residues and antibiotic resistance genes following land application of manure waste," Journal of Environmental Quality 38, no. 3 (2009): 1086–108. **https://doi.org/10.2134/jeq2008.0128.**

2. M. Pan and L. M. Chu,"Occurrence of antibiotics and antibiotic resistance genes in soils from wastewater irrigation areas in the Pearl River Delta region, southern China," Science of The Total Environment 624, (2018): 145–52. **https://doi.org/10.1016/j.scitotenv.2017.12.008.**

3. R. Nair et al., "Prospective multicenter surveillance identifies Staphylococcus aureus infections caused by livestock-associated strains in an agricultural state," Diagnostic Microbiology and Infectious Diseases 85, (2016): 360–6. **https://pubmed.ncbi.nlm.nih.gov/27198741/.**

4. J. Davies and D. Davies, "Origins and evolution of antibiotic resistance," Microbiology and Molecular Biology Reviews. 74, no. 3 (September 2010): 417–33. **https://doi.org/10.1128/MMBR.00016-10**.

5. "What is PCR (polymerase chain reaction)?," yourgenome.org, 2016, accessed March 11, 2021, **https://www.yourgenome.org/facts/what-is-pcr-polymerase-chain-reaction**.

6. "Real-time PCR (qPCR) technology basics," Bio-Sistemika, 2017, accessed March 11, 2021, **https://biosistemika.com/blog/qpcr-technology-basics/**.

7. R. Pei et al., "Effect of river landscapes on the sediment concentrations of antibiotics and corresponding antibiotic resistance genes (ARG)," Water Research 40 (2006): 2427–35. **https://pubmed.ncbi.nlm.nih.gov/16753197/.**

8. N. Devarajan et al., "Accumulation of clinically relevant antibiotic resistance genes, bacterial load, and metals in freshwater lake sediments in Central Europe," Environmental Science & Technology. 49, no. 11 (June 2, 2015):6528–37. **https://doi.org/10.1021/acs.est.5b01031**.

9. "FrameStar® 96 Well PCR & qPCR Plates," Brooks Life Science, accessed March 14, 2021, **https://www.brookslifesciences.com/products/framestar-96-well-plate**.

10. "Snap Cap Low Retention Microcentrifuge Tubes," ThermoFisher Scientific, accessed March 14, 2021, **https://www.thermofisher.com/order/catalog/product/3453#/3453.**

11. Kimble Kontes, "Kimble/Kontes Bottle Sq Tablet 1OZ CS288 5910133B | 31% Off w/ Free S&H" opticsplanet.com, accessed March 14, 2021, **https://www.opticsplanet.com/kimble-kontes-bottle-sq-tablet-1oz-cs288-5910133b.html.**

AUTHOR BIO

DENISE PEDRAZA '23

Denise Pedraza '23 is a biology major from McAllen, Texas who went to McAllen Memorial High School. Denise is motivated to help her community through her research findings and plans on continuing with her research and furthering her education.

An Egg-cellent Substitute for the Traditional Animal Model

By Hanna L. Hudson '21, Madilyn L. Feik '21, Brooke C. Grieme '21, Eileen Y. Chen '21, Jocelyn N. Mata '22, Robert T. Hayes '21

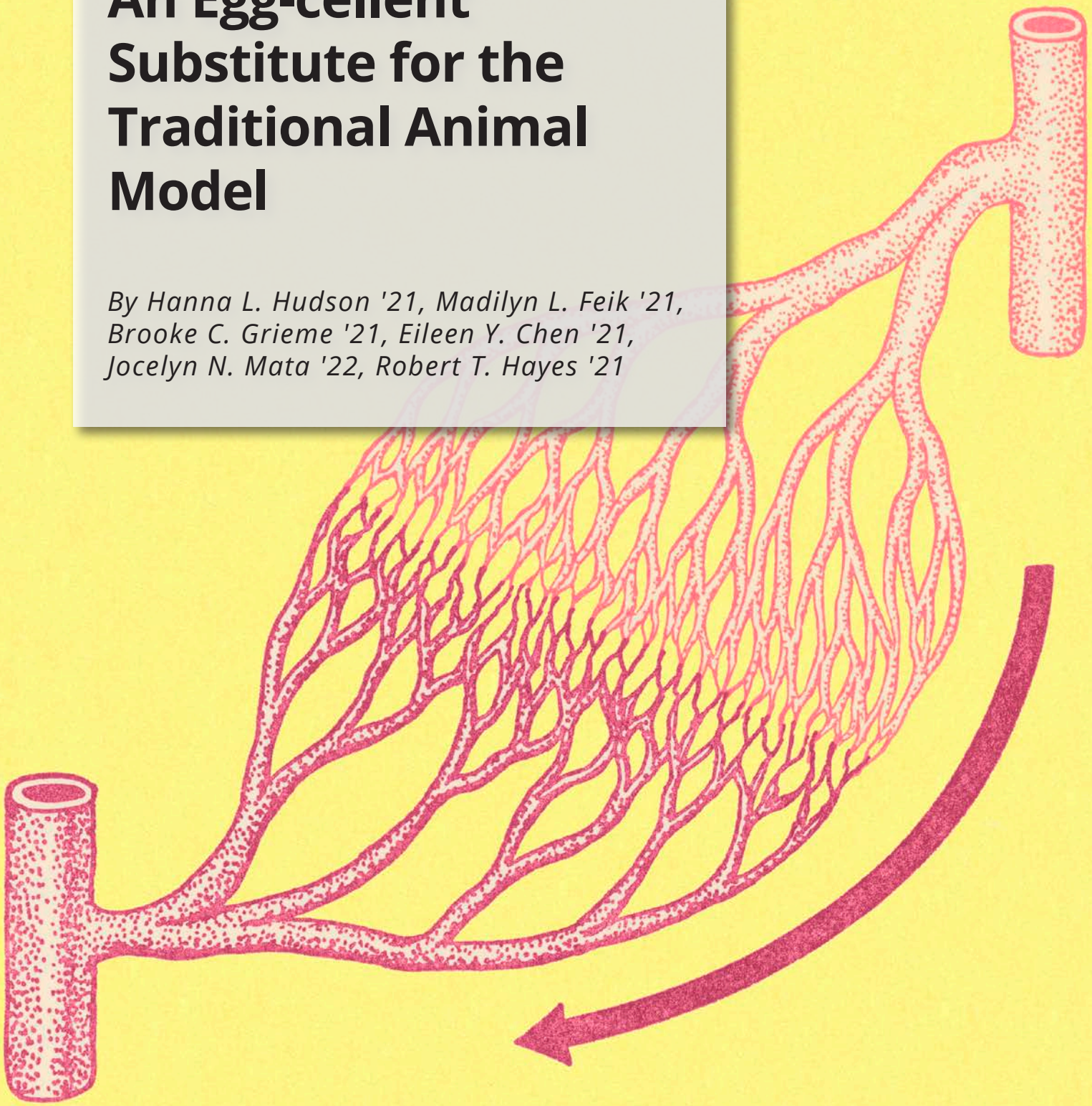

Aspartame (APM) is a widely used sugar substitute in many foods, beverages, and medications. It is most notably found in popular zero calorie drinks such as diet sodas. The sweetener is known to be harmful in large doses, but the effect of low doses of APM found in commonly consumed foods and beverages is less studied. To quantify the potential adverse effects of low-dose APM, a better method of investigation is needed to closely observe blood vessels over consecutive days.

APM affects the endothelial cell lining in the interior portion of blood vessels. Endothelial cells secrete nitric oxide through endothelial nitric oxide synthase (eNOS) to dilate blood vessels and increase blood flow. APM is immediately catabolized into three metabolites in the small intestine in mammals: 50% phenylalanine, 40% aspartic acid, and 10% methanol. APM metabolites downregulate eNOS function in high doses, decreasing the amount of nitric oxide available to dilate blood vessels.[1] APM is also potentially dangerous because it increases mitosis in endothelial cells which remodels the vasculature.[2] Microvascular tone, growth, and remodeling regulate endothelial shear stress, defined as the force of flow tangential to the wall of the blood vessel, in responses to changes in blood flow.[3] APM increases vascular endothelial growth factor (VEGF) release,[4] causing large elastic arteries to adapt to changes in blood flow through the modulation of vascular tone.[5,6] Although APM is known to be harmful in high doses, it is important to investigate APM's effect in lower doses common to human consumption. APM increases endothelial cell proliferation in vessels that elongate to relieve stress, rapidly establishing new blood vessels.[7] This abnormally rapid microvascular network development rapidly increases blood flow.

Conventional animal models used to evaluate subtle changes in microvascular radii and tone have severe limitations. Most animal models require multiple surgeries and vessel removal for observation. These surgical interventions require anesthesia which manipulates blood vessel radius, flow, and vascular tone. Additionally, it is difficult to monitor small vessels in conventional animal models. Shear stress increases during surgery which may cause vessel constriction or

...A BETTER METHOD OF INVESTIGATION IS NEEDED TO CLOSELY OBSERVE BLOOD VESSELS OVER CONSECUTIVE DAYS.

complete blockage of the vessel. Post-surgical inflammation alters vessel size by causing some vessels to dilate and some vessels to constrict, artificially resulting in zero net change.[8] Conventional animal models are also difficult to manage when they depend on the subject remaining compliant.[9]

An alternative animal model explored in this experiment is the Chick Chorioallantoic Membrane (CAM) model using in-vitro chicken eggs. With minimal manipulation, the CAM model allows measurement of both acute and chronic changes in microvascular radii in response to changes in blood flow over consecutive days. The easily accessible and extensive microvascular network in the CAM model is shown in

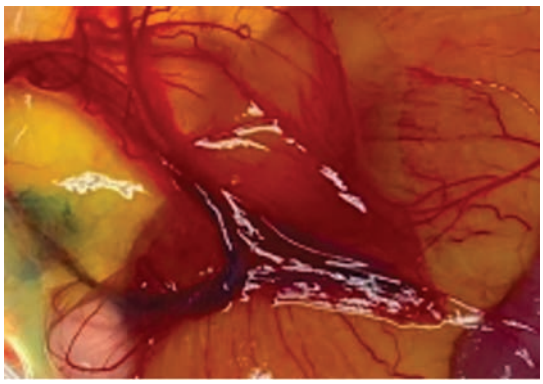

Figure 1. *Microvasculature of the Chick Chorioallantoic Membrane (CAM) model.*

Figure 1. In vitro chicken eggs have a high offspring yield, short generation time, and are inexpensive.

The CAM model is useful for studying shear stress and microvascular tone because the avian ge-

nome is homologous to the human genome.[10] The CAM vasculature is constantly developing and changing, so significant changes in microvascular radii, flow, and tone can be measured in a short period of time. Vessel adaptation can be observed through rapid changes in flow in the CAM. The purpose of the present work is to investigate the most efficient methods for injection into and incubation of the CAM to compare the CAM model's viability to conventional animal models. A viable CAM preparation method will help determine the effects of low-dose APM on endothelial cell progression in the future.

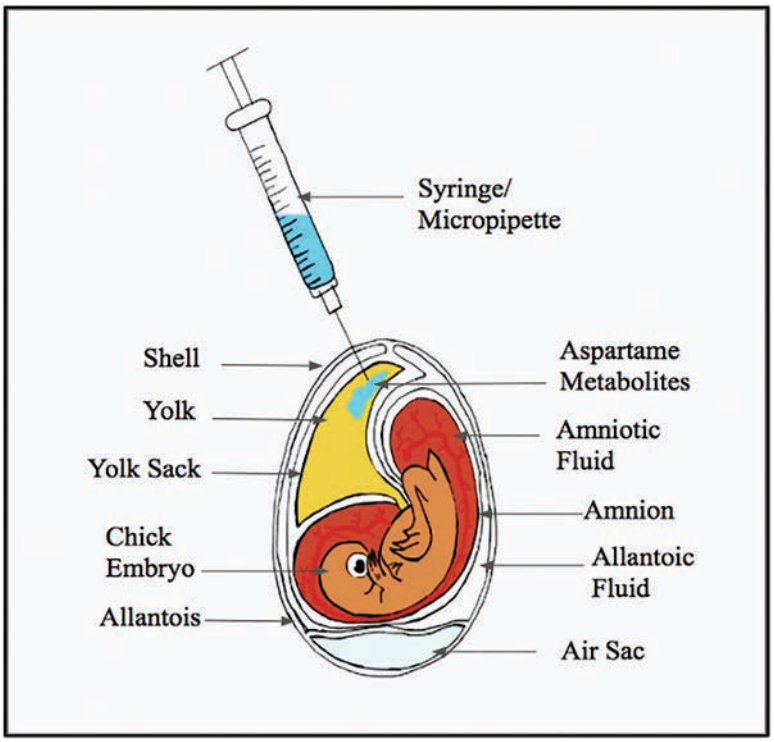

Figure 3. *Injection technique using the venting preparation method.*

METHODS

Fertilized White Leghorn chicken eggs were obtained from the Texas A&M University Poultry Science Department. Before intervention, the eggs were placed in an incubator at 37.7°C and 40 ± 1% humidity. The incubator automatically rotated the eggs to minimize adherence between the CAM and the inner shell membrane. Eggs were removed from the incubator and sterilized with chlorhexidine, ethanol, and iodine, respectively, to eliminate bacterial contamination on the outside of the shell. Eggs were divided into control and experimental groups.

To examine the most efficient method of injection into the CAM model, three methods of preparation were considered as shown in **Figure 2**: windowing, hammocking, and venting. In the windowing preparation method, a 2.5 cm hole was created in the shell of the egg superior to the yolk using tweezers. The hole was then covered by sterilized parafilm. In the hammocking method, the shell of the egg was cracked horizontally to completely remove the embryo, and the egg was placed on a sterilized strip of parafilm suspended over a water bath. The entire apparatus containing the water bath and suspended embryo was then covered with sterilized parafilm and the embryo was observed over consecutive days. In the venting preparation method, the yolk was located within each egg using a Novaflex fiber optic illuminator to position them for proper injection. A 1 mm hole was created in the shell of the egg superior to the yolk using tweezers without breaking the membrane and the hole was covered by parafilm to maintain a sterile environment as the embryo grew.

To clearly examine development of the vasculature, a bright Trypan Blue solution was injected into

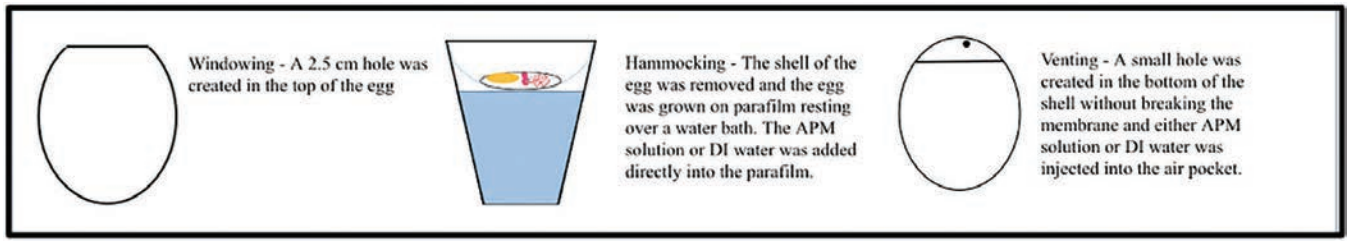

Figure 2. *Methods of preparation considered for microvascular injection.*

the yolk. Forty µL of 0.4% Trypan Blue solution with similar viscosity to the yolk was administered with a micropipette suspended 2 mm through the yolk sac. A micropipette containing 40 µL of 0.9% saline solution was injected into the yolk of the control eggs in the same manner. **Figure 3** details the injection technique using the venting preparation method. The egg was oriented with the air sac at the bottom so the yolk would span the top of the egg. Injection into the yolk of the egg maximized dye uptake into the microvasculature across samples. In the windowing and hammocking preparation methods, the Trypan Blue solution was similarly injected into the more visible yolk.

After injection, the eggs were placed back into the incubator so they could continue developing. The Trypan Blue solution was sealed to avoid contamination and stored at room temperature to maintain its stability. Following intervention, eggs were kept in the incubator for seven days to allow adequate vasculature development and Trypan Blue solution movement throughout the blood vessels. Experimental and control eggs were intermingled randomly within the incubator to ensure that the groups were not influenced by local incubator differences.

To compare vessel development and Trypan Blue dye movement, the embryos from each of the three preparation methods were successively compared. On the seventh day after fertilization, the embryos prepared with the windowing and venting methods were removed from their shells. Each embryo was placed into a petri dish lined with plastic wrap to allow for easy positioning and manipulation for viewing. The embryos were viewed using an Olympus SZX12 stereo microscope with a Basler ace USB 3.0 camera and a Novaflex fiber optic illuminator on its lowest brightness level. Due to natural vessel constriction and dilation in response to a new environment, five minutes were allowed to pass between removal of the embryos from the incubator and analysis of the vessels under the microscope to standardize the exposure of the embryos to the environment.

A VIABLE CAM PREPARATION METHOD WILL HELP DETERMINE THE EFFECTS OF LOW-DOSE APM ON ENDOTHELIAL CELL PROGRESSION IN THE FUTURE.

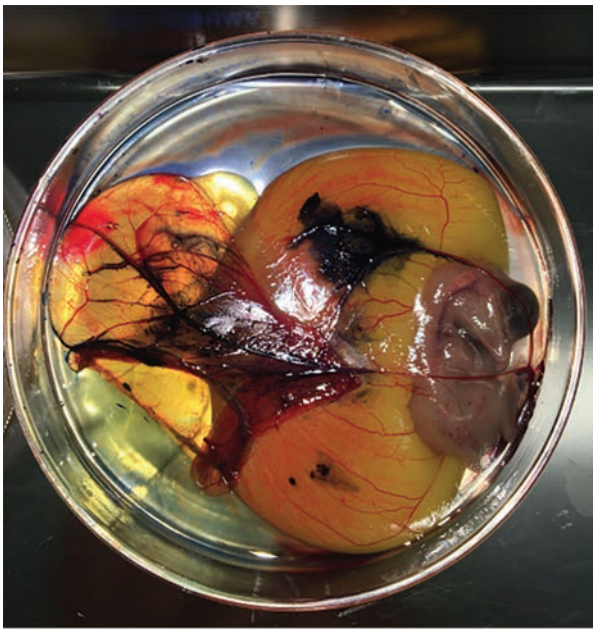

Figure 4. *Dye uptake into vessels.*

The umbilical artery is large and easy to visualize, therefore, it was used to detect changes within the CAM model with clear visualization of vasculature and blood flow. **Figure 4** shows optimal dye uptake into the umbilical artery and its branching vessels. Vessel diameter was measured under one of three randomly assigned conditions: without treatment, vasoconstrictor treatment to decrease vessel diameter, or vasodilator treatment to increase vessel diameter. The microvasculature of each embryo was measured before and after treatment using a video caliper and stage micrometer. The stage micrometer measurement on the stereo microscope was used as a point of reference for vessel changes.

The data collected via intravital microscopy

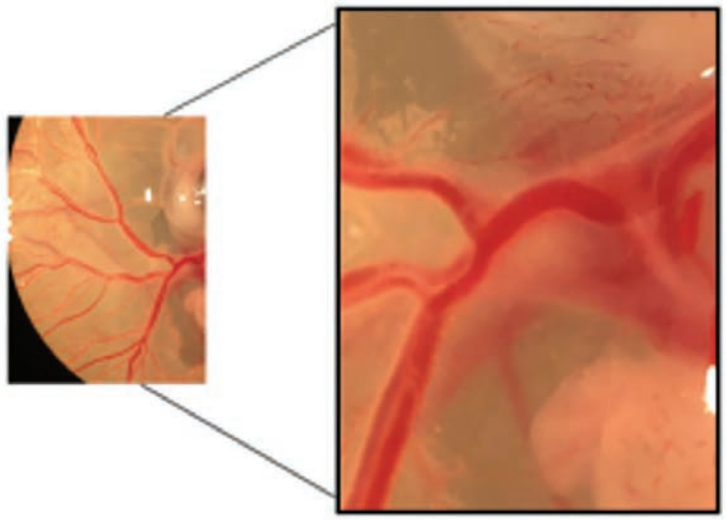

Figure 5. *Parent and daughter vessel branching radii analyzed with Murray's Law.*

was compared to Murray's law, which relates the radii of daughter branches to parent branches to determine standardized vessel branching.[11] A parent vessel with two daughter branches is shown in **Figure 5**. The standard deviation was calculated from the measured diameters of the umbilical artery both before and after vessel diameter treatment. The standard deviation from the first daughter branches of the umbilical artery was calculated under the same conditions. A chi-square statistical test was used to find standard deviation in comparison to Murray's Law. Currently, these values continue to be compared to the measurements for minimum and maximum vessel radii.

THE CAM MODEL WAS FOUND TO BE A VIABLE ALTERNATIVE TO CONVENTIONAL ANIMAL MODELS TO EVALUATE MEMBRANE MICROVASCULATURE AND VESSEL DEVELOPMENT.

RESULTS

After comparing the three CAM preparation methods, venting was determined to be the most viable ex-ovo preparation method. The advantages and disadvantages of the three preparation methods are summarized in **Table 1**. In the venting preparation method, dye injection through a small hole in the shell minimized manipulation of the CAM and prevented embryo contact with the outside environment, reducing contamination. Venting was the most effective method for Trypan Blue dye uptake and the method least susceptible to infection during development. While hammocking offered high visibility of the embryo during growth, it was the most susceptible method for infection. The microvasculature of embryos prepared with the hammocking method oftentimes grew significantly less and showed minimal dye circulation. When compared to venting and hammocking, the windowing method showed intermediate dye uptake, but the embryo was still susceptible to infection during development and required high disruption of the embryo for measurement.

In each of the three preparation methods, consistent transillumination and injection site precision were maintained. Standardized transillumination methods ensured that microvascular growth was observed accurately. Injection site precision helped ensure that the metabolites entered the embryo in the same manner. Consistent sanitation techniques were used to keep the eggs viable and healthy throughout incubation.

CONCLUSION

The CAM model was found to be a viable method to analyze changes in microvasculature and observe Trypan Blue dye uptake. The CAM model was used in a novel way to determine vessel branching

Table 1. *Advantages and disadvantages of the three preparation methods.*

Method Type	Advantages	Disadvantages
Venting	· Most successful Trypan Blue dye uptake · Least susceptible to infection · Lowest disruption of the embryo during treatment	· High disruption of the embryo for measurement · Low visibility of the embryo during growth
Hammocking	· Least disruption of the embryo for measurement · High visibility of the embryo during growth	· Highest susceptibility to infection · Highest disruption of the embryo during treatment · Least successful Trypan Blue dye uptake
Windowing	· Low disruption of the embryo during treatment · Intermediate Trypan Blue dye uptake	· High susceptibility to infection · Low visibility of the embryo during growth · High disruption of the embryo for measurement

patterns and teratogenic potential. After the development period, the dye progressed from the yolk into the microvasculature of each embryo, but the venting preparation method most effectively circulated Trypan blue dye and was the least susceptible to infection.

Using each of the three preparation methods, APM metabolites and other solutions' effect on shear stress and endothelial cells could be quantified with a velocimeter without disturbing the egg. APM is immediately catabolized into three metabolites in the small intestine in mammals: 50% phenylalanine, 40% aspartic acid, and 10% methanol. By replicating this cycle in the CAM model, the physiological effects of aspartame metabolites can be examined in order to determine if the minimal safe dosage of aspartame should be corrected. Using the venting preparation method, APM will be injected through a small hole in the posterior region of the egg where the yolk resides, resulting in a higher concentration in the region of interest and lower concentration throughout the rest of the body.[12,13] This method can also help evaluate how APM metabolites' effect on eNOS relates to inducible Nitric Oxide Synthase (iNOS).

The CAM model was found to be a viable alternative to conventional animal models to evaluate membrane microvasculature and vessel development. If APM's effect on shear stress and endothelial cells can be successfully measured in the chick CAM model using the venting preparation method, the effects of other metabolites can likely be studied in the same manner. Furthermore, the CAM model can be used to observe the effects of APM and other metabolites on embryonic development through an extended period, and daily observations can be noted without anesthesia. The injection procedures used in the CAM model have the potential to revolutionize the way in vitro studies are completed in the future.

REFERENCES

1. R. C. Jin and J. Loscalzo, "Vascular Nitric Oxide: Formation and Function," Journal of Blood Medicine 2010, no. 1 (2010): 147–62, **https://doi.org/10.2147/jbm.s7000**.

2. R. Alleva et al., "In Vitro Effect of Aspartame in Angiogenesis Induction," Toxicology in Vitro 25, no. 1 (2011): 286–93, **https://doi.org/10.1016/j.tiv.2010.09.002**.

3. J. J. Paszkowiak and A. Dardik, "Arterial Wall Shear Stress: Observations from the Bench to the Bedside," Vascular and Endovascular Surgery 37, no. 1 (2003): 47–57, **https://doi.org/10.1177/153857440303700107**.

4. Y. S. Chatzizisis et al., "Role of Endothelial Shear Stress in the Natural History of Coronary Atherosclerosis and Vascular Remodeling," Journal of the American College of Cardiology 49, no.

25 (2007): 2379–93, https://doi.org/10.1016/j.jacc.2007.02.059.

5. A. R. Pries, B. Reglin, and T. W. Secomb, "Structural Response of Microcirculatory Networks to Changes in Demand: Information Transfer by Shear Stress," American Journal of Physiology-Heart and Circulatory Physiology 284, no. 6 (2003): H2204–12, https://doi.org/10.1152/ajpheart.00757.2002.

6. N. Resnick et al., "Fluid Shear Stress and the Vascular Endothelium: for Better and for Worse," Progress in Biophysics and Molecular Biology 81, no. 3 (2003): 177–99, https://doi.org/10.1016/s0079-6107(02)00052-4.

7. Alleva et al., "In Vitro," 286–93.

8. S. M. Seyed Jafari et al., "Improvement of Flap Necrosis in a Rat Random Skin Flap Model by In Vivo Electroporation-Mediated HGF Gene Transfer," Plastic and Reconstructive Surgery 139, no. 5 (2017): 1116e–27e, https://doi.org/10.1097/prs.0000000000003259.

9. R. M. Dongaonkar et al., "Venomotion Modulates Lymphatic Pumping in the Bat Wing," American Journal of Physiology-Heart and Circulatory Physiology 296, no. 6 (2009): H2015–21, https://doi.org/10.1152/ajpheart.00418.2008.

10. M. Giannaccini et al., "Non-Mammalian Vertebrate Embryos as Models in Nanomedicine," Nanomedicine: Nanotechnology, Biology and Medicine 10, no. 4 (2014): 703–19, https://doi.org/10.1016/j.nano.2013.09.010.

11. C. D. Murray, "The Physiological Principle of Minimum Work: I. The Vascular System and the Cost of Blood Volume," Proceedings of the National Academy of Sciences 12, no. 3 (1926): 207–14, https://doi.org/10.1073/pnas.12.3.207.

12. Alleva et al., "In Vitro," 286–93.

13. S. L. Burgert et al., "Metabolism of Aspartame and Its 1-Phenylalanine Methyl Ester Decomposition Product by the Porcine Gut," Metabolism 40, no. 6 (1991): 612–18, https://doi.org/10.1016/0026-0495(91)90052-x.

AUTHOR BIOS

JOCELYN N. MATA '22

Jocelyn Nicole Mata is a biomedical sciences major with a minor in psychology from Houston, Texas. Jocelyn has been an advocate for Brazos county's Sexual Assault Resource Center for two years and is a part of A&M's Aggie Research Program. Jocelyn plans to further her education by attending medical school in hopes of specializing in psychiatric medicine.

EILEEN Y. CHEN '21

Eileen Chen is a biomedical science major with a certificate in biomedical research from Sugar Land, Texas. During her sophomore year, she began her research journey and in her junior year, she was a part of two research teams. Eventually, she became a research team leader for a group of undergraduates. She plans on attending medical school and using her background in research to contribute to the medical field.

HANNA L. HUDSON '21

Hanna Lee Hudson is a Biomedical Sciences major from Waco, Texas. She has minors in Public Health and Spanish and certificates in Biomedical Research & Development and Cultural Competency & Communication in Spanish. Hanna was the leader of her research team studying novel experimental models and aspartame, driven by the desire to further current medical knowledge and the safety of the community. She aspires to be a physician and will be moving to Conroe with her husband, Jacob, in order to attend Sam Houston State University College of Osteopathic Medicine after graduation.

BROOKE C. GRIEME '21

Brooke Grieme is a Biomedical Sciences major, Spanish minor with a certificate in Biomedical Research from Corpus Christi, Texas, where she attended London High School. Research was a way for Brooke to apply the knowledge she had gained in the classroom to her project in the lab. She immensely enjoyed spending time in lab where she was able to evolve her experiment until it was able to produce the best results possible.

MADILYN L. FEIK '21

Madilyn Feik is a biomedical sciences major with a neuroscience minor, public health minor, and biomedical research certificate from Houston, Texas. Her left brain and right brain get along well; she has enjoyed combining her passions for writing, neuroscience, and animal model optimization in her two undergraduate research projects. After graduating, Madilyn plans to earn her Doctor of Medicine degree and prioritize research while working in the medical field.

ROBERT T. HAYES '21

Robert Trenton Hayes at Texas A&M University, is a biomedical sciences major from Corsicana, Texas who attended Corsicana High School. Robert joined the biomedical research certificate program with hopes of exploring the effects of consumable chemicals and inspiring others to do the same. Robert hopes to attend medical school in Texas and become a doctor with a dedication to individuals with special needs like his brother.

Analysis of Fin Whale Lunge-Feeding in Southern California Using Multisensory Biotags

By Leah K. Bogan '21

INTRODUCTION

Oceanic research challenges

The Earth's oceans are a mysterious and complex network of systems driving the planet's many vital processes. These remote regions truly are the last frontiers of scientific research, the adage still holds: we know more about the surface of the moon, maybe our entire solar system, than we do our oceans. The depth, pressure, darkness, and salinity converge into a perfect storm, essentially obscuring almost 70% of our planet from study.[1] Consequently, it is difficult to quantify population size for some of the largest creatures that reside there. In fact, new populations of whales are continuously being discovered. Without an accurate count, it is a challenge to measure, and more importantly exemplify, which conservation efforts are successful and where modification is still needed.

Modern breakthroughs in marine mammal study have been primarily due to the advancement of multi-sensory biotags. Although this technology has streamlined methodologies, marine animal research continues to be an expensive undertaking. In addition, with an increase in the ability to gather data necessitates the accumulation and storage of data. Data processing and visualization in this field has quickly become as much of a limitation as a goal.[2] Prioritizing data that has the most intersections of value is of particular importance in these cases. The objective for this work is to highlight viable short-term solutions for whale conservation in areas with high ship traffic and feeding whales. This has caused an uptick in annual ship-strikes worldwide, a leading cause of fatalities for the larger baleen whales.

Dynamics of multisensory biotags

Marine animal research has undergone significant advancements in recent decades. Biotag innovations have expanded how marine research is conducted, particularly for whales and deep-diving pinnipeds. The tags contain customizable sensors and recording equipment designed to be affixed to the dorsal side of a whale. Biotag data offers a non-invasive way to observe the animals they are attached to for a few hours or up to several days. Acoustics, acoustical telemetry, and multisensory bio-readings capitalize on the physical properties of water to "see" with sound where visual observation ends.

BIOTAG DATA OFFERS A NON-INVASIVE WAY TO OBSERVE THE ANIMALS THEY ARE ATTACHED TO FOR A FEW HOURS OR UP TO SEVERAL DAYS.

Balaenopterids compared to other whales

Within the recently reconfigured Cetartiodactyla order, there are two suborders of whale: mysticetes, or baleen whales, and odontocetes, toothed whales. Baleen whales have keratin plates instead of teeth which are used for straining small crustaceans or schooling fish from the water. Within the suborder Mysticeti is the family Balaenopteridae whose members may prove to exhibit the "greatest biomechanical action in the animal kingdom." [3]

This biomechanical action is a specialized form of filter-feeding known as lunge-feeding. Lunges require an exceptional amount of energy to produce the extreme physical transformation necessary to feed in this way. An almost reptilian-shaped head and a distinct set of jaw joints allow an up-to 90-degree gape, which inflates the buccal cavity, or throat, like a parachute. This morphology and behavior is found only in balaenopterids. During a lunge as much as 70,000 liters of water is forced into a whale's mouth within just a few seconds. The drag generated from this action, inverts the tongue and expands ventral pleats to as much as four times their resting size allowing the whales to forage up to a ton of krill a day.[4]

QUANTIFYING A WHALE'S LUNGE-FEEDING PROVIDES INFORMATION ON VITAL STATISTICS, FORAGING TIME, ENERGY STORES, AND OTHER COMPLEX PHYSIOLOGICAL PROCESSES.

Quantifying a whale's lunge-feeding provides information on vital statistics, foraging time, energy stores, and other complex physiological processes. Feeding is also when baleen whales, which are among the larger whales, are especially vulnerable to ship strikes. This is particularly true at night when visibility is further reduced. Many baleen whale populations are in recovery, however, the populations of grays, blues, and fins that migrate annually through the southern California bight still have critically low numbers. Currently, most efforts to estimate whale populations are typically based on irregular surface counts, passive acoustic monitoring, and centuries-old whaling data.[5] Continuing to develop a more precise understanding of how, where, and when baleen whales feed, would lay the groundwork for shifting focus to probabilities based on density estimates rather than population counts.

Balaenopterids and krill

Krill are a small red crustacean and are the primary source of food for many animals in the ocean. These tiny crustaceans are found in abundance in areas with strong upwelling such as off the southern coast of California.[6] Upwelling is typically a coastal occurrence but also happens along the equator or anywhere surface water is displaced by nutrient-rich water from the deep. This process of upwelling seeds the higher trophic levels with organic detritus and other nutrients, combining with sunlight at the surface, causing massive blooms of phytoplankton. These blooms result in great swarms of grazing krill.

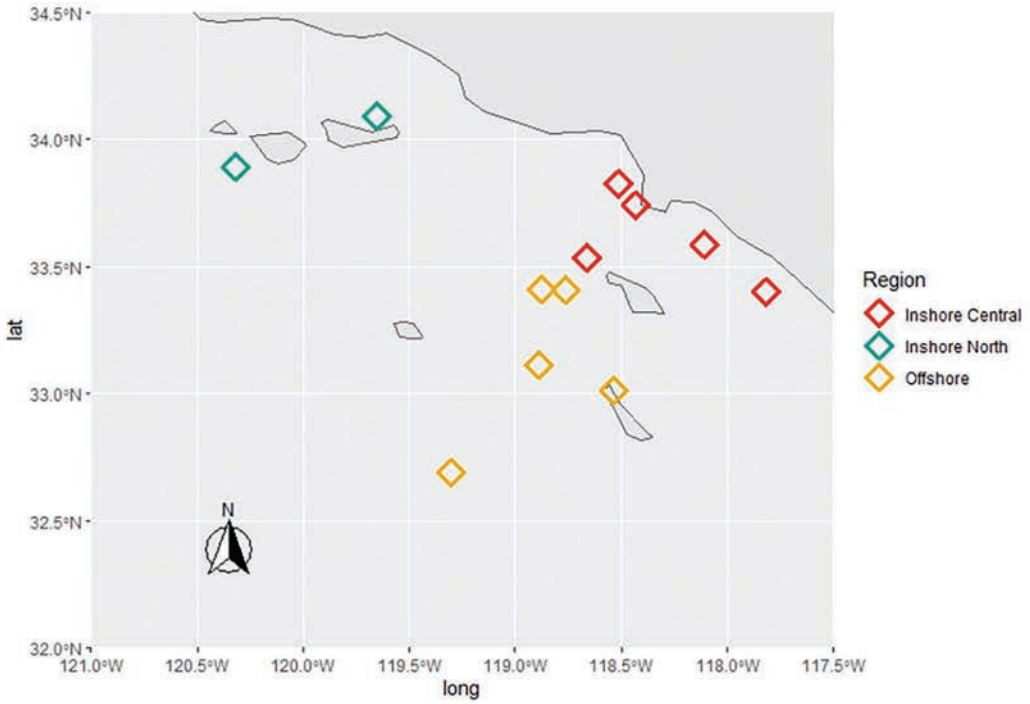

Figure 1. *Area of Southern California where 24 whales were tagged in three regions (Inshore North, Inshore Central and Offshore; separated by color), over eight years (2010-2018) for a total of 247 recorded hours.*

Though individually they are small (~6 cm), aggregations of krill swarm can reach densities of 30,000-100,000 individuals per 1 m^2 and span several miles across and hundreds of meters in depth. Under these conditions whales take up as much as 10 kg of krill per 70,000 liters or per full-gaped lunge.[7] Krill are a foundational species to the global marine food web, so to avoid widespread predation, krill have developed a method of prey-defense known as Diurnal Vertical Migration (DVM).[8] This is considered one of the greatest migrations on earth happening daily. During the daylight hours zooplankton (including krill) travel several hundred meters down into the darkness, away from visual predators. At night they venture back to the surface to feed under cover of darkness.[9]

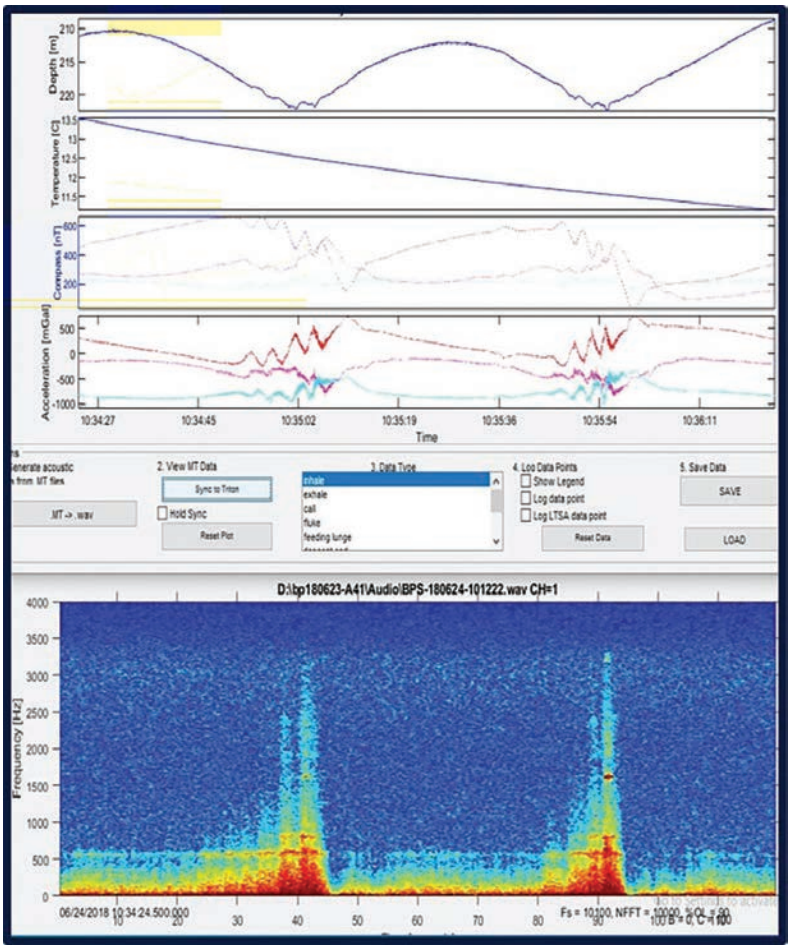

Figure 2. *MTViewer, a plug-in program used on the Triton platform within MatLab, designed for raw biotag signal processing. This viewer displays depth (A, top band), temperature (B, 2nd band from top), compass coordinates (C, 3rd band from top), accelerometer triaxial positioning (3D position in space) (D, 4th band from top), the event logger (E, central buttons), and the full color spectrogram that reads audio signal amplitude by color (F, full color chart along bottom). This logging screen shows two lunging events on the spectrogram and other sensors.*

METHODS

Data Collection

Types of multisensory biotags

DTAG (digital acoustic recording tag) and Acousonde tags were originally designed for passive acoustic audio surveillance, which focused on recording audio in the environment but have evolved to include a suite of compact digital sensors housed in a buoyant and water-resistant capsule designed to be affixed to the dorsal side of a whale. The tag contains a lithium rechargeable battery, digital signal processor, pressure sensor for depth measurements, compass, temperature sensor, audio board, preamp, hydrophones, analogue-to-digital converter, and a suite of movement sensors including accelerometers (a tri-axial coordinate reading for measuring the 3D movements of the whales in space), magnetometers and flash memory. Data from the tags were read, tabulated and prepared for analysis.

I specifically analyzed datastreams from 24 different multisensory biotags. The tags selected had over 3,000 lunging events across 247 recorded hours in and around the southern California bight. The effort for these tag deployments focused on three regional sites: Inshore North, Inshore Central and Offshore (**Figure 1**) between 2010-2018.

Tag Tabulation

Raw data from the biotags was tabulated via MatLab through Triton and its MTViewer remora, a program developed specifically for reading Acousonde tag signals (**Figure 2**). The Triton MatLab plug-in visualizes raw tag data into a series of visual charts that read out as depth, temperature, compass coordinates, accelerometer coordinates that give a 3D position of the whale. When a known visual signature for an inhala-

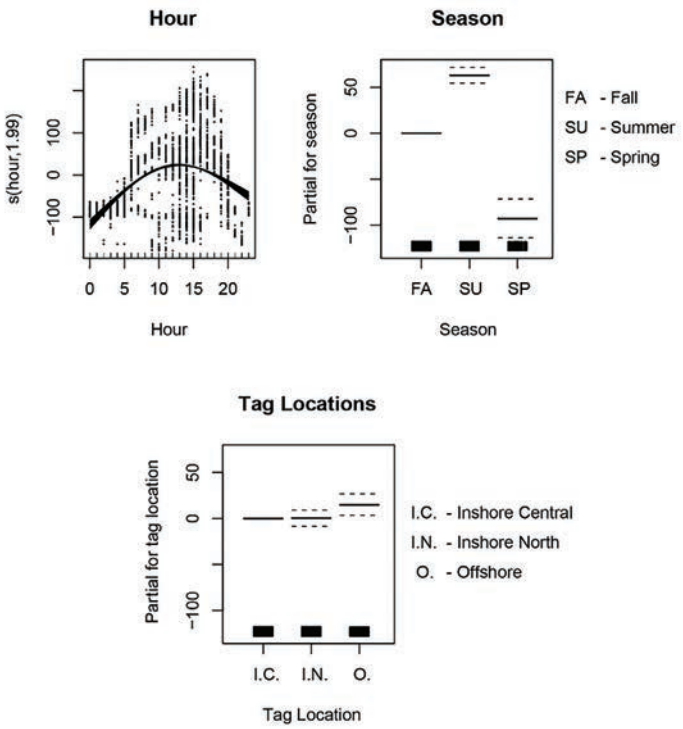

Figure 3. *Mean-adjusted partial fits of lunge-feeding along the y-axis for the predictor variables: hour (top left), season (top right) and location (bottom).*

tion, tail fluke, or feeding lunge is identified, the event is logged and labelled along with depth, GPS coordinates, and temperature (**Figure 2**).

The analysis portion primarily investigated the relationship between the response variable, fin whale lunge-feeding depths, as a function of the predictor variables, hour, season, and three different tagging locations in the southern California bight. I used a generalized additive modeling (GAM) framework with a Gaussian distribution for the two and three-way interaction terms (**Equation 1**).

The R package (mgcv) was used to model the data to fit a GAM using the following equation:

Equation 1.

lunge_depth ~ 1 + s(hour, bs = "ts", k = 3) + season + tag_location

The independent variables used in the model were hour (numerical), season (spring, summer and fall), and location (Inshore North, Inshore Central, and Offshore) which were treated as categorical variables with three factor levels each (**Figure 3**; **Table 1**).

RESULTS

Lunge-depths at night were significantly shallower (<135 m) than the lunges during the day (>135 m) (**Figure 3**).

Lunges deeper than 135 m are indicated by the dashed line above the mean or zero on the y-axis and lunges shallower than 135 m are indicated by the dashed line below the mean or zero on the y-axis. For the tags in this study, the hour variable (top left) shows that between 5:00 a.m. and 8:00 p.m. the parabolic GAM rises above the mean, which represents lunge-depths exceeding 135 m. The seasonal variable (top right) which consists of spring, summer and fall show the lunge-depths in the fall sit predominantly at the mean (135 m), the summer months show lunges significantly deeper than the (>135 m) mean depth, and in spring the lunge-depths are significantly shallower (<135 m) than the other seasons. The location variable (bottom) which represents the three-level factor of Inshore Central (closest to shore), Inshore North (Santa Cruz and Santa Rosa Islands) and Offshore (beyond Catalina Island).

There was a significant effect of location on

Predictor Variable	df	std. error	F	t-value	p-value
Intercept		2.42		41.79	2e-16
hour	1.993*		197.1	84.56	2e-16
season	2				
summer		4.27		14.75	2e-16
spring		10.51		-8.83	2e-16
tag_location	2				
Inshore North		4.38		0.074	0.941
Offshore		5.80		02.59	0.010

Table 1. *Degrees of freedom (df for hour is effective*), standard errors, t-values, and P-values for the predictor variables hour (7 p.m-5 a.m. PST = night, 5:01 a.m-6:59 p.m. PST = day), season (spring, summer, fall) and location (Inshore North, Inshore Central, and Offshore).*

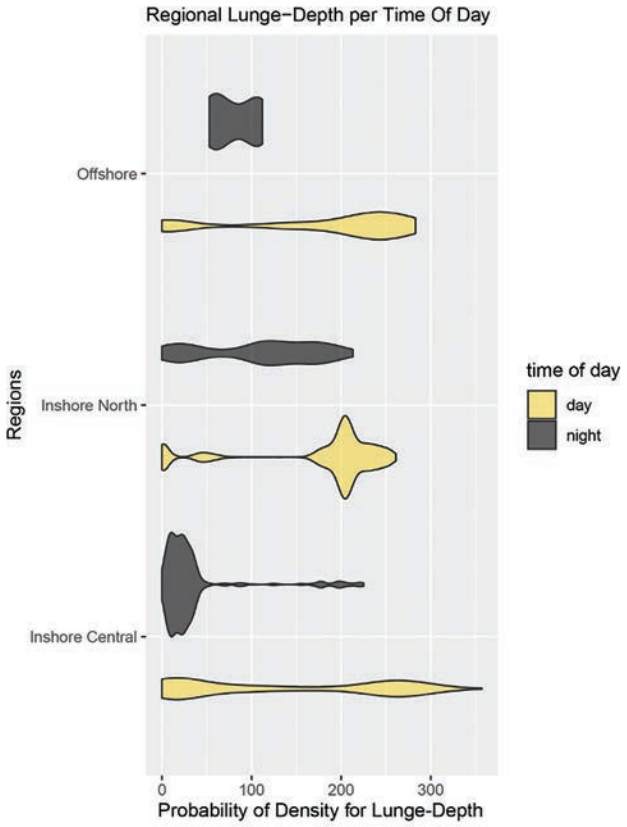

Figure 4. *Probability of feeding lunge depths for day and night per region sampled; the more vertical distribution of spread along the y-axis, the higher the probability of a lunge at that depth. Lunge-depth is indicated along the x-axis.*

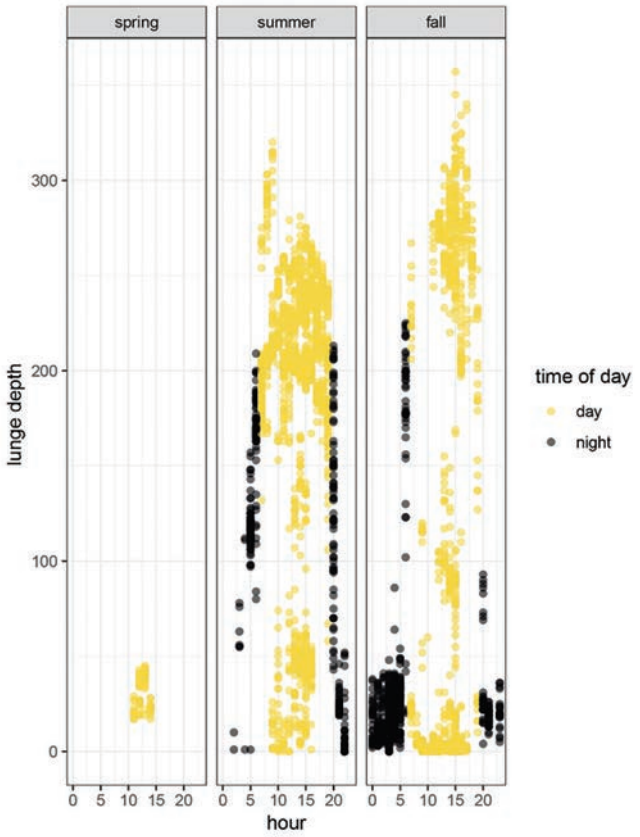

Figure 5. *Lunge-depth density per hour for each season; from Left: spring, shows the depth distribution of daytime lunges (yellow) occurring at 20-50 m (y-axis) between 10 a.m.-7 p.m. PST (x-axis). Center: summer depth distributions show night-lunges (black) from 0 -200 m and day lunge-depths (yellow) >320 m. Right: fall lunge-depth distributions show night lunges >225 m and daytime lunges >350 m.*

the depth of lunges as well (**Figure 3**; **Figure 4**; **Table 1**). This was driven by significant differences in lunge-depths between Inshore Central and Offshore, where Offshore had deeper than average (>135 m) lunge-depth distribution than Inshore Central. Offshore and Inshore North showed no significant difference from each other (**Figure 2**; **Figure 3**; **Table 1**).

Season also influenced lunge-depth (**Figure 5**), with significant differences across all seasons (**Figure 3**; **Figure 5**; **Table 1**). Spring had the shallowest distribution of lunge-feeding depths with a daytime range between 20-45 m (more spring data is stored and available for analysis). Summer showed an increase in depth and frequency with the deepest dives occurring during the daylight hours in excess of 300 m. The fall season has the most lunging variability with daytime lunge-depths in excess of 350 m and night lunges from as shallow as 20 m to deepest night lunges at 225 m.

Overall, the deepest lunges (>135 m) occurred along the shelf-edge, in the late summer and early fall months between the afternoon and early evening hours of the day, with shallower dives (<135 m) occurring at night.

CONCLUSION

Currently, population estimations remain the most crucial yet most challenging statistic of whale conservation.[10] Populations of these leviathans are slow to rebound even a quarter of a century after the moratorium on whaling. This makes them doubly difficult to locate in an environment already with its own set of challenges. With this in mind, my research focused on the probability of a whale feeding under specific con-

ditions. To do this, I began a deep dive into the spatial and temporal fluctuations of feeding-lunge depths for fin whales. This focus supported the already verified hypothesis that baleen whales base their lunge-feeding predation on the density of a krill patch.[11] In contrast to the great whales, krill are easier to predict, find, and measure. The density of a krill patch fluctuates most significantly with the rise and set of the sun in a DVM. Because we know the whales change their feeding depth based on the density of krill patches, krill density estimates could be correlated with tagged whale feeding densities through an expanded platform of study. In this way, with the aid of machine learning algorithms designed to predict probability densities, krill-density could be approached as a proxy for feeding whales. When a krill patch reaches a density that has a high probability of feeding whales, a mechanism could be put in place to trigger an alert. This approach would reorient research towards a whale proxy as opposed to the whales themselves. Doing so in this case could potentially circumvent years-long bureaucratic processes stymieing time-sensitive conservation measures.

Developing an automated classifier would be the initial step towards expediting the time-consuming analysis of tag data.[12] The more data applied to a classifier, the more precise it will become, the more precise the classifier, the better our probability estimates. Eventually, an in-house automated classifier could be added to the tags themselves. Data can be upload to surface vessels or buoys nearby, giving real-time krill-density estimates. Autonomous gliders have already been in use for conducting krill-density measurements, enabling real-time readings of krill aggregations, within a surface/satellite relay system in the antarctic.[13]

Future goals include the development of a "whale probability" alert system, informed by gliders in areas of high ship traffic. Programs have already been cleared to take continuous bio-geochemical measurements with autonomous gliders.[14] The sensors used for krill-density estimations could be cost-efficiently added to the instrument arrays, taking krill-density readings concurrently with other measurements.[15] Alerts from these gliders could signal when krill-swarm densities reach a level of high whale-feeding probability within a certain meter radius. Ports with high traffic in the North Atlantic have reported an 86% decrease in whale ship-strikes when speeds are reduced to ten knots or less.[16] An alert system of this kind could inform real-time shipping routes, speeds and schedules, regulating one of the greatest threats to the recovery of these rare giants.

ACKNOWLEDGMENTS

Contributors

I would like to thank my faculty advisor, Dr. Ana Širović and my colleagues in the bioacoustics lab for their guidance and support throughout the course of this research.

Special thanks goes to Dr. Pablo Crespo ’13, a Senior Data Scientist who helped me navigate my coding process.

Thanks as well to my friends, colleagues, faculty, and staff in the Marine Biology department for making my time at Texas A&M University at Galveston such a formative experience.

Last but certainly not least, thanks go to my family for their encouragement, unending patience and support, without which none of this would have been possible.

The data used for this research was provided by Dr. Ana Širović. The analyses were conducted by the author, independently throughout the academic year 2020–2021.

Funding sources

Undergraduate research was supported by Texas Sea Grant College Program at Texas A&M University.

REFERENCES

1. H. van Haren, “Grand challenges in physical oceanography,” Front Mar Sci, 5 (2018).
2. N. Allen et al., “Development of an automated method of detecting stereotyped feeding events in multisensor data from tagged rorqual whales,”

Ecology and Evolution, 6 no. 20 (2016): 7522–35. https://doi.org/10.1002/ece3.2386.

3. Paul F. Brodie. Noise generated by the jaw actions of feeding fin whales. Canadian Journal of Zoology. 71(12): 2546-2550. https://doi.org/10.1139/z93-348.

4. J. Calambokidis et al., "Insights into the underwater diving, feeding, and calling behavior of blue whales from a suction-cup-attached video-imaging tag (crittercam)," Marine Technology Society Journal 41 (2007): 19–29.

5. A. Širović et al., "Seven years of blue and fin whale call abundance in the southern california bight," Endangered Species Research 28, (2015). https://doi.org/10.3354/esr00676.

6. J. Fiechter et al., "Krill hotspot formation and phenology in the california current ecosystem," Geophysical research letters (2020). https://doi.org/10.1029/2020GL088039.

7. J. A. Goldbogen et al., "Kinematics of foraging dives and lunge-feeding in fin whales," J Exp Biol. 209, no. 7 (2006): 1231–44. https://doi.org/10.1242/jeb.02135.

8. D. Bianchi and K. S. Mislan, "Global patterns of diel vertical migration times and velocities from acoustic data," Limnology and Oceanography 61, no. 1, (2016): 353–64. https://doi.org/10.1002/lno.10219.

9. Bianchi and Mislan, "Global patterns," 353–64.

10. A. Širović et al., "Seven years of blue and fin whale" 28.

11. Szesciorka AR, Ballance LT, Širović A, et al. Timing is everything: Drivers of interannual variability in blue whale migration. Scientific Reports. 2020;10(1):19.doi: 10.1038/s41598-020-64855-y.

12. Allen et al., "Development of an automated method," 7522–35.

13. D. Guihen et al., "An assessment of the use of ocean gliders to undertake acoustic measurements of zooplankton: The distribution and density of antarctic krill (euphausia superba) in the weddell sea," Limnology and Oceanography: Methods 12, no. 6 (2014): 373–89. https://doi.org/10.4319/lom.2014.12.373.

14. Ruiz S, Garau B, Martínez-Ledesma M, et al. New technologies for marine research: Five years of glider activities at IMEDEA. 2012. doi: 10.3989/scimar.03622.19L

15. D. Mellinger et al., "Gliders, floats, and robot sailboats: Autonomous platforms for marine mammal research," The Journal of the Acoustical Society of America 131 (2012): 3493. https://doi.org/10.1121/1.4709197.

16. J. Calambokidiset al., "Differential vulnerability to ship strikes between day and night for blue, fin, and humpback whales based on dive and movement data from medium duration archival tags," Front. Mar. Sci. (2019). https://doi.org/10.3389/fmars.2019.00543.

AUTHOR BIO

LEAH K. BOGAN '21

Leah Kathleen Bogan is a senior majoring in marine biology at TAMUG. After graduation, she plans to continue the research she began in the Bioacoustics Lab, through higher education opportunities. Leah is excited to integrate developing technology, bioacoustics and multisensory biotags together to explore the wildlife in the ocean. Her passion is in expanding conservation efforts through sustainable, creative, and community-focused and inclusive practices.

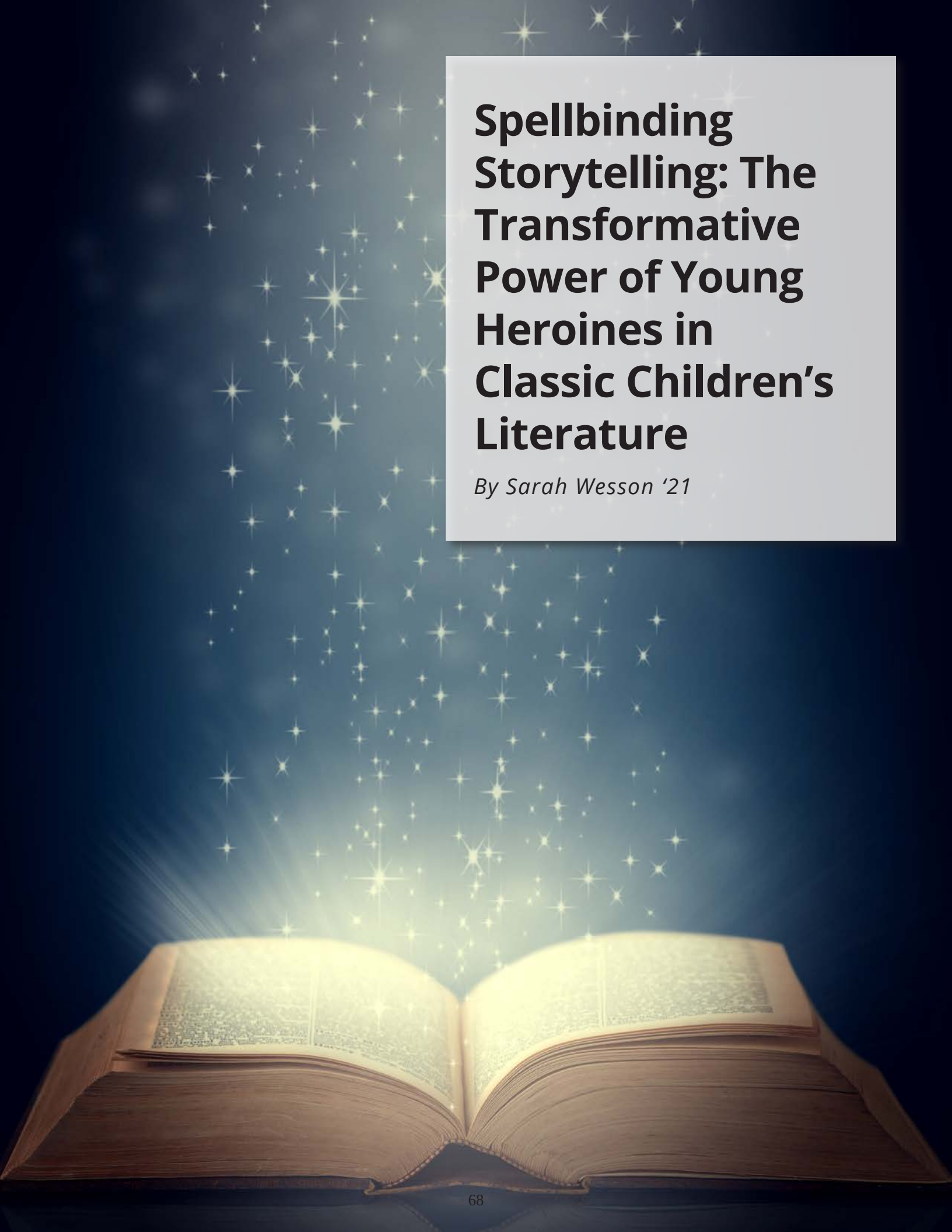

Spellbinding Storytelling: The Transformative Power of Young Heroines in Classic Children's Literature

By Sarah Wesson '21

In 1965, the American rock band The Lovin' Spoonful sang about a truth greater than they were perhaps aware when they famously asked their listeners, "Do you believe in magic in a young girl's heart?"[1] There certainly is magic there—a magic that has been noticed for centuries by rock bands and authors alike. In particular, the Golden Age of Children's Literature, from the mid-1800s to the early 1900s, heavily featured young female protagonists with a certain enchanting element about them. Even in the realistic fiction of this period, these protagonists possess figurative magic; they bring about transformation in the world around them. The young heroines of classic children's literature use words to affect this magic. Why is this "magic"—and the resulting degree of autonomy afforded to young heroines—significant, and what does it mean for modern readers? In this article, I attempt to answer these questions by examining Anne Shirley from *Anne of Green Gables* and Sara Crewe from *A Little Princess*, two key literary figures from the Golden Age of Children's Literature, in light of available literary criticism.

CHILDREN'S LITERATURE WAS CONSIDERED A "LOWLY" GENRE,[4] AND THUS FREE FROM INTENSE PUBLIC SCRUTINY, WOMEN WRITERS HAD A RARE OPPORTUNITY OF SOVEREIGNTY.

BACKGROUND

Anne Shirley and Sara Crewe are anomalies in women's literary power. Considering their time period, the autonomy that Anne, Sara, and other similar heroines possess is the exception to the misogynistic rule. During the Victorian period, empowered female characters were portrayed as "an unnatural aberration, a monster, a witch."[2] Female power, because it was unfitting with the gender norms of the time,[3] was malevolent. Strong female characters had to be diminished by the end of a novel, and if the author chose to keep these characters strong, they had to be evil to fit within societal codes.

Even for a female author in the Victorian period, the possibility of empowerment through mainstream authorship was difficult, but children's literature offered a creative safe haven for women and fictitious young heroines alike. Children's literature was considered a "lowly" genre,[4] and thus free from intense public scrutiny, women writers had a rare opportunity of sovereignty. Women writers of children's literature were "a specially marginalized group writing for an equally disregarded audience."[5] Consequently, they could "adopt a subversive position through articulating the child's viewpoint."[6] Because of the genre's low public regard, it was possible for children's literature of this period to feature prominent, powerful young female protagonists. Some of these novels of girl power are still classics today. From Anne of Green Gables to A Little Princess, the young female protagonists of this era are the primary influencers within their novels, yet they are not arbitrarily portrayed as bad. On the contrary, their power is good—enchanting, even. These girls transform their surroundings with words, speaking new realities into existence, to suit their particular needs. As feminist literary critics Simons and Foster note, they "adopt the [role] of storyteller, replicating the position of author as they use narrative as a means of empowerment."[7] So curiously, Golden Age children's literature offers an autonomous space for young heroines in which they are free to be empowered without negative connotations. Like the authors who wrote them into existence, these girls transform their worlds with words.

DISCUSSION

The word witch is an unlikely first term to come to mind when one thinks of Anne of Green Gables. But in fact, a witch is exactly how Anne is

ON THE ISLAND, ANNE'S POWERS ARE MANIFESTED IN HER TENDENCY TO NAME THINGS AROUND HER, THUS MAKING HER ORDINARY WORLD EXTRAORDINARY, AND INVITING OTHERS TO ENTER INTO THIS ENCHANTING SPACE.

described several times in L.M. Montgomery's classic novel.[8] During one of Anne's first scenes, in which both Anne's future foster father Matthew Cuthbert and the reader are introduced to the heroine, Montgomery notes that "this freckled witch [is] very different."[9] She is also described as doing several things to fulfill this archetype, such as having "bewitched" Matthew after her first interaction with him[10] and "casting a spell" over the Cuthberts.[11] Anne is also a "witch" because of her notable creative abilities, with which she manipulates her world by colorfully renaming landmarks and spinning elaborate speeches. She possesses the qualities of the "witch" that Sandra Gilbert and Susan Gubar describe in their feminist literary criticism classic, *The Madwoman in the Attic*: "a plotter, a plot-maker, a schemer … a woman of almost infinite creative energy."[12] Montgomery seems to be aware of the term's negative connotations and role in literature, yet in describing Anne as a witch, Montgomery gives the archetype of witch a new dimension: if Anne is a witch because of her creativity, then perhaps other witches in women's literary history are misunderstood creatives as well. Montgomery's description of Anne as a witch also commingles the genres of fantasy and realistic fiction, which suggests the power that Anne's abilities have.

The reader and Matthew, in their first encounter with Anne, spend an entire scene listening to "her chatter" in which Anne casts enchantments over the local sights by renaming them. She later reveals the origin of this ability: that she used her words and imagination to cope with the dark and difficult environment at the asylum from which she originates.[13] Explaining this, Anne says to Matthew, "there is so little scope for the imagination in an asylum … I used to lie awake at night and imagine things."[14] In addition to coping with her dismal surroundings in the asylum, Anne uses her imagination to deal with her lowly status as an orphan girl. She feels "ashamed" of her neglected appearance, and to transform this miserable situation, she "[goes] to work and imagine[s] that [she has] on the most beautiful pale blue silk dress" and "[feels] cheered up right away."[15] Anne uses her creative abilities to transform a dire situation into one of her own fantastic invention, and thus exerts a sort of magic within her world. Her creative power derives from a need to escape her awful surroundings, and now she can use these powers to enchant her new home, Prince Edward Island. On the island, Anne's powers are manifested in her tendency to name things around her, thus making her ordinary world extraordinary, and inviting others to enter into this enchanting space. During her first interaction with Matthew, Anne brings color and enchantment to his world by renaming the landmarks that are ordinary to him, such as the Avenue, saying, "They should call it … the White Way of Delight. Isn't that such a nice imaginative name? When I don't like the name of a place or a person I always imagine a new one and always think of them so."[16] Renaming is Anne's way of transforming the world around her into one that suits her needs and whimsy. She no longer lives in a mundane Canadian town, but in an enchanting world of her own creation.

Anne also renames herself, in an attempt to form her identity or put forth certain publicly-perceived characteristics. Upon first meeting her future foster mother Marilla, Anne views her own name as "unromantic" and desires to be called, what is according to Anne, a much more romantic name, Cordelia, or at the very least, Anne with an e, because "[the e] makes such a difference. It looks so much nicer … A-n-n-e looks so much more distinguished."[17] Anne, desiring a certain romantic perception of herself, turns to words. Even

as a disadvantaged orphan girl, Anne demonstrates her power over words to transform both herself and her surroundings.

At Green Gables, others' perceptions of Anne are crucial, because her safety and happiness are at stake. If the adults on Prince Edward Island disapprove of her, Anne is more likely to return to the asylum. Anne is already in a disadvantaged position because she, a manically creative young girl, is the opposite of what Marilla and Matthew originally wanted in a child, a "smart, likely boy of about ten or eleven."[18] While her position at Green Gables is not yet secure, Anne weaves elaborate word tapestries in order to gain the favor of the adults in her life and thus ensure her new-found home and happiness. The most distinguishable and transformative instance of this is early in the novel: Anne must apologize to her neighbor, Mrs. Lynde, for losing her temper after Mrs. Lynde insults Anne's appearance. This is a critical moment for Anne, because without the approval of the adults in her life, including Mrs. Lynde, she will likely be sent back to the asylum—and so, even though the situation is unjust, Anne must work it to her advantage with her magical witchcraft of words. The readers are aware of the dramatic irony in this scene: that Anne is actually insincere, but Mrs. Lynde believes every bit of Anne's embellishment. After Anne's dramatic apologetic speech, the narrator notes:

> There was no mistaking her sincerity—it breathed in every tone of her voice. Both Marilla and Mrs. Lynde recognized its unmistakable ring … [Marilla understood that Anne] was reveling in the thoroughness of her abasement … Anne had turned [Marilla's punishment] into a species of positive pleasure.
>
> Good Mrs. Lynde, not being overburdened with perception, did not see this. She only perceived that Anne had made a very thorough apology and all resentment vanished from her.[19]

Anne uses her words to not only construct an elaborate, believable lie about her sincerity and emerge victorious out of an unjust situation; she also uses her words to turn an unjust punishment into an amusing, imaginative personal drama. Her witchy abilities are at work in her elaborate apology, in order to ensure the retention of her new home at Green Gables via making an ally of Mrs. Lynde—and in her characteristic whimsical charm, to transform an unjust situation into amusing stagecraft.

Like Anne, Sara Crewe of Frances Hodgson Burnett's A Little Princess uses her powerful words to transform her often difficult and unfair environment to her advantage. Sara's words focus on comfort, for herself and those around her. Her words are how she transforms dire situations into manageable ones. Sara's storytelling ability is her most notable quality: "the greatest power Sara possessed … was her power of telling stories and of making everything she talked about seem like a story, whether it was one or not."[20] Sara's storytelling is what causes her to emerge as an admired leader among her peers, and gives herself and others the power to withstand difficulties. Her storytelling gives her invincibility; through it, she transforms her ever-unfair world into a manageable one.

The comforting power of Sara's words is especially prevalent when she is suddenly thrown into poverty, a sharp departure from her previously lavish lifestyle. She uses her words to take control over her situation and thus bear her immense hardships. Like Anne, Sara is imaginative in her use of words. In particular, Sara uses her words to craft a new living situation for herself: instead of living in the dingy upstairs attic of an English girls' school, she is in "a beautiful little room,"[21] or a cell in Bastille,[22] or a tropical forest.[23] This imaginative wordcraft makes her hardship manageable. As Sara says, recognizing the power she possesses in her storytelling, "what you have to do with your mind, when your body is miserable, is to make it think of something else."[24] In a situation where Sara should have no power—she is an orphan girl with no fortune—she has complete control over her happiness through her words.

Sara's words not only affect herself; they also have immense comforting power over people of all social statuses. Both in her wealth and in her poverty, Sara's words, and the magical, comforting power they hold, are her gift to her classmates. In the midst of her

impoverished life, Sara notes that "[w]hen [Ermengarde, a fellow classmate] comes into the attic I can't spread feasts, but I can tell stories, and not let her know disagreeable things."[25] Even without worldly possessions or high social status, Sara invites others into her comforting musings, and thus exercises power over not only herself, but her peers as well. Lottie, a young motherless girl whom Sara has figuratively adopted, is distressed upon seeing Sara's new lowly living situation. Through her verbal enchantments, Sara imaginatively transforms the attic before Lottie's eyes, and Lottie is comforted again: "[Sara] was walking round the small place, holding Lottie's hand and making gestures which described all the beauties she was making herself see. She quite made Lottie see [the imagined beauties], too."[26] Her storytelling is what keeps drawing her friends up to her dismal attic, and sustaining them through their own difficulties, even though Sara has no physical comfort to offer them. Especially in her poverty, Sara continues to "[dispense] generously of the one hospitality she could offer—the dreams she dreamed—the visions she saw—the imaginings which were her joy and comfort."[27]

LIKE THE EMPOWERED CHARACTERS THEY CREATED, THESE AUTHORS ALSO POSSESSED A SOVEREIGN, GENERATIVE POWER OF WORDS BY NATURE OF THEIR VOCATION.

CONCLUSION

It is important to note that Sara and Anne are the only figures with this magical power of words in their particular novels. Some of the adults in the novels may appreciate their musings, but certainly all of the adults lack this creative power. The other children in the novels also notably lack this ability; Montgomery and Burnett go so far as to say they are envious of it.[28,29] Thus Anne and Sara, and similar young heroines of the Golden Age of Children's Literature, are afforded the principal position of transformative power within their novels. Anne, Sara, and their literary compatriots are enactors of positive change through their words. They bring about powerful transformations, yet their medium is not wicked spells or violence; it is life-giving, enchanting words.

The female empowerment that heroines like Anne and Sara offer does not end at the last page of their novels. These empowered characters granted autonomy to their authors as well, in a time when the female voice was limited. Because Montgomery and Burnett, and other similar female authors, wrote children's literature, they had a rare opportunity to have a voice through writing. Like the empowered characters they created, these authors also possessed a sovereign, generative power of words by nature of their vocation. Montgomery and Burnett's voices in their classic novels also serve to empower the often young and female reader. In reading such novels as Anne of Green Gables and A Little Princess, readers are invited into this fantastical creative power, put forth by the protagonists and the authors. Readers are afforded the opportunity to escape their present world and thus experience the heroines'—Anne and Sara's—and the authors'—Montgomery and Burnett's—transformative wordcraft. Readers and authors share in Anne and Sara's ability to create and transform with words, making Golden Age Children's Literature significant for female empowerment, at the textual, author, and reader levels. Over a century later, children's classics like Anne of Green Gables and A Little Princess continue to remind readers of the immense potential of words to empower the marginalized.

REFERENCES

1. "The Lovin' Spoonful – Do You Believe in Magic." Genius, July 17, 1965. https://genius.com/The-lo-

vin-spoonful-do-you-believe-in-magic-lyrics.

2. Edith Lazaros Honig, Breaking the Angelic Image: Woman Power in Victorian Children's Fantasy (Westport, CT: Greenwood Press, 1988), 112.
3. Honig, Breaking the Angelic Image, 112–3.
4. Shirley Foster and Judy Simons, What Katy Read: Feminist Re-Readings of 'Classic' Stories for Girls (Iowa City: University of Iowa Press, 1995), 21.
5. Foster and Simons, What Katy Read, 20.
6. Foster and Simons, 22.
7. Foster and Simons, 30.
8. L.M. Montgomery, Anne of Green Gables (New York: Bantam Books, 1998), 15, 51, 249.
9. Montgomery, 15.
10. Montgomery, 29.
11. Montgomery, 35.
12. Sandra M. Gilbert and Susan Gubar, The Madwoman in the Attic: The Woman Writer and the Nineteenth-Century Literary Imagination. (New Haven, CT: Yale University Press, 2020), 38.
13. Montgomery, Anne of Green Gables, 13–15.
14. Montgomery, 13.
15. Montgomery, 13–14.
16. Montgomery, 18.
17. Montgomery, 25
18. Montgomery, 6.
19. Montgomery, 74.
20. Frances Hodgson Burnett, A Little Princess (Enhanced Ebooks, 2014).
21. Burnett, 61.
22. Burnett, 65.
23. Burnett, 87.
24. Burnett, 87.
25. Burnett, 102.
26. Burnett, 62.
27. Burnett, 102.
28. Burnett, 24.
29. Montgomery, Anne of Green Gables, 210.

AUTHOR BIO

SARAH WESSON '21

Sarah Wesson '21 is an English major with minors in French and German from San Diego, California. Her research was motivated by her long-standing interest in classic children's literature and reading about strong heroines in Dr. Elizabeth Robinson's Young Adult Literature class. She plans to continue studying enchanting young heroines, and through teaching, show others the wonder and power of children's literature.

How Children's Curiosity Predicts School Readiness: Examining Moderation by Socioeconomic Status and Parenting

By Kathryn N. Gray '21

INTRODUCTION

Curiosity is a natural way to gather information about the world, making it directly relevant to learning. However, little research has examined whether an association exists between children's early curiosity and formal learning. Even less has examined the role critical environmental factors play in this association, such as socioeconomic status (SES) and parenting. A clearer understanding of how children's curiosity relates to outcomes like school readiness could illuminate economical and effective strategies for preparing children for formal learning.

Previous research suggests that curiosity is positively related to intrinsic motivation[1,2] which is an important aspect of academic achievement[3] and long-term retention.[4] Curiosity in children has been associated with cognitive ability,[5] and especially for children from poverty-level homes, cognitive growth.[6] Recently, empirical findings show a positive association between curiosity and academic achievement.[7] This association was strongest for children with low family SES, which was evaluated using income and education level. Children with low family SES may benefit more from curiosity because they do not have the advantages that children with high family SES have. Though this work has yet to be replicated, such findings imply a possible association between children's early curiosity and readiness for entry into formal schooling and suggest a possible pathway for reducing socioeconomic disparities in educational achievement by strengthening children's curiosity.

CHILDREN'S CURIOSITY HAS BEEN POSITIVELY CORRELATED WITH PARENTAL ENCOURAGEMENT OF CURIOSITY AND PARENTAL DEMONSTRATION OF CURIOSITY.

At all levels of SES, parents serve as the primary scaffolding for children's early learning.[8] Parents are the most frequent social partners of young children and the primary figures

Table 1. *Descriptive statistics of participants across the three visits.*

	Initial Visit	Second Visit	Third Visit
Number of Children Participating	108	98	91
Mean Age of Children (years)	3.59	4.57	5.52
Standard Deviation of Children's Age	0.15	0.15	0.12
Mothers' Mean Age	34.53		
Fathers' Mean Age	36.14		

in a child's environment before formal schooling.[9] Children's curiosity has been positively correlated with parental encouragement of curiosity[10] and parental demonstration of curiosity.[11] Thus, parents may be viable targets for interventions aimed at enhancing school readiness. Because parent-based strategies for encouraging curiosity are inexpensive and do not require advanced education, they may be particularly appealing for families with low SES, though parent behaviors almost certainly play a critical role for children of all socioeconomic strata. However, as is true for the association between curiosity and academic achievement, there is limited formal research aimed at understanding whether and how parent behaviors affect the association between early curiosity and children's school readiness.

To expand our knowledge about the role of curiosity in young children's readiness for formal schooling, this study examined preschoolers' curiosity at age three as a predictor of academic readiness for entry to formal schooling at age five. The association between early curiosity and school readiness was evaluated in light of family SES and parenting behaviors.

This study had three hypotheses. First, curiosity and school readiness would be positively correlated. Second, the link between curiosity and school readiness would be stronger at lower levels of SES than at high SES. Third, the link between curiosity and school readiness would be greater when parents showed more frequent curiosity-encouraging behaviors (e.g., exploring the objects themselves, asking their child about the objects, etc.) and more thorough responses to children's questions.

METHODS

Participants

As part of a larger longitudinal study of child development, 121 children (female = 59%) came to the laboratory three times between spring 2014 and winter 2017. The initial visit occurred when children were three years old, the second visit at age four, and the final visit at age five (**Table 1**). The full range of parents' gross annual incomes are represented in **Figure 1**. Parents reported their race and ethnicity, which is summarized in **Figure 2**. Due to missing data for the specific variables that this study examined, the final sample included 61 children.

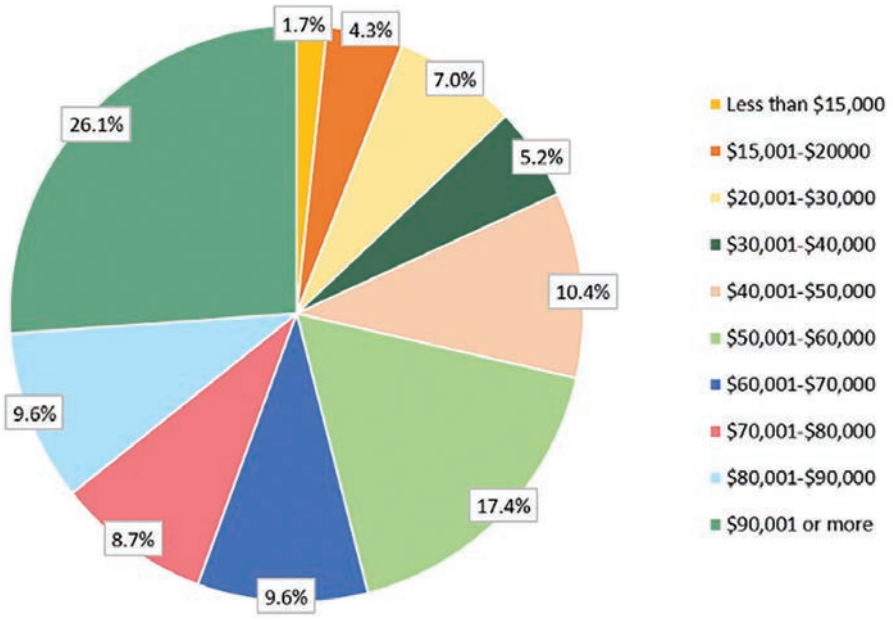

Figure 1. *Reported gross annual incomes (maternal and paternal reports were averaged).*

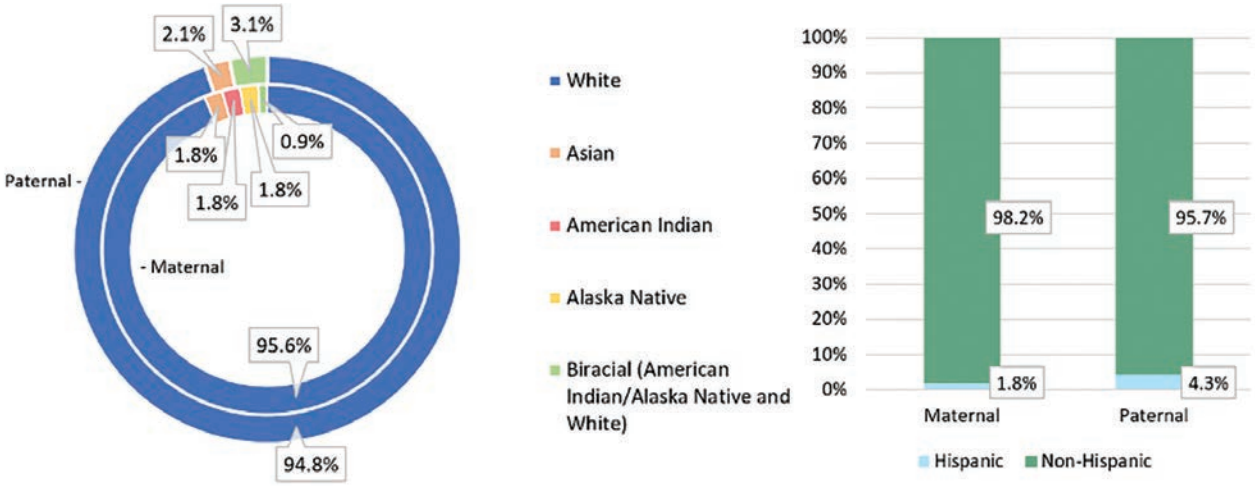

Figure 2. *Parents' reported race and ethnicity.*

Child Curiosity

Children's behavioral curiosity and vocal curiosity were observed during a laboratory episode. As part of the age three assessment, each child came to the lab accompanied by their primary caregiver and participated in a Risk Room episode designed to measure children's reactions to novel contexts.[12]

Children investigated a set of novel, age-appropriate toys in whatever manner they chose. The child was told they could play with the toys in any way they wanted, and the parent and child were left alone in the room for 3 minutes. To quantify behavioral curiosity, the number of objects children engaged with was recorded and exploratory behavior was rated on a five-point scale, ranging from not engaging with any of the objects (0) to attentively manipulating at least one object with variation to their actions (4). Variation was defined as the child playing with the same object in different ways (e.g., putting their arm inside the monster box and stroking its teeth). Vocal curiosity was scored as a count of the number of information-seeking questions that children asked.

Parent Behaviors

Three aspects of parent behavior were also coded during the Risk Room episode. The quality of parents' general responsiveness to questions from children across the episode was rated on a four-point scale, ranging from not typically responding (1) to answering with information and elaboration (4). Parental encouragement of curiosity was similarly coded on a four-point scale, ranging from parents not exhibiting any curiosity-orienting behavior (0) to parents consistently encouraging their children to explore (3). Parental encouragement of curiosity included instances where parents encouraged their children to play with new objects, asked their children questions about the objects, or explored the objects themselves. Finally, parent interference with children's curiosity, such as separating their child from an object, telling them to stop asking questions, or influencing them to stop exploring the room, was noted as present or absent.

Socioeconomic Status

At the age three assessment, family SES was calculated using the Hollingshead Four Factor Index of Social Status.[13] Parents self-reported the highest grade that they had completed on a 7-point scale, ranging from less than 7th grade (1) to receiving graduate/professional training (7). Parents also self-reported their current occupation which was coded on a nine-point scale, based on occupation title and responsibilities

Table 2. *Results from the multivariate regression model including behavioral curiosity and SES as predictors of school readiness.*

	β	*SE*	*p*
Behavioral curiosity	-0.37	0.14	0.009
SES	0.42	0.14	0.002
Interaction of behavioral curiosity and SES	-0.13	0.14	0.366

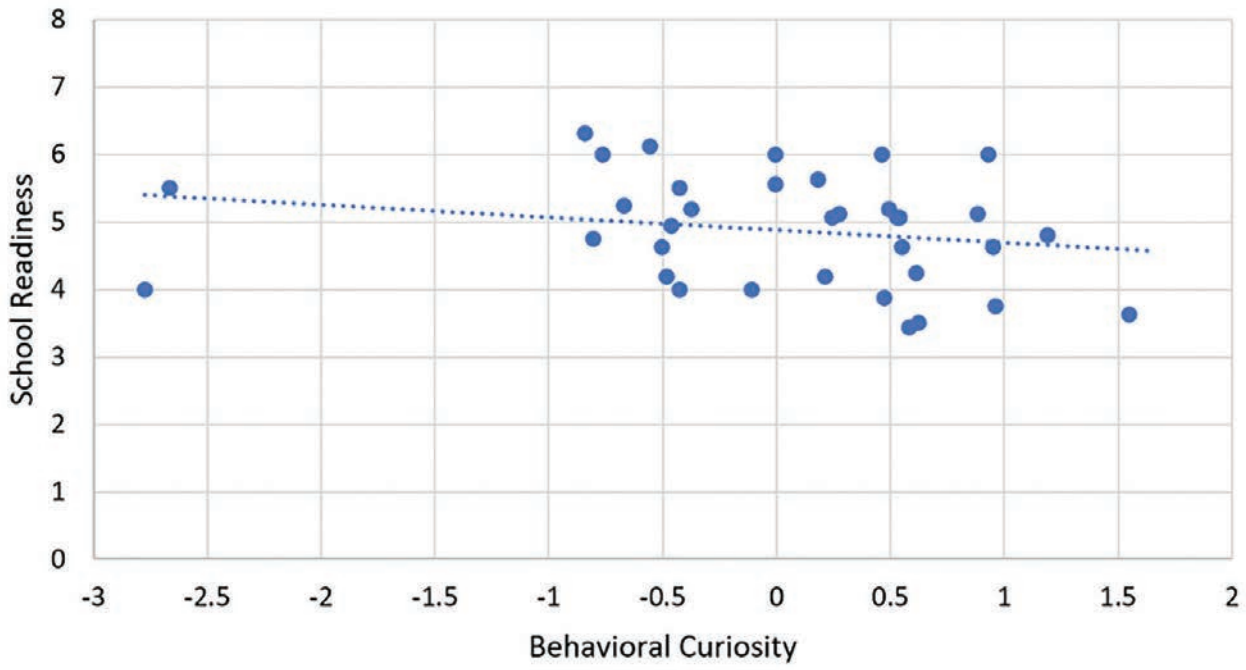

Figure 3. *Behavioral curiosity at age three predicts decreased school readiness at age five.*

as described in the Hollingshead scoring instructions. Education and occupation levels were weighted and combined for each parent, then the maternal and paternal scores were averaged to determine family SES.

School Readiness

To evaluate school readiness, parents completed the School Experiences section of the MacArthur Health and Behavior Questionnaire[14] when their child was five years old. Parents only completed this section of the instrument if their child had started kindergarten. The section consisted of eight questions that asked parents to rate, on a 1 to 7 scale, their child's math and reading abilities. Ratings were averaged together such that each child received a single score for school readiness, with higher ratings indicating greater readiness for formal schooling.

RESULTS

To test hypothesis one, two regression models were used, examining behavioral curiosity and vocal curiosity separately. Neither behavioral curiosity nor vocal curiosity was significantly associated with school readiness, so hypothesis one was not supported.

To test hypothesis two, multivariate regression models were used that predicted age five school readiness from curiosity (behavioral or vocal), the putative moderator (family SES), and the interaction between curiosity and putative moderator. Sixty-one participants were included in the analyses, reflecting the subset of families for whom children had begun kindergarten.

The model including behavioral curiosity found that greater behavioral curiosity predicted lower levels of school readiness. That is, school readiness decreases as behavioral curiosity increases (**Figure 3**).

Consistent with previous research, higher SES predicted greater school readiness (**Figure 4**) when behavioral curiosity was included in the model. However, contrary to study hypotheses, SES did not affect the association between behavioral curiosity and school readiness, suggesting that the association between behavioral curiosity and school readiness was the same at all levels of SES.

Vocal curiosity and SES were both unrelated to school readiness, and SES did not affect the relation between vocal curiosity and school readiness.

To test hypothesis three, a univariate ANOVA model was used that predicted age five school readi-

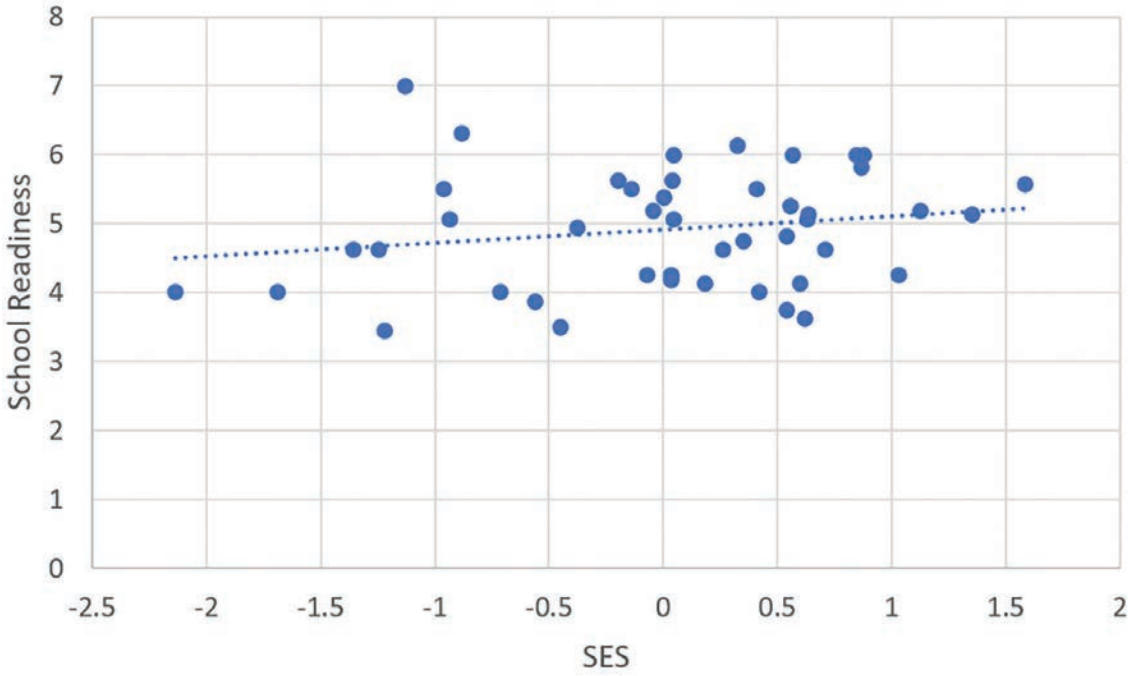

Figure 4. *Socioeconomic status at age three predicts school readiness at age five.*

ness from curiosity (behavioral or vocal), the putative moderator (parent encouragement or responsiveness), and the interaction between curiosity and the moderator. This model was used in place of regression models given the categorical nature of the parent variables.

There was no difference in school readiness levels for children with parents who typically did not respond, responded incompletely, answered their questions, or answered with information and elaboration. Thus, parent responses did not affect the association between vocal curiosity and school readiness (**Figure 5**).

Finally, the effect of parental encouragement of curiosity on the association between age three behavioral curiosity and age five school readiness was tested using a univariate ANOVA. Parental encouragement of curiosity did not affect the association between behavioral curiosity and school readiness (**Figure 6**). There was no difference in school readiness for children with parents who did not encourage curiosity, encouraged curiosity once or twice, often encouraged curiosity, or consistently encouraged curiosity.

DISCUSSION

The primary hypotheses were not supported in this study. Rather, it found a negative association between behavioral curiosity and school readiness and a positive association between socioeconomic status and school readiness. Although neither of these findings

...PRIORITIZING AMELIORATING CHILDHOOD POVERTY WOULD BE A MORE EFFECTIVE STRATEGY TO ENHANCE CHILDREN'S LONG-TERM EDUCATION OUTCOMES RATHER THAN EFFORTS FOCUSED ON ENHANCING UNDERPINNINGS OF CHILD LEARNING OR PARENT BEHAVIOR.

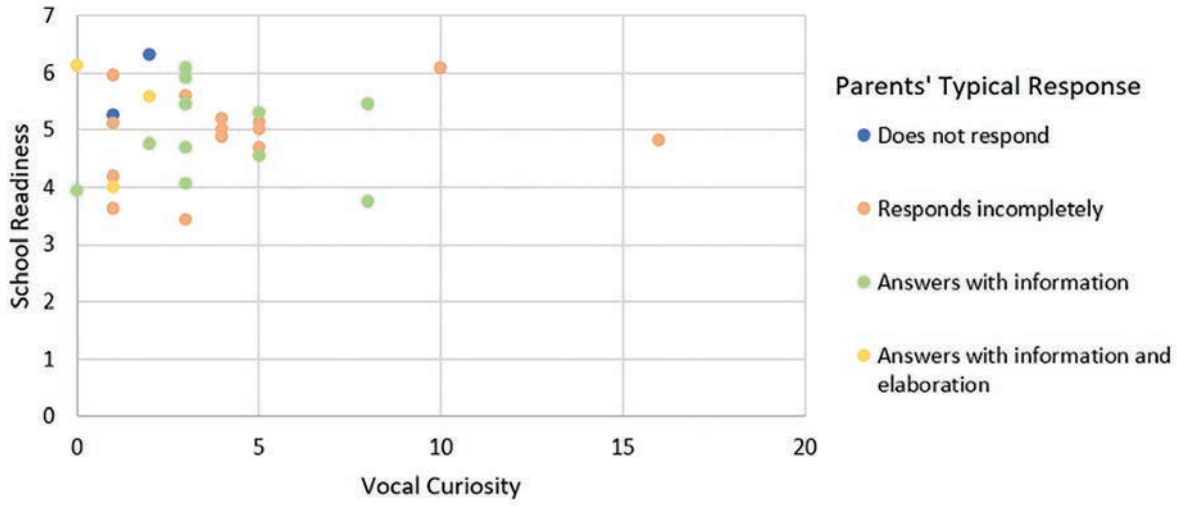

Figure 5. *Parent responses did not affect the link between vocal curiosity and school readiness.*

were hypothesized, some important implications can be taken from them.

First, this study underscored previous assertions about SES as a robust predictor of school readiness. Because SES is such a robust measure, its association with school readiness was not disrupted by the inclusion of other factors. This is in line with a substantial amount of literature showing SES disparities in early learning,[15] including disparities in early vocabulary[16] and math ability.[17] It should also be noted that SES was assessed two years prior to children's levels of school readiness, underscoring the long-term impact of being raised in a low SES household. This highlights SES as the critical intervention point across all of the variables investigated, suggesting that prioritizing ameliorating childhood poverty would be a more effective strategy to enhance children's long-term education outcomes rather than efforts focused on enhancing underpinnings of child learning or parent behavior. Thus, future research should continue to investigate the relationship between SES and school readiness, aimed at creating effective methods to reduce the socioeconomic achievement gap.

There was also an unexpected negative association between behavioral curiosity and school readiness. This could be because children's behavioral curiosity demonstrated a gap in their knowledge, similar to the suggestions of Lowenstein,[18] rather than indicating an internal drive for deeper or higher-level knowledge. Children who were less curious on our rating scale may have appeared as such because they already knew about the toys they were offered and found them less novel. This rationale explains why behavioral curiosity was a significant predictor only when accounting for SES. Children with low family SES may not have as many opportunities for learning experiences because parents may not have the time, information, or resources needed to provide these experiences.[19] Families with low SES generally have less stimulating home environments, such as not owning as many toys intended

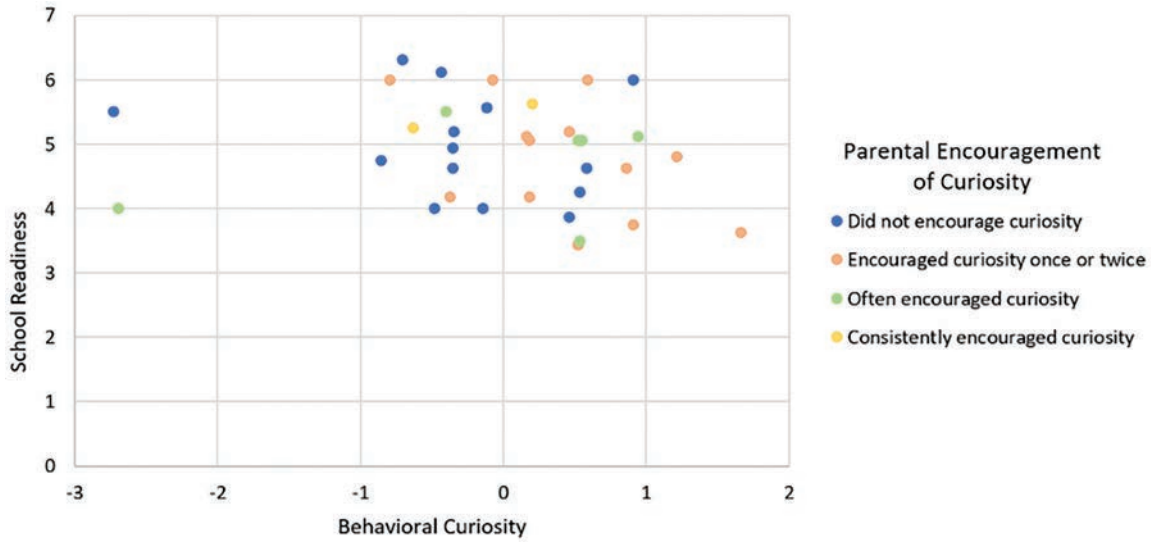

Figure 6. *Parental encouragement did not affect the link between behavioral curiosity and school readiness.*

for learning.[20] Future research should examine the relationship between learning experiences and school readiness, and whether curiosity or SES affect that relationship.

It is important to note that there were limitations to this study. Data was already collected to evaluate behavioral inhibition. Upon further reflection, this data was well-suited for this study. However, because the data was not initially intended for this project, the sample was relatively small and there was missing data in multiple variables.

There were also limitations regarding the measures. The objects in the laboratory may not all have been novel to every participant, because it would not be feasible for parents to know every object their child had seen or interacted with, given that a child could see these objects at a friend's house, in preschool, or online. Also, vocal curiosity and behavioral curiosity were statistically different concepts, though we initially intended to examine curiosity overall. This was likely due to the small amount of time children had during the episode: it seemed they had time either to explore or to ask questions. The short amount of time could explain why the findings indicated that vocal curiosity is not a predictor of school readiness. Another limitation was that school readiness was only accessed via parent report, which was used because it suited the needs of the initial study. To have a more robust measure, future studies could incorporate direct measures of children's academic competence. Furthermore, the parent's questionnaire only asked about math and reading competence, so exploratory behavior may benefit children in a different academic domain, such as science. Having a direct measure of academic competence that includes other subjects can allow for a greater understanding of

THE FINDINGS ALSO SHOWED THAT CURIOSITY IS RELATED TO SCHOOL READINESS, AS DEMONSTRATED BY THE NEGATIVE ASSOCIATION BETWEEN CHILDREN'S BEHAVIORAL CURIOSITY AND SCHOOL READINESS WHEN ACCOUNTING FOR SES.

the association between curiosity and school readiness.

Ultimately, this research highlighted how strong a predictor SES is for school readiness. The findings also showed that curiosity is related to school readiness, as demonstrated by the negative association between children's behavioral curiosity and school readiness when accounting for SES. Behavioral curiosity may demonstrate a lack of learning opportunities for children with low family SES. Future research could examine the impact of children's learning experiences on school readiness and whether children with low family socioeconomic status have fewer learning opportunities.

ACKNOWLEDGMENTS

I would like to thank my faculty advisor, Dr. Rebecca Brooker, for her guidance and support during this project. I have learned so much from her about the research process, and words cannot express my gratitude for the time and effort she spent reviewing and providing feedback for all of my materials.

I would like to thank my friends and family for their love and encouragement over the course of this project and throughout my time at Texas A&M University. I am also grateful for Robert Tirso and Sejal Mistry, who have guided me in my research and professional development.

REFERENCES

1. Vered Halamish, Inbal Madmon, and Anat Moed, "The Long-Term Mnemonic Benefit of Curiosity in Intentional Learning," Experimental Psychology 66, no. 5 (2019): 1–12, **https://doi.org/10.1027/1618-3169/a000455**.

2. Richard M. Ryan and Edward L. Deci, "Intrinsic and Extrinsic Motivations: Classic Definitions and New Directions," Contemporary Educational Psychology 25, (2000): 54–67, **https://doi.org/10.1006/ceps.1999.1020**.

3. Kourosh Amrai et al., "The Relationship Between Academic Motivation and Academic Achievement Students," Procedia Social and Behavioral Sciences 15, (2011): 399–402, **https://doi.org/10.1016/j.sbspro.2011.03.111**.

4. Halamish et al., "Long-Term Mnemonic Benefit," 1-12.

5. Eric T. Alberti and Sam L. Witryol, "The Relationship Between Curiosity and Cognitive Ability in Third- and Fifth-Grade Children," The Journal of Genetic Psychology 155, no. 2 (1994): 129–45, **https://doi.org/10.1080/00221325.1994.9914767**.

6. Patricia Minuchin, "Correlates of Curiosity and Exploratory Behavior in Preschool Disadvantaged Children," Child Development 42, (1971): 939–50, **https://www.jstor.org/stable/1127460**.

7. Prachi E. Shah et al., "Early Childhood Curiosity and Kindergarten Reading and Math Academic Achievement," Pediatric Research 84, (2018): 380–6, **https://doi.org/10.1038/s41390-018-0039-3**.

8. Claire B. Kopp, "Regulation of Distress and Negative Emotions: A Developmental View," Developmental Psychology 25, no. 3, (1989): 343–54, **https://doi.org/10.1037/0012-1649.25.3.343**.

9. Kopp, "Regulation of Distress," 343-54.

10. Richard C. Endsley et al., "Interrelationships among Selected Maternal Behaviors, Authoritarianism, and Preschool Children's Verbal and Nonverbal Curiosity," Child Development 50, no. 2 (1979): 331–9, accessed on May 25, 2020, **https://www.jstor.org/stable/1129407**.

11. Robert M. Saxe and Gary E. Stollak, "Curiosity and the Parent-Child Relationship," Child Development 42, no. 2 (1971): 373-384, **https://www.jstor.org/stable/1127473**.

12. Jerome Kagan, J. Steven Reznick, and Jane Gibbons, "Inhibited and Uninhibited Types of Children," Child Development 60, no. 4 (1989): 838–45, **https://www.jstor.org/stable/1131025**.

13. August B. Hollingshead, "Four Factor Index of Social Status" (unpublished manuscript, 1975), typescript.

14. Jeffery M. Armstrong, Lauren Heim Goldstein, and The MacArthur Working Group on Outcome and Assessment, "The MacArthur Health and Behavior Questionnaire (HBQ 1.0)," MacArthur Foundation Research Network on Psychopathology and Development, accessed December 13, 2020, **https://macarthurhbq.files.wordpress.com/2014/05/**

hbq-manual-1-0-05-29-2014.pdf.

15. Robert H. Bradley and Robert F. Corwyn, “Socioeconomic Status and Child Development,” Annual Review of Psychology 53, no. 1 (2002): 371–99, https://doi.org/10.1146/annurev.psych.53.100901.135233.

16. Betty Hart and Todd R. Risley, “The Early Catastrophe,” Education Review 117, no. 1 (2003): 110–8, https://www.maine.gov/doe/sites/maine.gov.doe/files/inline-files/hart%2B%26%2Brisley%2B2003%5B1%5D.pdf.

17. Milagros Nores and W. Steven Barnett, “Access to High Quality Early Care and Education: Readiness and Opportunity Gaps in America,” Center on Enhancing Early Learning Outcomes, (2014), accessed March 27, 2021, https://nieer.org/wp-content/uploads/2014/05/ceelo_policy_report_access_quality_ece.pdf.

18. George Loewenstein, “The Psychology of Curiosity: A Review and Reinterpretation,” Psychological Bulletin 116, no. 1 (1994): 75–98, https://psycnet.apa.org/doi/10.1037/0033-2909.116.1.75.

19. Theresa Hawley, “Starting Smart: How Early Experiences Affect Brain Development,” Ounce of Prevention Fund and Zero to Three, (2000), accessed March 27, 2021, https://startearly.org/app/uploads/pdf/StartingSmart.pdf.

20. Jeanne Brooks-Gunn, Pamela Kato Klebanov, and Fong-ruey Liaw, “The Learning, Physical, and Emotional Environment of the Home in the Context of Poverty: The Infant Health and Development Program,” Children and Youth Services Review 17, nos. 1-2 (1995): 251–76, https://doi.org/10.1016/0190-7409(95)00011-Z.

AUTHOR BIO

KATHRYN N. GRAY ‘21

Kathryn N. Gray '21 is a psychology major from College Station, Texas. The motivation behind her project was to explore ways to increase children's academic achievement. Kathryn plans to pursue a Ph.D. in developmental psychology, with a focus on improving children's success in schools and reducing the socioeconomic achievement gap.

The Whole as the Part: An Analysis on the Arrangement of Permanent Supportive Housing Neighborhoods

By Maggie Martin '22

INTRODUCTION

Permanent supportive housing (PSH) neighborhoods are a somewhat recent strategy for assisting the unhoused by providing long-term housing for individuals and families with extremely low incomes. According to the National Alliance to End Homelessness, investments in permanent supportive housing have helped decrease the number of chronically homeless individuals by twenty percent since 2007.[1] However, there is evidence of a lack of architectural design in the arrangement of PSH neighborhoods. Many promote or even require community engagement and interaction, which makes the configuration of the community vital. There is no question that PSH neighborhoods are beneficial; however, the primary question lies in what steps can be taken to improve the overall arrangement of the communities.

Aldo Rossi in *The Architecture of the City* said, "the comfort of any building consists of three principal items: its site, its form, and the organization of its parts."[2] By considering the whole as a part, it can also be said that the comfort of a site is dependent on the city as the larger site, its form, and the organization of its parts. In "Design and Affordable American Housing," Gwendolyn Wright said "site plans are more significant than architectural styles. They orchestrate the natural environment, of course, but they also affect safety and social life, both planned and serendipitous, for residents of all ages."[3] The success of any community relies heavily on the arrangement of its parts. Historically, social housing has primarily been designed as high density, presenting numerous challenges which ultimately lead to the failure of many projects. Unfortunately, low density supportive housing comes with many of its own challenges. The primary issue is the tendency to create a scaled down model of the traditional American suburban home and neighborhood. In the post-war American suburban neighborhood, a resident interacts primarily with only their home or lot, whereas in a supportive housing neighborhood the home is scaled down significantly often removing elements that require the residents to leave for simple tasks, yet these neighborhoods are arranged in a similar manner. This attempt to fulfill the supposed American dream ultimately leads to a juxtaposition of the traditional neighborhood and the PSH neighborhood.

THIS ATTEMPT TO FULFILL THE SUPPOSED AMERICAN DREAM ULTIMATELY LEADS TO A JUXTAPOSITION OF THE TRADITIONAL NEIGHBORHOOD AND THE PSH NEIGHBORHOOD.

METHODS

Research began with an in-depth analysis on the arrangement of four diverse permanent supportive housing communities. Between the four communities, variables in scale from 30-100 units, locations including Texas and Washington, and design approach such as tiny homes and quadruplexes allowed for a wide analysis. In addition to their heterogeneousness, commonalities were identified through each aspect of the projects, both good and bad. Qualities were then

Figure 1. *Quail Trail analogical illustration, "Wood Blocks," draws the site plan of the community as a curved rug with the housing as a child's building blocks.*

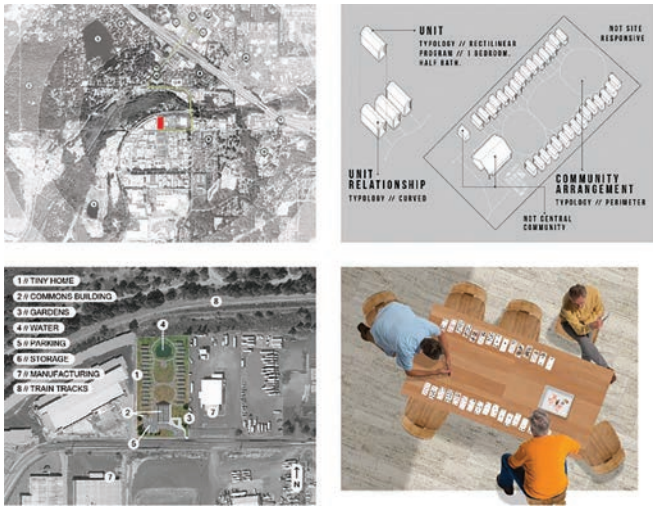

Figure 2. *Quixote Village. Bottom right: analogical drawing, "House of Cards," illustrating the site as a table and the housing as cards in play.*[6]

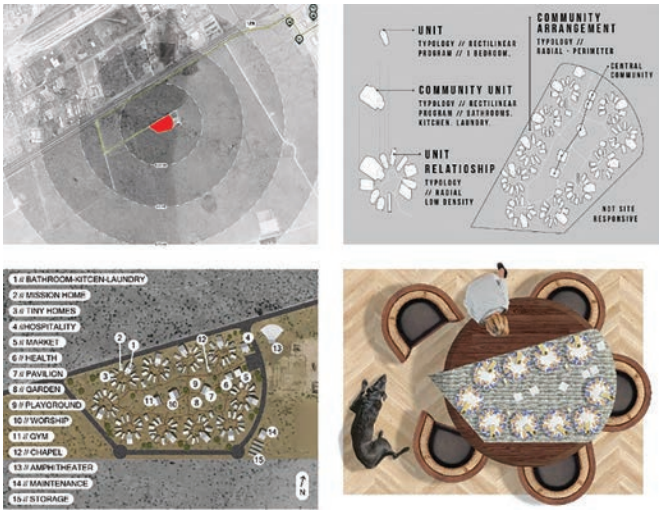

Figure 3. *Field's Edge. Bottom right: "Wheat Crackers" illustrates each collection of units as cheese and crackers on a plate.*[7]

displayed in a series of analytical drawings at each scale of the projects from city to individual unit, beginning with a land sustainability analysis to evaluate the lot and later analyzing the arrangement of spaces on that lot. Additionally, analogical drawings were created to playfully draw a line from site plans to the mundane arrangement of objects within the home (**Figure 1**). These illustrations attempt to relate the complexities of architecture to something even a child could understand, bringing the arrangement down to the most basic concepts of composition. While conducting research, it became clear that though motivations in the designs are pure, they can be severely misleading and result in inefficient designs for the city and the residents of the communities. This led to a motivation to develop accessible and understandable information on the crucial aspects to consider in order to design a successful housing community. Which begs the question, what

Figure 6. *Full spread of the toolkit. Each image in the composite is an individual 8.5x11" page.*

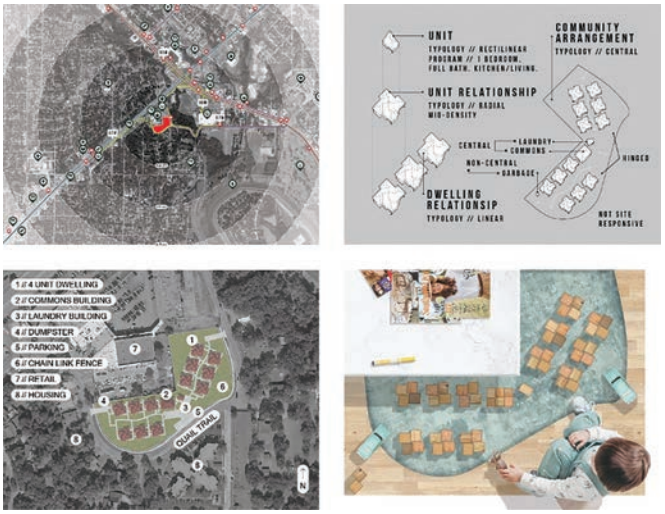

Figure 4. *Quail Trail. Bottom Right: "Wood Blocks," draws the site plan of the community as a curved rug with the housing as a child's building blocks.*[8]

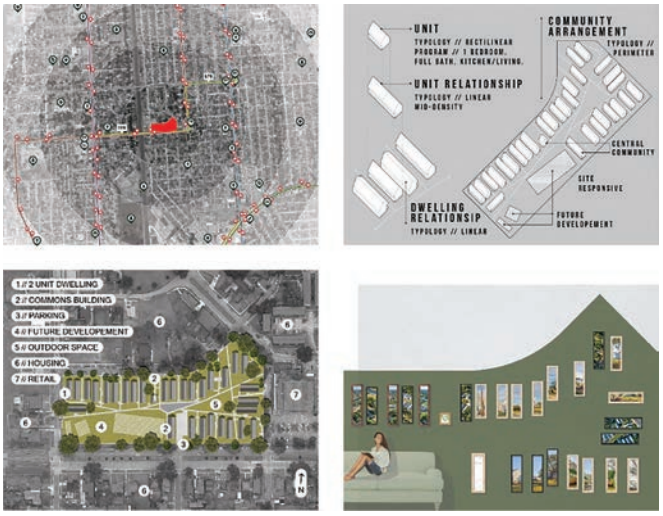

Figure 5. *Bastion. Bottom Right: "Picture Perfect," displays each dwelling as a framed picture on a wall, using photographs of the realized project.*[9,10]

elements of design can be established to assist in the successful planning of the arrangement of permanent supportive housing neighborhoods?

RESULTS

Based on the successes and shortcomings of Quixote Village in Tumwater, Washington (**Figure 2**); Field's Edge in Midland, Texas (**Figure 3**); Quail Trail in Fort Worth, Texas (**Figure 4**); and Bastion in New Orleans, Louisiana (**Figure 5**) a series of steps and strategies were established and organized into a toolkit. This strategy is often used when spaces are actively being designed or built by untrained people. One such example is the Self-Build Manual by Comunal.[4] The group found that families in rural Mexico were building their homes with little to no structural knowledge. On their Who We Are page they state, "we do not conceive architecture as an individual author's work or as a static, artistic and unmodifiable object; but as a collaborative, live, open and constantly evolving social process."[5] By recognizing architecture as a social process, Comunal empowers users with decision making and acknowledges them as the most central part of projects. Their toolkit provides an accessible resource to ensure that not only do the users have decision making power, but also that they are making informed and safe decisions in terms of structure. **Figures 2–5** are each a composite of four images created for one of the four communities showing in the top left a city analysis assessing accessibility; in the top right a site analysis on the relationships and quality of private, semi-private, and semi-public spaces; in the bottom left is a site analysis on the program of the site, and the bottom right is an analogical illustration drawn from the site plan in the bottom left.

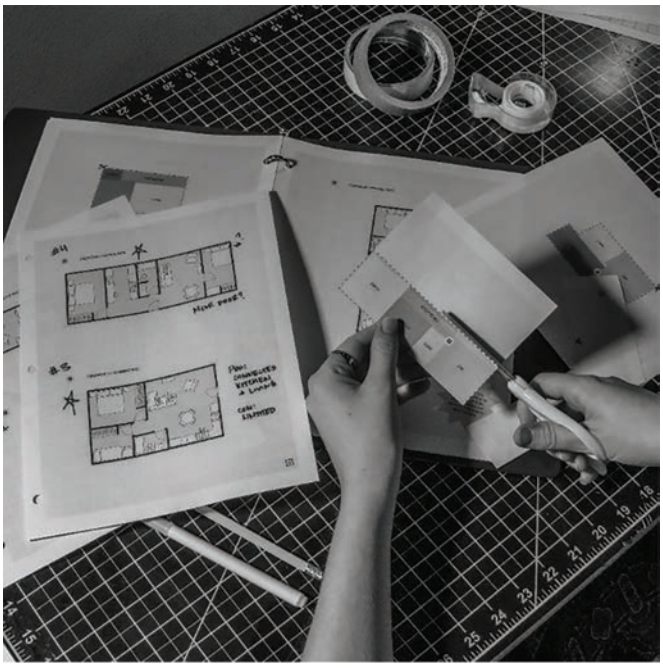

Figure 7. *Example of the toolkit in use. Photos of the toolkit in use are dispersed throughout the book as a visual guide to assist with written and illustrated instruction.*

Figure 8. *Axonometric drawing of the application of the toolkit in Baytown, Texas*

In a similar way, the toolkit (**Figure 6**) produced from this research seeks to provide a resource so that organizations along with the users are making informed design decisions to ensure optimal living spaces, a real sense of ownership, and community. The organization of chapters was done intentionally and is meant to be followed in order so that each element of the community is given correct priority and focus. This resource is intended to be printed out and used through a series of steps involving cutting out pieces, taping things together, drawing, and taking notes (**Figure 7**). By following each step of the process, users will explore the arrangement possibilities as they see instructions on how to plan a community without a computer program or prior architectural knowledge. After the toolkit was completed, a design was created using the tool for a site in Baytown, Texas (**Figure 8**). By using the toolkit to design a potential community, the images created serve both as examples of the application to assist users as well as a source of reflection on the effectiveness of the product. Throughout each step of the process, users can see examples of the toolkit's application because of the community designed using it. This toolkit gives the proposed elements for designing a permanent supportive housing community in practical and tangible ways. Furthermore, it continues the concept of the analogical illustrations by scaling down the elements of a community to pieces small enough to fit within a home. Lack of architectural quality in PSH neighborhoods is largely due to the lack of design in arrangement, but with the consideration of the elements and strategies proposed, these communities can be designed as both programmatic and aesthetic.

CONCLUSION

Although there are organizations that offer education workshops on planning supportive housing neighborhoods, they are almost all for tiny home villages. The creative artifact produced from this research proposes breaking from this approach. One aspect of design the toolkit focuses on is a solution to the desire to build single family homes in order to fulfill the supposed "American dream." This usually leads to the tiny home model; however, the toolkit proposes another solution. By suggesting the development of mid-density housing, the designs can satisfy the American dream through an illusion of single-family homes. Supportive housing units are small enough that when arranged into dwellings of 2-4 units, they can still appear to be a single-family home. This creative artifact seeks to answer the primary question of this research in a format that is accessible not only to architects, but anyone with the hope of housing the unhoused. Though it may not fully solve the problem at hand, by establishing a set of guidelines it opens a line of discourse for others to agree or disagree on.

ACKNOWLEDGMENTS

I would like to thank my faculty advisor, Professor James Michael Tate, for his guidance and support throughout the course of this research. Thanks also go to my friends, classmates, and the department faculty and staff for making my time at Texas A&M University a great experience. The materials used to produce drawings for the analysis on Field's Edge in Midland Texas were provided by Laura Chandler from The Field's Edge. The materials used to produce drawings for the analysis on Quail Trail in Fort Worth Texas were provided by Mark Dabney from Boka Powell. Thanks to Mina Gerall, Shannon S. Van Zandt, and Jaime H. Masterson for their valuable feedback on the toolkit. Finally, I would like to acknowledge Luke Redus from Compassion United for inspiring the creation of a toolkit to be used for the planning of permanent supportive housing neighborhoods.

This research was supported by the Department of Architecture and LAUNCH: Undergraduate Research at Texas A&M University, with additional funding from the Academy for the Visual and Performing Arts at Texas A&M University.

REFERENCES

1. "Permanent supportive housing," National Alliance to End Homelessness, last modified January 27, 2020, accessed March 01, 2021, **https://endhomelessness.org/ending-homelessness/solutions/permanent-supportive-housing/**.
2. A. Rossi, The architecture of the city (Cambridge, Mass: MIT Press, 2007), [40].
3. Wright, Gwendolyn. "Design and Affordable American Housing." Cityscape 16, no. 2 (2014): 69-86. Accessed August 20, 2021. **http://www.jstor.org/stable/26326884**.
4. Manual, accessed April 03, 2021, **https://en.comunaltaller.com/copia-de-tequiocalco** (page discontinued).
5. "Who we are," Comunal, accessed April 03, 2021.
6. Olympia Quixote Village, accessed September 14, 2020, **http://www.quixotecommunities.org/olympia-quixote-village.html**.
7. "About," The Field's Edge, accessed January 24, 2021, **http://www.thefieldsedge.org/about**.
8. S. Nishimura, "New 48-Unit Project in West Fort Worth to Provide Homes for the Homeless," Fort Worth Magazine, July 21, 2020, **https://fwtx.com/news/new-48-unit-project-in-west-fort-worth-to-provide-homes-for-/**.
9. Bastion, **https://www.officejt.com/our-work/bastion** (page discontinued).
10. D. Tapia, "Bastion Community Housing / OJT," Arch Daily, June 27, 2019, **https://www.archdaily.com/919835/bastion-community-housing-ojt**.

AUTHOR BIO

MAGGIE MARTIN '22

Maggie Martin '22 is an honors Environmental Design major with a double minor in New Media Art and Leadership in the Design and Construction Professions. Born and raised in Conroe Texas, Maggie is part of a line of 100 years of Aggies. With interests in architectural visualization, housing issues, graphic design, and design education, Maggie plans to attend graduate school for Architecture after graduating from Texas A&M. Her research stems from these interests and focuses on providing an accessible design education resource for cities or organizations working towards designing a permanent supportive housing neighborhood.

BOARD BIOGRAPHIES

MACK CLEVELAND ‘23

Mack Cleveland is a class of 2023 Materials Science and Engineering major, from Bedford, TX. After graduation, he plans to go to graduate school to earn a PHD in materials science to pursue a career in research.

ANNALIESE FOWLER '23

Annaliese Fowler is a class of 2023 Biomedical Engineering major, from Houston, Texas. After graduation, she plans to go to graduate school for bioinformatics or biostatistics.

THAO HO ‘22

Thao Ho is a class of 2022 Bioinformatics major, from Houston, TX. After graduation, she plans to go to graduate school for economics.

EUNHYE "GRACE" JEON

Eunhye is a class of 2021 Biology major, from Harker Heights, Texas. After graduation, she plans to become a physician scientist.

SUCHITAA SAWHNEY '24

Suchitaa Sawhney is a class of 2024 Biomedical Engineering major, from Flower Mound, TX. After graduation, she plans to attend medical school.

ARYAN SHETTY '22

Aryan Shetty is a class of 2022 Computer Science major, from Dubai, United Arab Emirates. After graduation, he plans to continue studying by pursuing his masters in Machine Learning!

MIRIAM STEIN '24

Miriam Stein is a class of 2024 Molecular and Cell Biology major, from San Antonio, Texas. After graduation, she plans to pursue a career in medical research.

JEREMY THOMAS '23

Jeremy is a class of 2023 Biomedical Engineering major, from Flower Mound, Texas. After graduation, he plans to pursue a career in academia.

BOARD BIOGRAPHIES

CATHERINE JOHNSON ‘23

Catherine Johnson is a class of 2023 Mathematics major, from Nashville, TN. After graduation, she plans to earn a masters of financial management.

AMY LONG '24

Amy Long is a class of 2024 Computer Science major, from Katy, TX. She is not 100% sure on what she’ll be doing post-graduation. She will either work for a few years then go to grad school or go to grad school immediately.

ALYSSA LOW '22

Alyssa is a class of 2022 Biochemistry and Genetics major, from McKinney, Texas. After graduation, she plans to career in medicine.

VISHAY RAM '24

Vishay is a class of 2024 Molecular and Cell Biology major, from Katy, Texas. After graduation, he plans to pursue a career or higher education in healthcare.

NIKITA VALLURI '22

Nikita Valluri is a class of 2022 Biomedical Sciences major, from Houston, TX. After graduation, she plans to go to medical school. In her gap year, she would like to continue research, work in EMS, or get a Masters Degree.

ANDREA VAN RAVENSWAAY ‘23

Andrea “Andie” van Ravenswaay is a junior applied math major with a double minor in art history and economics from Houston, Texas. Andie loves to travel whenever she can and is an aspiring actuary, who hopes to work in underwriting for art insurance.

REBECCA ZIVLEY ‘23

Rebecca is a class of 2023 Mechanical Engineering major, from Houston, TX. After graduation, she plans to go to graduate school to become an engineering professor.

LAUNCH

UNDERGRADUATE RESEARCH

Explorations: The Texas A&M Undergraduate Journal
114 Henderson Hall, 4233 TAMU
College Station, Texas, 77843-4233
United States of America

ISSN 2668-7525 (print)
ISSN 2688-7533 (online)

explorations.tamu.edu